

**Republic of Iraq**  
**Ministry of Higher Education & Scientific Research**  
**University of Kerbala**  
**College of Engineering**  
**Civil Engineering Department**



## **Improving Efficiency of Storm Water Network Using a New Galley Design-Filter Bucket**

A thesis Submitted to the Department of Civil Engineering, University of Kerbala in Partial Fulfillment of the Requirements for the Degree of Master of Science in Infrastructure Engineering

By

**Karrar Abdullah Mohsen**

BSc. in Civil Eng./ University of Kerbala (2016)

Supervised by

**Prof . Dr. Basim Khalil Nile**

**Prof. Dr. Waqed Hammed Hassan**

بِسْمِ اللّٰهِ الرَّحْمٰنِ الرَّحِیْمِ

وَقُلْ رَبِّ زِدْنِيْ عِلْمًا

صدق الله العلي العظيم

سورة طه الآية (114)

## **SUPERVISOR CERTIFICATE**

We certify that this thesis entitled “**Improving Efficiency of Storm Water Network Using a New Galley Design-Filter Bucket.**” which is prepared by " **Karrar Abdullah Mohsen** " under our supervision at University of Kerbala in partial fulfillment of the requirements for the degree of Master of Science in Civil Engineering (Infrastructure Engineering ).

**Supervisor**

Signature:

Prof. Dr. Basim Kh. Nile

Date:     /     / 2020

**Supervisor**

Signature:

Prof. Dr. Waqed H. Hassan

Date:     /     / 2020

## **Examination Committee' Certificate**

We certify that we have read the thesis entitled “**Improving Efficiency of Storm Water Network Using a New Galley Design-Filter Bucket**” and as an examining committee, we have examined the student " **Karrar Abdullah Mohsen**" in its content and that in our opinion, it meets the standard of a thesis for the degree of **Master in Civil Engineering Science (Infrastructure Branch)**.

### **Member and Supervisor**

Signature:

Name: Prof. Dr. Basim Kh. Nile

Date:     /     / 2020

### **Member and Supervisor**

Signature:

Name: Prof. Dr. Waqed H. Hassan

Date:     /     / 2020

### **Member**

Signature:

Name: Assist. Prof. Dr. Musa H. J. Al-shammari

Date:     /     / 2020

### **Member**

Signature:

Name: Dr. Raid R. A. Al-muhanna

Date:     /     / 2020

### **Chairman**

Signature:

Name: Prof. Dr. Riyad H. H. Al-anbari

Date:     /     / 2020

**Approved by the Head of Civil Engineering Department**

Signature:

Name: Dr. Raid R. A. Almuhanha

Date:     /     / 2020

**Approved by the Dean of College of Engineering**

Signature:

Name: Assist. Prof. Dr. Laith Sh.Rasheed

Date:     /     / 2020

This thesis is dedicated to:

My parents and my family, brothers, sisters and friends for their  
love and continuous support

## **ACKNOWLEDGEMENTS**

I would like to thank my parents for their continuous support and love. This accomplishment would not have been possible without them. I would also like to thank in particular their directors of study and academic supervisors **Professor. Dr. Basim Khalil Nile** and **Professor. Dr. Waqed Hammed Hassan** for their valuable assistance, suggestions, advice, continuous guidance and encouragement throughout the research.

# Abstract

Storm networks as urban infrastructure are important elements in the society. One of the most critical problems facing such networks is the clogging of pipes due to sediment inlet into the sewer systems, which can cause flooding during heavy rain. This study aims to improve the efficiency of storm network by using a new filter.

This study presents an experimental model, in which a buildup model contained a network of pipes used to simulate the rain as well as the street surface with two sides, in the first side contains gully with filter, while the other side contains gully without filter. Several variables effects on the passing ratio from gully with filter to gully without filter were studied, such as rainfall intensity, length of filter, duration of intensity and slope of floor.

A numerical model FLOW-3D was verified by using experimental work, and the purpose of numerical model to study a new variable not getting in the present experimental work like diameter of sediments. Five different intensities of rainfall were used 30, 37, 44, 51 and  $58\text{mmh}^{-1}$ , each intensity is runoff on the floor with five slopes 1,1.5,2, 2.5 and 3. For a length of filter were also used 100,150,200,250 and 300mm, while the duration of rainfall intensities were 5, 10, 15, 20 and 25 minutes.

Results indicated that the slope of the ground and the length of filter were

the most influential factors affecting on passing ratio of gully with filter to gully without filter ( $Mf/Mg$ ). The relationship between the efficiency of filter and passing ratio ( $Mf/Mg$ ) was the inversely related. The passing ratio ( $Mf/Mg$ ) was 35% for the minimum slope of the ground, and 11% for the maximum slope of ground. It was observed that the passing ratio decreases when the length of filter in filed is more than 400mm. The duration of intensity has a less important effect on the passing ratio than other variables. The results also showed that the passing ratio ( $Mf/Mg$ ) was 34% at a low rain intensity of  $30 \text{ mmh}^{-1}$  and 12.5% at a high rain intensity of  $58 \text{ mmh}^{-1}$ , while it was 37% and 13% for minimum and maximum diameter of sediment, respectively.

The results also concluded that the use of FLOW-3D to simulate these phenomena gave acceptable results, as the maximum error between numerical and laboratory model was less than 16%. The dimensional analysis prediction model provides effective methods to predict the behavior of passing the ratio of gully with filter to gully without filter. The numerical model helped in providing a statistical equation to calculate the passing ratio ( $Mf/Mg$ ), where the using of SPSS model to estimate the passing ratio gives result that agree with ( $R^2 = 0.88$ )



# CONTENTS

ABSTRACT.....	I
CONTENTS.....	III
LIST OF FIGURES .....	VI
LIST OF TABLES .....	VIII
LIST OF SYMBOLS .....	VIII
ABBREVIATIONS/ACRONYMS.....	IX
CHAPTER ONE .....	1
Introduction .....	2
1.1 Introduction .....	2
1.2 Statement of the problem .....	3
1.3 Objectives of the study .....	3
1.4 Structure of the thesis .....	4
CHAPTER TWO .....	5
Literature review .....	7
2.1 Introduction .....	7
2.2 Rainfall simulators .....	7
2.3 Rainfall performance simulator.....	9
2.4 Types of filters in the rain network .....	11
2.5 Transmission of sediments .....	20
2.6 Summary .....	22
CHAPTER THREE.....	24
Theoretical Concept and Numerical Model .....	25
3.1 Introduction .....	25
3.2 Theory concept.....	25

3.4 Numerical model approach .....	26
3.4.1 Turbulence model.....	28
3.5 Model setup .....	30
3.5.1 Physical items.....	30
3.5.2 Model geometry .....	31
3.5.3 Meshing.....	32
3.5.4 Boundary and initial conditions .....	35
3.6 Material properties .....	36
3.7 Solving options.....	36
3.8 Steps of work in Flow 3D software.....	36
3.9 Statistical Analysis Model.....	37
3.9.1 The definition around statistical and goodness of fit .....	37
3.10 Dimensional Analysis .....	39
<b>CHAPTER FOUR .....</b>	<b>43</b>
Experimental work .....	44
4.1 Introduction .....	44
4.2 Laboratory model.....	44
4.3 Materials and equipments .....	44
4.3.1 Steel frame.....	44
4.3.2 Rain system .....	44
4.3.3 Rain collection floor .....	47
4.3.3.1 Floor slopping.....	48
4.3.3.2 Gully without filter.....	49
4.3.3.3 Gully with filter .....	49
4.3.3.4 Lifting devices and sieves .....	50

4.4 Laboratory tests .....	54
4.4.1 Uniformity and intensity rainfall .....	55
4.4.2 Permeability test .....	56
4.4.3 Porosity test .....	57
4.4.4 Sieve analysis .....	58
4.4.5 Density .....	58
4.5 Testing procedure .....	59
4.6 Methodology of laboratory test .....	60
4.7 Summery .....	62
CHAPTER FIVE.....	63
Results and Discussion.....	64
5.1 Introduction .....	64
5.2 Experiential results .....	58
5.2.1 Effect of rain storm intensity on filter.....	64
5.2.2 Effect length of filter .....	65
5.2.3 Effect duration of intensity .....	69
5.2.3 Effect of slope .....	72
5.3 Numerical model Flow-3D.....	74
5.3.1 Verification the result of numerical and experimental models .....	76
5.3.2 Effect the diameter of sediments .....	80
5.4 Dimensional analysis and prediction model.....	82
CHAPTER SIX .....	88
Conclusions and Recommendations.....	89
6.1 Introduction .....	89
6.2 Conclusions .....	89

6.2 Recommendations .....	90
References .....	91
Appendix-A .....	A-1
Appendix B.....	B-1
Appendix-C .....	C-1

## LIST OF FIGURES

<b>FIGURE NO</b>	<b>TITLE</b>	<b>PAGE</b>
Figure(2-1)	Plastic containers to assess the spatial distribution of rainfall intensity	11
Figure (2-2)	Storm water inlet filter	13
Figure (2-3)	Curb inlet gravel sediment filter	14
Figure (2-4)	Curb inlet filter	15
Figure (2-5)	Street curb drain filter	17
Figure (2-6)	Clogging filter	19
Figure (2-7)	Schematic representation of experimental	21
Figure (3-1)	Numerical model geometry representation of Flow-3D	32
Figure (3-2)	Meshing of numerical model (Flow-3d)	33
Figure (3-3)	FAVOR option with different cell size	34
Figure (3-4)	Boundary conditions uses in this study	35
Figure (4-1)	Installation process of rain system nozzle	45
Figure (4-2)	Gauge pressure and pump	46
Figure (4-3)	Rain water distribution and angle of nozzles of the model	47
Figure (4-4)	Floor slopping	48
Figure (4-5)	Top view of gully without filter	49
Figure (4-6)	Gully with filter	50
Figure (4-7)	Lifting devices	51

<b>FIGURE NO</b>	<b>TITLE</b>	<b>PAGE</b>
Figure (4-8)	Both gully details at top view	52
Figure (4-9)	Sketch of the frame, nozzle for experimental work	53
Figure (4-10)	Shape of the frame, nozzle for experimental work	54
Figure (4-11)	Distribution of container according to Christiansen theory	56
Figure (4-12)	Permeability devices	57
Figure (4-13)	Research methodology	61
Figure (5-1)	Relation between intensity and passing ratio ( $Mf/Mg$ )	66
Figure (5-2)	Relation between intensity and passing ratio for different slopes	67
Figure (5-3)	Relation between length of filter and passing ratio( $Mf/Mg$ )	69
Figure (5-4)	Relation between length of filter and passing ratio( $Mf/Mg$ )	70
Figure (5-5)	Relation between duration of intensity and passing ratio ( $Mf/Mg$ )	71
Figure (5-6)	Relation between duration of intensity and passing ratio for different slopes	72
Figure (5-7)	Relation between slope and passing ratio( $Mf/Mg$ )	74
Figure (5-8)	Relation between slope and passing ratio for different durations	75
Figure (5-9)	Relationship between passing ratio in experimental and numerical (FLOW-3D) for 5 mm grid size	76
Figure (5-10)	Relation between intensity and passing ratio (FLOW-3D)	78
Figure (5-11)	Relation between length of filter and passing ratio (FLOW-3D)	79
Figure(5-12)	Relation between intensity duration and passing ratio (FLOW-3D)	79
Figure (5-13)	Relation between slope and passing ratio (FLOW-3D)	80
Figure (5-14)	Comparison between the result for numerical and experimental work	81
Figure (5-15)	Effect diameter of sediments on passing ratio from (FLOW-3D)	82
Figure (5-16)	Effect slope on passing ratio ( $Mf/Mg$ )	84
Figure (5-17)	Relationship between passing ratio and $(I * T)/Lf$	85
Figure (5-18)	Relationship between passing ratio and $D/Lf$	86
Figure (5-19)	Caparisons between the observed and predicted passing ratio( $Mf/Mg$ )	87

## LIST OF TABLES

TABLE NO	TITLE	PAGE
Table (2-1)	Experimental details (Hatt et.al, 2007)	19
Table (4-1)	list of laboratory tests	59
Table (4-2)	Variable in experimental work	60
Table (5-1)	The correlation coefficient for different grid size	77
Table (5-2)	The correlation coefficient for different variables	83

## LIST OF SYMBOLS

Symbol	Definition	Dimension
$(\rho)$	Dry density of the sediments	$M L^{-3}$
(I)	Intensity of rainfall	$L T^{-1}$
(g)	Acceleration of gravity (g)	$L T^{-2}$
(T)	Duration of intensity	T
(S)	Bed slope	-
$(L_f)$	Length of filter	L
$(D_s)$	Diameter of sediments	L
$(M_s)$	Mass of sediments	M
$(M_f)$	Mass sediments pass through gully with filter	M
$(M_g)$	Mass sediments pass through gully without filter	M

## ABBREVIATIONS/ACRONYMS

<b>Symbol</b>	<b>Description</b>
ANOVA	Analysis of Variance
MAE	Mean Absolute Error
MAPE	Mean Absolute Percentage Error
$MS_E$	Mean Square of Residual
$MS_R$	Mean Square of Regression
RMSE	Root Mean Square Error
SPSS	Statistical Product and Service Solutions
$SS_E$	Residual Sum of Squares
$SS_R$	Regression Sum of Squares
$SS_T$	Total of Sum Squares
CFD	Computational Flood Dynamic

*Chapter One*  
*Introduction*



## *Chapter One*

### *Introduction*

#### **1.1 Introduction**

Water drainage networks are one of the most important segment in the construction of streets, highways, residential housing developments, commercial developments, schools, airports and other types of construction projects. Thereafter, the storm water drainage system for the development is constructed; it typically includes underground sewer, collection basins, culverts, and drop inlets that form the connection between the Storm water drainage system and a finished street side curb-and-grate inlet. As the construction of the development continues, government regulations and building codes generally require that the storm water drainage system be kept substantially free of silt and sediment that might enter through the curb-and-grate inlet. Keeping silt and sediment out of the collection basins difficult given construction on site that can dislodge or disturb silt and sediment. If silt and sediment are washed in collection basins and other parts of the sewage system or otherwise collected, the collection basins can become clogged. In that event, it becomes necessary to send workers down into the collection boxes to clean out the dirt and/or debris manually in order to comply with clean water regulations. These cleaning operations are difficult because the pipes are fairly tight, making it difficult to maneuver(Earl, 2006).

Storm networks like every urban infrastructure, are critical elements of life in society. They were designed to meet the increasingly diverse challenges protection against floods and discharge limitation in the natural environment, with an aging underground infrastructure, the burden on municipal agencies to prioritize and maintain the rapidly deteriorating sewer pipelines is increasing(Chughtai and Zayed, 2008).

## **1.2 Statement of the problem**

Stormwater is a major cause of urban flooding. Urban flooding is the inundation of land or property in a built-up environment caused by stormwater overwhelming the capacity of drainage systems, such as storm sewers. One of the most important problems facing such networks is the clogging of pipes due to sediment inlet into the sewage systems, which can cause flooding during heavy rain. Indeed, runoff water created by storm water (or melting water) can create erosion on the land due to flooding and/or increase pollutant discharges in a natural stream. All types of surfaces from natural permeable soil to impermeable surface are affected differently by runoff water. The best way to tackle this problem is to be aware of it at the design stage of the project in order to be able to implement sustainable and affordable solutions.

## **1.3 Objectives of the study**

This study aims to evaluate the efficiency of storm sewer networks by trying a new suggested filter. The use of this filter might have many benefits such as reducing maintenance of networks, reducing flooding during rainfall, and preventing water overflow that can be harmful to grass and plants.

**1.4 Structure of the thesis**

This study contains six chapters as follows

1. Chapter one presents the introduction of the problem and the objectives of this study.
2. Chapter two contains basic concept and previous studies about the simulation of rainfall and development of filter and storm water network.
3. Chapter three contains the dimensional analysis for the effect some parameter on the study and the numerical modeling. This chapter describes the numerical modeling by using FLOW-3D software simulation.
4. Experimental work details are shown in chapter four. Attribute of the experimental procedure and model are also presented.
5. Chapter five consists of the result, and discussion of all experimental and numerical work.
6. Conclusions, recommendations and suggestions to conduct other studies are presented in chapter six.

*Chapter Two*  
*Literature Review*

## *Chapter Two*

### *Literature Review*

#### **2.1 Introduction**

This chapter studying the previous works related to the rainfall simulation and filters. Rainfall simulation divided according to the areas and factors that affect in both of rainfall intensity and regular rain. There are many types of filters used in rain networks; these filters are made of iron, plastic and at various shapes and designs.

#### **2.2 Rainfall simulators**

The primary purpose of a rainfall simulator is to simulate natural rainfall accurately and precisely. At the same time, rainfall simulators control the intensity and duration of the rainfall which is otherwise random. Rainfall simulators are advantageous because rainfall can be produced quickly on demand, wherever necessary without having to wait for natural rain at the intensity and duration required.

For areas (up to about 10 meters per side), there are two standard options for rainfall simulators: rows or nozzle arrays and sweeping sprinklers. (D. Moore et al, 1983) represented the simulations of nozzle type, it is suitable for both large and small scale studies of the erosion, infiltration, and runoff processes. Rainfall intensities ranging from 3.5 to 185  $mmh^{-1}$  can be produced, and the measured uniformity coefficients range from 80.2 to 83.7.

There are several different types of rainfall simulators, each with its own application, benefits, and shortcomings. Many researchers explained the

standard small or laboratory scale ( $1m^2$  or smaller). (Cerdà et al, 1997) studied  $0.24m^2$  rainfall simulator given  $55 mmh^{-1}$  with a spatial uniformity coefficient of 93 %; the rainfall intensity and distribution depends on the type and number of nozzles used. In his study explores the description of a sprinkling-type portable rainfall simulator, which was designed to be used in rugged terrain conditions, and has been used for a decade in semi-arid environments with good results.

Another type of small plot rainfall simulator can use nozzles with a rotating disk that directs water to the plot originally (Grierson and Oades, 1977). These devices also attain uniformity coefficients of at least 75% for a full range of intensities. In general, small plot rainfall simulators are easily portable due to their small size. However, their limited size (approx.  $1m^2$ ) makes them not well suited to capturing plot-scale heterogeneity in surface properties.

(Foster *et al.*, 2000) explained seven case to demonstrating the successful use of drip-screen rainfall simulator. The majority of experiments utilized a simulator with an upper  $1 \times 0.5$  m perspex plate, which contained 627 drop formers in 19 rows of 33, produced intensities ranging from 7.74 to  $28.57 mmh^{-1}$  with temporal coefficients of variation for intensity ranging from 5.04 to 11.55 %,.. The experimental results led to the recognition of various philosophical and practical problems associated with the realistic simulation of rain.

Most significant intensities are also probable; for example, (Fernández et al., 2008) applied a simulator with a domain of  $0-120 mmh^{-1}$  are with an

intentionally various distribution. The rainfall simulator is designed to be used over 50×50 cm plots and consists essentially of a drop forming chamber which is supported over a metal structure at a certain height above the soil surface.

(Fister *et al.*, 2012) developed a rainfall simulator for a 2.2m<sup>2</sup> plot that achieves 85–96 mmh<sup>-1</sup> with a mean uniformity coefficient of 60 %; the emphasis was placed on reproducibility rather than uniformity in this case. The analysis presented in his study suggested, in particular, very good reproducibility of wind and rain conditions.

According to (Wilson *et al.*, 2014) achieving high drop speeds than trickle tanks due to water pressure in the nozzles is one of the major features of these types of fixed nozzle systems. As well, these devices tend to expand into bigger spaces by reproducing the base unit. The design can comprise complex parts and may need to be powered by a computer, making the system's calculation and complexity a typical flaw to simulate rainfall by sweeping or oscillating spraying. Also, the spray may be choppy rather than steady as the nozzles sweep back and forth or rotate around a piece of land. Arrays of drizzle nozzles or rows are that they tend to be less the uniformity coefficients due to fixed nozzle patterns represent a typical defect.

For larger plots on the hillslope scale, the standard design is a rotating boom rainfall simulator, first developed by Swanson as mentioned in (Wilson *et al.*, 2014). A single unit of this simulator irrigates two parallel plots of 4.3m×10.7m at up to 120mmh<sup>-1</sup> intensity, with two units used to cover plots up to about 23m long. In addition to covering large areas, these systems can

be mounted on a trailer, simplifying transportation between sites. However, trailer-mounted systems cannot be used on steep hillslopes or in other areas that vehicles cannot reach, such as forests, which does not make them well suited for use in the wide range of soil and vegetation combinations needed for the present research. Additionally, these systems are usually more complicated than drip tanks or stationary nozzle systems, and due to the circular spray pattern, these systems are less efficient for covering square or rectangular plots. Overall, lacking standard designs for rainfall simulators, individual researchers develop devices that suit their particular needs.

### **2.3 Rainfall performance simulator**

Precipitation pattern, uniformity, precipitation granules, rain drop velocity and kinetic energy represent simulated properties in precipitation simulation. The simulated precipitation characteristics depend on the applied pressure, the type of nozzle used, and how the nozzles are transported by a rotating bar and arranged. In addition, the intensity of precipitation and even the method of measurement effect the distribution of drop size (Kincaid et al, 1996).

Through repetition testing, uniformity in the spatial distribution of precipitation on the frequency of both the scale of the decrease volume and low kinetic energy, the network performance of the nozzles can be assessed to simulate precipitation. The drop size distribution can be predicted by the width of the nozzle fan for a bell-shaped distribution while reducing a larger

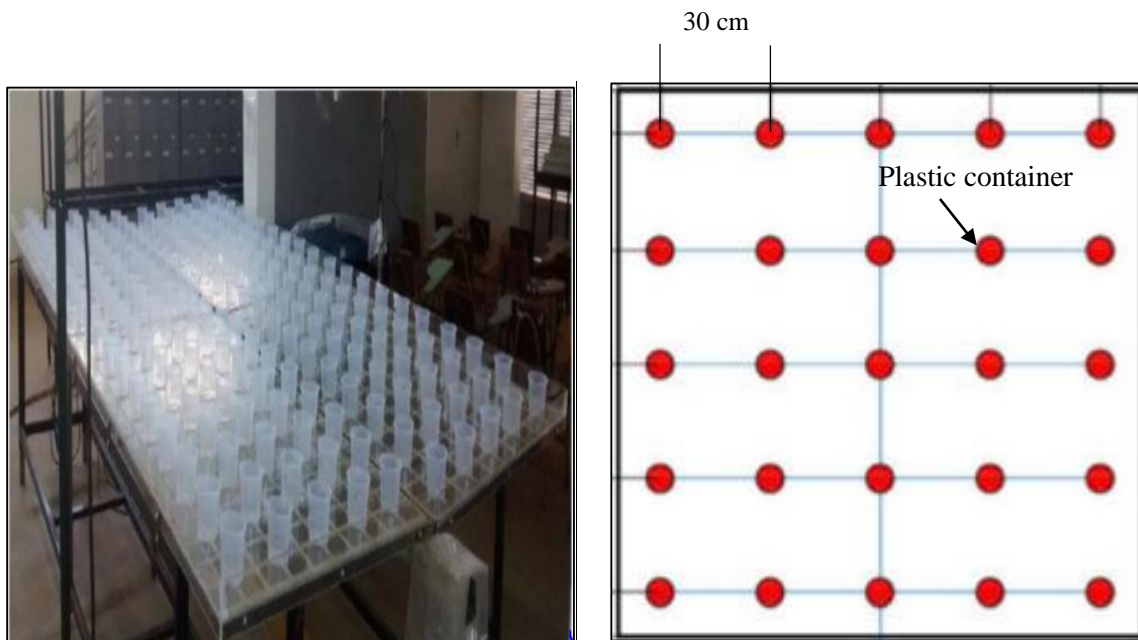


volume at a central location while smaller droplets include fan edges. Through the arrangement and movement of the nozzles can overcome this defect. However, multiple nozzle precipitation simulators naturally tend to improve local areas of high precipitation connect with overlapping patterns of spray from adjacent nozzles (Grismer, 2011)

Rainfall drizzle falls on the surface of the earth periodically, that is, rainfall, followed by a rest period. Thus, the intensity and uniformity of rainfall depends on the frequency of oscillation of the fan, nozzle water pressure(Aksoy *et al.*, 2012). Increasing nozzle oscillation frequency increases the rainfall intensity and uniformity, both of which are determined by the test plot size considered. Longer plot length requires a greater sweep time that results in possible unacceptable periods of repose. This could require more openings to sweep the edge of the test plot. Determination of the almost used spatial uniformity is the coefficient of uniformity (CuC) defined by Christiansen as mentioned in (Wilson *et al.*, 2014)

$$(CuC) = \left(1 - \frac{\sum_1^N |Xi - \bar{X}|}{N\bar{X}}\right) 100 \dots\dots\dots(2-1)$$

where Xi is the amount of rainfall at location i, N is points number where measuring container are placed on the ground to collect rain and  $\bar{X}$  is the average amount of precipitation. The CuC is an important indicator of spatial uniformity of precipitation. The more uniform the pattern of rainfall is the closer CuC approaches to 100%. A rainfall can be considered uniform when CuC is higher than 80%



A. Shape of containers

B. Sketch of containers

Figure(2-1) Plastic containers to assess the spatial distribution of rainfall intensity(Wilson et al., 2014)

## 2.4 Types of filters in the rain network

In this review one take a look on how the filters used in the rain networks developed, and how the researchers improved the types of filters. Previously, storm water is collected through a series of grated or recessed inlets placed in pavement or curb sections, and then conveyed by storm sewer piping to an outfall in an existing drainage way or stream. There is no treatment or attempt to remove sediment, trash or other pollutants. This arrangement quickly conveys storm water away from structures and property and avoids water or flood damage and protects life and limb. However, it also contributes to the pollution of surface and subsurface water supplies: oils, greases, solvents, sediments, trash, etc., are washed from impervious areas, such as streets and parking lots, as well as storage yards rooftops, etc., by the

storm water and are discharged with that water into streams, lakes and ground water recharge areas, contributing to the accumulative pollution of the water supply. Moreover, the sight of waste material, such as food and beverage containers, floating on streams and waterways is a visible reminder to the public of contamination and pollution of the water supply.

(George W. Murfae, 1992) made invention comprise inlet purification system consisting of filter basin, removable filtration basket inside the basin and auxiliary connections of traditional storm collector system, this invention purification system use for traditional storm water collection sewers. The basket fixed in the direction upstream of the traditional stormwater inlets would be placed in the inlet filtration system. Preferably, the filtration basket is constructed of metal and is suitable to arrive a forklift assembly of a traditional waste-disposal collection vehicle. The basket has a hinged metal lid arranged to swing open when the basket is inverted over the waste-disposal vehicle's waste holding cavity. The filter tub array and therefore, the expected weight/ volume of load controls the material requirements and basket strength.

(Thomas E. Hegemier, 1993) try to improve filter without moving parts placed on steel supports attached to the walls of the storm sewer inlet to filter debris, rubbish and sediments transported by stormwater runoff. The deposition of the above materials in the storm sewer pipes and the receiving waterways because storm water runoff flows unfiltered into storm sewer conveyance systems as shown in figure (2-2).

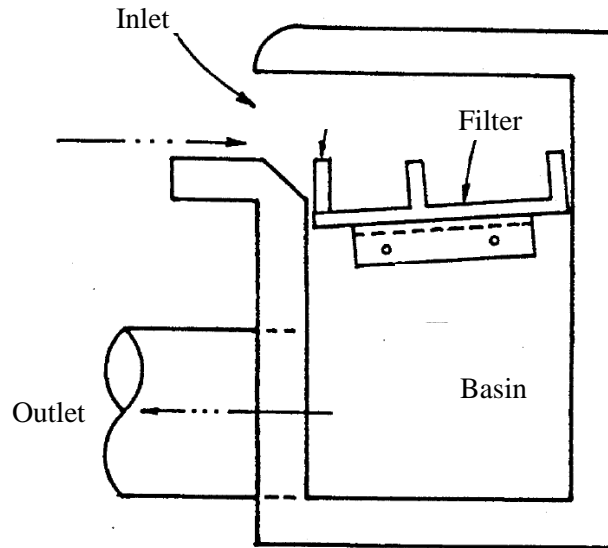


Figure (2-2) Thomas suggest stormwater inlet filter(Thomas E. Hegemier, 1993)

(Grant R. Emery, 1995) suggest filter made with the content of a square grid filter frame includes a rectangular panel at the bottom , a rectangular rear panel, a rectangular front panel, and two side panels as shown in figure (2-3). The major baffle divides the filter frame into the filter room that includes a filter particle medium, like gravel, and the flood room. The flood room is peripherally separated into a hydraulic opening and one or two end cap rooms by a mesh flood baffle panel. Two flood plates are used and the two end cap rooms are also loaded by the filter materials in order to be one enough filter to extend the narrow inlets, and attract sediment from the water escaping around the front panel and into the hydraulic opening through the side panels. The invention also looks forward to a wide range of filters, with a single-sided cap, tightly connected, side plate to side plate, across the full range of wider

entrances. In this way, the end cap rooms at the end of each station of the water inlet have a filter medium.

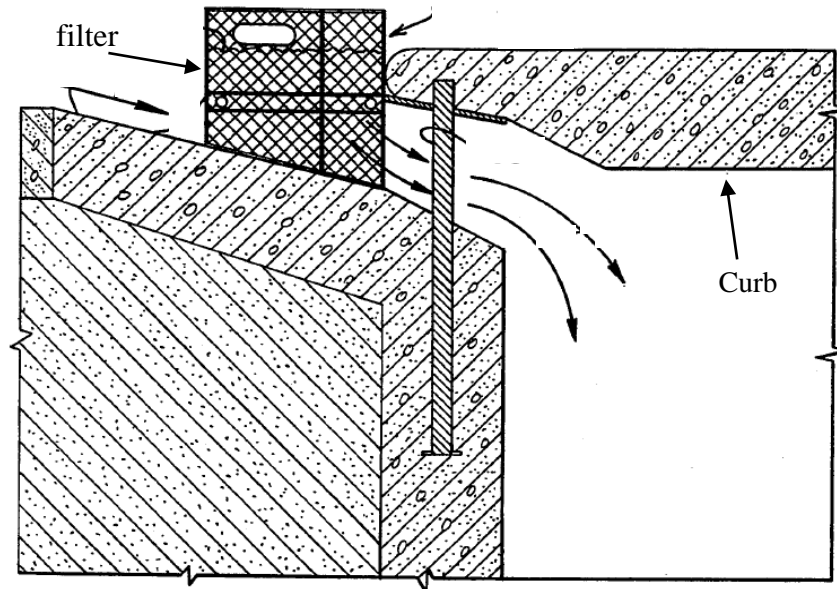


Figure (2-3) Curb inlet gravel sediment filter(Grant R. Emery, 1995)

The portable street or curb inlet sediment filter disclosed herein is characterized by the fact that it is self-contained for temporary erosion control, easily adapted to different inlet sizes, fits safely and securely adjacent to the curbside, and is designed for ease of installation and maintenance.

(Montagu *et al.*, 1997) in this study invention is designed to provide an easy path to install and keep an environmental filter system. The invention comprises an wrapper of a filter material that is proper for receiving an input device such as a storm sewer system. The invention may include a porous fabric that may be sewn, glued, welded, erected or otherwise formed in a container or envelope to accommodate an inlet device. In a separate embodiment, the presented invention may also include the wrapping of a mat

of corrosion. The roll can be used alone or with the filter material casing to prevent silt rocks. and Debris, etc. from entering the curb entrances.

(Larry and Bridgette, 2000) try to suggest an invention consists of one-piece molded device with the formation of an exposed network of spaced vertical ,as shown in figure(2-4). Additional contain horizontal part to allow liquids and small debris to go inside the storm sewer system while intercepting large-sized debris. The invention allows the release of accumulated debris collected for release into a storm sewer system, usually during heavy rainfall events.

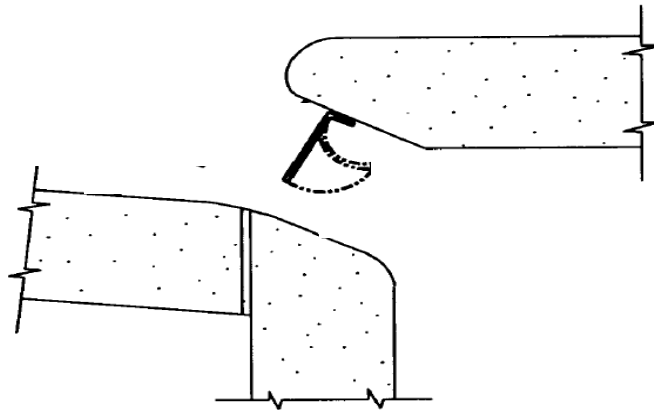


Figure (2-4) Curb inlet filter(Larry and Bridgette, 2000)

(Happel, 2004) the invention is a catch basin filter to filter storm water runoff. It is designed for curb inlet catch basins own a ramp along the curb front to permit rainfall into the catch basin and which also permit water to come in through a grate covering the catch basin. Stormwater drain filters are installed within a storm water catch basin at the entrance to the catch basin to filter the storm water runoff prior to it passing through a drain and out an outfall into a lake, pond, or retention area. The drain water loaded with waste

and grass clippings, sand and gravel and a lot of collected from streets, which are fed through a grated inlet into the storm water catch basin and then into a lake or detention pond or the like. The runoff water which is a lot loaded with grass clippings, trash, sand, tree limbs, gravel and other forms of sediment, which is collected from parking lots, streets, and other areas into a runoff inlet where it is directed into a network drain pipe system. The detention sump can tolerate a certain amount of grass scraps but cannot tolerate hydrocarbons from cars used in parking lots or on the streets.

(Earl, 2004) try to suggest an invention comprises a curb inlet filter that forms a temporary barrier or filter for filtering runoff water entering a curb inlet connected to a storm water drainage system. The curb inlet filter enables water to pass there through and into the curb inlet, while preventing a substantial portion of silt and debris flowing with the water from passing into the curb inlet. The curb inlet filter generally includes an elongated body having a first end and a second end to which first and second weighted anchors are attached, respectively. The elongated body further typically includes one or more support members encapsulated within a filter medium that assists in the filtering of water running to the curb inlet by blocking silt and debris, while allowing water to travel there during. Other support member arrangements are also contemplated, including those where at least a portion of the filter media provides support to the body. The filter medium generally includes geosynthetic materials, wire screens, meshes, polyesters, nylons, natural woven fibers and combinations thereof, or other appropriate filtration material. The filter medium typically is formed into a sleeve or cover that encloses one or more support members of the body.

(Charles R. Fleischmann, 2005) suggest a street curb drain filter is comprised of U-shaped brackets for attaching to an inside wall of a street curb drain adjacent an inlet, as shown in figure(2-5). A horizontal retaining bar is attached to the outer ends of the brackets. The lower edge of a horizontally elongated flexible net is attached to the retaining bar. The upper edge of the net is connected to the interior ceiling of the drain with eye bolts and S-hooks. A horizontally elongated debris basin is supported within the brackets. A filter media pack is positioned inside the basin adjacent a perforated outer wall of the basin. Water flowing from the street into the drain is directed through the filter. When runoff is relatively light, debris flowing into the drain is collected inside the basin. When runoff is relatively heavy or when the basin is clogged, debris bypassing the basin is filtered by the net

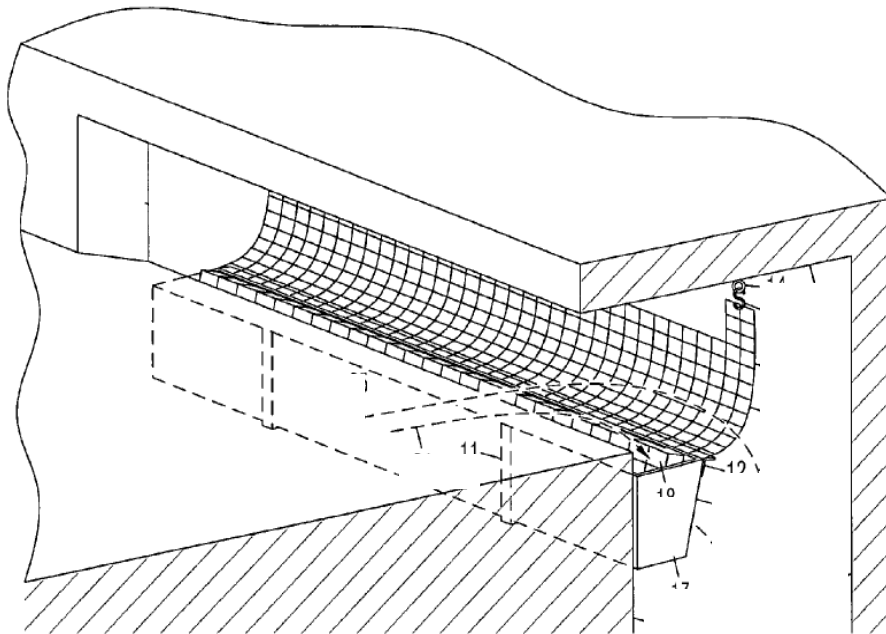


Figure (2-5) Street curb drain filter(Charles R. Fleischmann, 2005)



There are several other researchers studied the effect or stages of blockage that occurs in the filter among them (Hatt, et.al 2007; Siriwardene et.al, 2007; Nilmini et.al, 2007). (Siriwardene et.al,2007) studied one-dimensional rig was built from detachable perspex section (high 10 or 20cm, for each 20 cm in diameter). The 90cm high filter was built on top of 70cm of soil. The filter media was gravel with characteristics typically consistent with those recommended by storm water infiltration guidelines, as shown in figure(2-6). The median particle size ( $d_{50}$ ) of 10.5mm, ( $d_{10}$ ) of 6.4mm and  $d_{90} = 13$ mm. The soil layer was act by very fine sand with  $d_{90} = 300 \mu\text{m}$ ,  $d_{50} = 215 \mu\text{m}$  and  $d_{10} = 115 \mu\text{m}$ , and a hydraulic conductivity of  $2-8 \times 10^{-5} \text{ m/s}$  (in the above domain of natural soils in which these systems are typically built). The porosity of the soil and gravel filter were about 0.38 and 0.48, respectively. Semi-synthetic rainwater, containing sediments with typical characteristics of urban storm water, was prepared in a 500-liter tank. The sediments collected from the storm water inlet of the basin were passed through a  $300 \mu\text{m}$  sieve, then mixed with tap water. Total suspended solids (TSS) were aimed concentrations between 300 and 80 mg/L of , with particles having a  $25-60 \mu\text{m}$  of  $d_{50}$  . Air was injected constantly at the bed of the water tank to own sediment condensation uniformly mixed. Precipitation was added in the column just above the filter medium using rotary sprinklers.

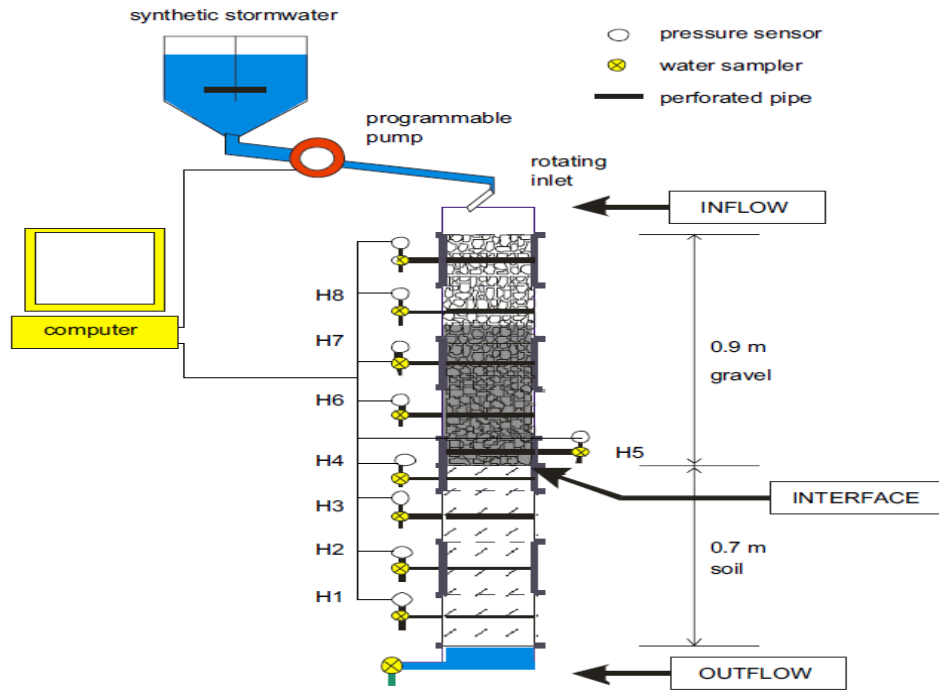


Figure (2-6) Clogging filter( Siriwardene et.al, 2007)

Flow from the water tank to the rig was the computer under controlled according to the required water level in the column, as shows results in table(2-1)

Table (2-1) Experimental details (Siriwardene et.al,2007)

Experiment	Media		Water level		Hydraulic loading (m/day)			Duration (days)	Remarks
	Top	Bottom	Regime	Level below surface (m)	Initial	Final	Final/initial (%)		
1	Gravel	Sandy Loam	Constant	0.45	0.87	0.06	7	15	Clogged
2	Gravel	Sand	Constant	0.45	4.1	1.4	35	36	Reached steady-state flow
3	Gravel	Sand	Constant	0.85	3.9	1.0	27	15	Pump failure
4	Gravel	Sand	Varied	0.05-0.85	2.6	0.12	5	13	Clogged
5	Gravel	Sand	Varied	0.05-0.85	3.1	3.0	96	7	Pressure sensor failure
6	Gravel	Sand	Varied	0.15-0.85	4.7	0.12	3	16	Clogged
7	Gravel	Sand	Constant	0.15	5.1	2.3	44	12	Power outage

## **2.5 Transmission of sediments**

One of the objectives of this study were to measure the transport capacity of interrill flow generated under simulated rainfall, and to isolate the contributions to transport capacity from raindrop impact and from surface runoff. Laboratory study was conducted to examine the transport capacity of interrill flow. Experiments were performed in flows with and without rainfall to isolate the contributions to transport capacity from surface runoff and raindrop impact. Theory and measurement indicated that the runoff contribution was determined by discharge and bed slope. The transport capacity was greatly enhanced by raindrop impact, and the enhancement depended on rainfall intensity and bed slope. Rainfall momentum and kinetic energy fluxes were also significant in explaining the transport enhancement. Inter rill transport capacity equations based on the separate runoff and raindrop impact contributions were developed. Simpler equations, with the two contributions lumped, were also investigated. Rainfall-disturbed flows were better able to transport the larger particles of the sediment mixture. However, observations of restricted flow competence suggested that the transport capacity of interrill flow is dependent on soil, as well as on hydraulic and rainfall properties(Guy, WT and Rudra, 1987) , as shown in figure(2-7). The effects of rainfall pattern on runoff and rainfall-induced erosion were quantitatively studied by simulating four rain storms, each with a different temporal rainfall pattern but all delivering the same total kinetic energy, and using two soil types. No consistent differences were observed in runoff across

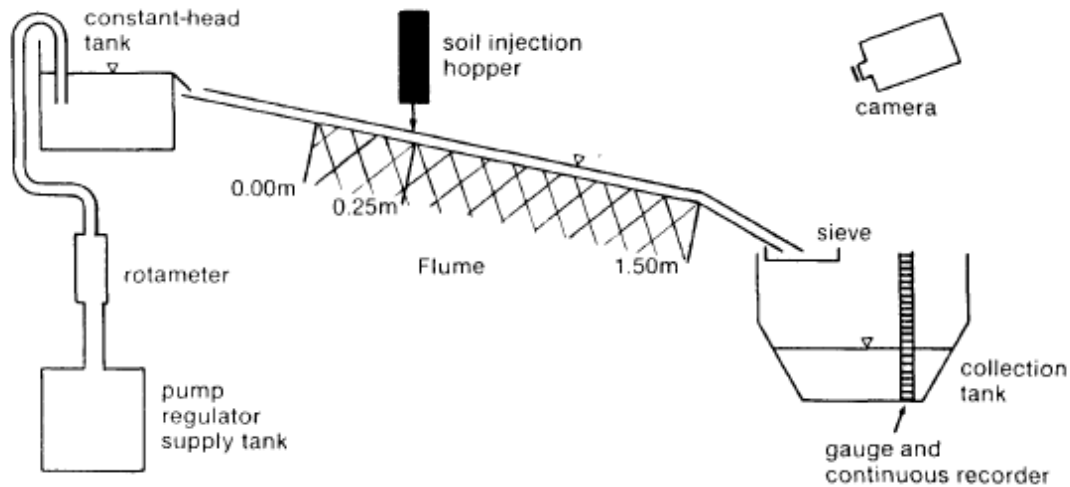


Figure (2-7) Schematic representation of experimental apparatus for transport capacity of soil (Guy and Rudra, 1987)

the two soil types, but soil losses from the same rainfall intensity were significantly affected by rainfall pattern and stages. In particular, the average soil loss from the varying-intensity rainfall patterns was almost equal to that from the constant-intensity pattern. Analysis of the interrill erosion rate equations indicated that models that derive interrill soil erosion directly from rainfall intensity can be expected to perform poorly in predicting soil erosion from varying-intensity rainfall patterns. Obvious differences were observed in the temporal variation of sediment concentration among rainfall patterns implying that the rainfall pattern controlled the sediment transport mechanism. In general, in rainfall-induced erosion at small scale, the dominant sediment transport mechanism depends on both rain drop

detachment and the resultant over land runoff. The findings of this study revealed that rainfall patterns significantly affect interrill erosion at small scales. The findings in this study should assist in better understanding of the effects of rainfall patterns on the interrill soil erosion process and provide new insight for developing process-based erosion prediction models (Alavinia, Saleh and Asadi, 2018)

## **2.6 Summary**

The literature shows that there are number of researchers they studied rainfall simulators and filter development, as shown

A. Rainfall simulation divided according to the areas and factors that affect in both of rainfall intensity and regular rain

1- For areas (up to about 10 meters per side), there are two standard options for rainfall simulators rows or nozzle arrays and sweeping sprinklers (D. Moore et al, 1983) represent one of the first simulations of nozzle type.

2-Standard small area or laboratory scale ( $1m^2$  or less) (Cerdà et al, 1997) studies  $0.24m^2$  rainfall simulator given  $55 mmh^{-1}$  with a spatial uniformity coefficient of 93 %; the rainfall intensity and distribution depends on the type and number of nozzles used.

B. (Charles R. Fleischmann, 2005) study the street curb discharge filter consists of U-shaped brackets to be installed on the inner wall of the street drainage adjacent to the entrance

C. Other researchers study soil corrosion process and provide a new look for improve process-based corrosion prediction models (Alavinia et.al, 2018).

D. The implementation of a new system thus generally improves the rain network, and the objective of this study is thus to enhance efficiency of storm networks by introducing and using a new filter. (Grant R. Emery, 1995) represent the nearest previous study to the current study, where the filter made with the content of a square grid filter.

*Chapter Three*  
***Theoretical Concept and Numerical Model***

***Chapter Three***  
***Theoretical Concept and Numerical Model***

**3.1 Introduction**

This chapter presents a general overview of the theoretical concept and the methodology of the numerical model for the present study by using the program Flow-3D

**3.2 Theory concept**

There are several ways to calculate rainfall discharge. The rational method is the simplest of the methods used for storm sewer design. It's one of the most popular runoff prediction methods used for the designs of urban drainage facilities in a small area. The rational hydrograph method was further tested for various hydrologic simulation scales including an experimental event at a laboratory scale. It used to calculating the peak flows from small drainages area less than 200 acres( James, 2001).

$$Q = C . I . A \dots\dots\dots(3-1)$$

where Q = max. runoff discharge(m<sup>3</sup>/s) ,C= runoff coefficient, A=area(m<sup>2</sup>) and I =intensity of rainfall(m/s). The average value of C , depending on the specific values chosen for the individual areas.

One of the most public used equations governing open channel flow is known as the Manning's equation. It was introduced by Manning in 1889 as an alternative to the Chezy equation. The Manning's equation is an empirical



## **Chapter Three      Theoretical Concept and Numerical Model**

equation that applies to uniform flow in open channels and is a function of the channel velocity, channel slope and flow area (equation 3-2).

$$Q = V.A = \left(\frac{1.49}{n}\right) \cdot A \cdot R^{\frac{2}{3}} \cdot S^{\frac{1}{2}} \dots\dots\dots(3-2)$$

Where:

Q = Flow rate, (m<sup>3</sup>/s)

V = Velocity, (m/s)

A = Flow area, (m<sup>2</sup>)

n = Manning's roughness coefficient

R = Hydraulic radius, (m)

S = Channel slope, (m/m)

The Manning's n is a coefficient which represents the roughness or friction applied to the flow by the channel. Manning's n-values are often selected from tables, but can be back calculated from field measurements. In many flow conditions the selection of a Manning's roughness coefficient can greatly affect computational results.

### **3.3 Numerical model approach**

The purpose of numerical simulation is that rather than of design and construction a physical model with using expansive appurtenance instrument like velocimeter. The fluid behavior can be obtained through Computational Fluid Dynamics (CFD) software such as FLOW-3D. This software is developed to deal with fluid behavior by solving partial differential equations based on the conservation of mass, conservation of energy etc.

## **Chapter Three      Theoretical Concept and Numerical Model**

FLOW-3D is a public-aim computational fluid dynamics program (CFD). It uses specially sophisticated digital techniques to solve motion equations of liquids for 3D transient solutions to multi-physics flow problems. A range of physical and numerical options allows users to apply FLOW-3D to a wide range of fluid flow and heat transfer phenomena (FLOW-3D manual,2014)

The logarithm of the numerical solutions studied in FLOW-3D follows the part of motion equations. The numerical model usually beginning with a mathematical grid or a mesh, consists of a number of interrelated cells or, elements. Physical space by divide these cells into small volumes with various nodes connected to each such volume. The nodes are used to store values of the unknowns, such as pressure, temperature and velocity. The mesh is in fact the numerical size that replaces the main physical size and provides a method for determining flow parameters at separate positions, setting boundary conditions and, certainly, for setting numerical parataxis to fluid motion equations. The FLOW-3D method is to divide the flow field into a grid of rectangular cells, sometimes called brick elements. (FLOW-3D manual,2014)

Arithmetic meshes effectively estimate the physical area. Each fluid parameter in a grid is explain by a set of values at separate points. If the mesh between nodes is a small spacing will gives a better impersonation to the reality than a large one, because the truth physical parameters change continuously in space. Then reach at a basic property of numeric parataxis any valid numerical parataxis approaches the main equations where the grid spacing is reduced. It should be considered incorrect if rounding does not meet this requirement. Reducing purifying the grid, or the grid spacing, for the

## **Chapter Three      Theoretical Concept and Numerical Model**

similar physical space leads to more nodes and elements, thus increasing the size of the numerical model(FLOW-3D manual,2014).

This software uses the Volume of Fluid (VOF) method to follow the free surface. Flow 3D makes it easy to produce detailed velocity profiles and rating curves for a complex model, counting the impact of shape, flow depth, contraction ratio and discharge. Flow 3D is usually used to verify the hydraulic performance of bridge pier designs and to assist professionals rally pier safety requirements(Hirt and Nicolos, 1981).

### **3.4 Turbulence Model**

The governing equations incompressible, viscous fluids are continuity and momentum equations. These equations are known as Navier- Stokes equations. These equations express conservation of mass and momentum mathematically. Yakhot and Orszag, 1986 derived an improved  $k-\varepsilon$  turbulence model named RNG (renormalization group)  $k - \varepsilon$  model, in which the coefficients are obtained from theoretical analysis, not from experimental data. The RNG  $k - \varepsilon$  model has the ability to adapt than standard  $k - \varepsilon$  model. In this study uses RNG  $k - \varepsilon$  model to simulate the gravel filter, combines with the standard wall function method to deal with the near wall. The governing equations are as follows (FLOW-3D manual, 2014)

$$\frac{\partial \rho}{\partial t} + \frac{\partial u_i}{\partial x_i} = 0 \quad (3 - 3)$$

## Chapter Three      Theoretical Concept and Numerical Model

$$\frac{\partial \rho u_i}{\partial t} + \frac{\partial (\rho u_i \varepsilon)}{\partial x_i} = -\frac{\partial P}{\partial x_i} + \frac{\partial}{\partial x_i} \left( (\mu + \mu_i) \left( \frac{\partial u_i}{\partial x_j} + \frac{\partial u_j}{\partial x_i} \right) \right) + \rho G_i \quad (3-4)$$

$$\frac{\partial \rho u_i}{\partial t} + \frac{\partial (\rho u_i k)}{\partial x_i} = \frac{\partial}{\partial x_i} \left( \left( \mu + \frac{\mu_i}{\sigma_k} \right) \frac{\partial k}{\partial x_i} \right) + G + \rho \varepsilon \quad (3-5)$$

$$\frac{\partial (\rho \varepsilon)}{\partial t} + \frac{\partial (\rho u_i \varepsilon)}{\partial x_i} = \frac{\partial}{\partial x_i} \left( \left( \mu + \frac{\mu_t}{\sigma_\varepsilon} \right) \frac{\partial \varepsilon}{\partial x_i} \right) + C_{1\varepsilon} \frac{\varepsilon}{k} G - C_{2\varepsilon} \rho \frac{\varepsilon^2}{k} \quad (3-6)$$

In which: t=time,  $u_i$  = velocity component;  $\rho$ = density,  $\mu$ =molecular viscosity;

$$\bar{P} = P + \frac{2\rho k}{3}$$

The generation of turbulent kinetic energy (G) due to mean velocity gradients can be defined as:

$$G = \mu_i \left( \frac{\partial u_i}{\partial x_j} + \frac{\partial u_j}{\partial x_i} \right) \frac{\partial u_i}{\partial x_j} \quad (3-7)$$

Where:  $\bar{P}$  is modified pressure and P is the pressure. The parameter  $\mu_i$ =turbulence viscosity, which can be calculated by turbulence kinetic energy (k) and turbulent dissipation rate ( $\varepsilon$ ) as:

$$\mu_i = \rho C_\mu \frac{k^2}{\varepsilon} \quad (3-8)$$

Where:  $C_\mu$ ,  $C_{1\varepsilon}$ ,  $C_{2\varepsilon}$ ,  $\sigma_k$ , and  $\sigma_\varepsilon$  are all dimensionless user-adjustable parameters, and have a values of 0.085, 1.42, 1.39, 0.7179 and 0.7179, respectively (FLOW-3D manual,2014).

### **3.5 Model setup**

The process of building any model passes through steps fixed well defined. The start with the physical characteristics of all the details of the model, then defining the characteristics of fluids used, finally building the model with meshing.

#### **3.5.1 Physical items**

There are many available optional physics in FLOW-3D, but in this study, only four selections are necessary to activate in order to obtain the accurate simulations of the data desired in this study. The first option of the gravity is activated with gravitational acceleration in the vertical direction being set to negative  $9.81 \text{ m/sec}^2$ .

Second option is porous media the soils, fractured rock, sponges, and paper are all examples of porous media. Porous media refers to solid materials with connected interstitial voids through which fluid can flow. On a microscopic scale the velocities and pressures in the void spaces are highly irregular but from a macroscopic viewpoint, a volume averaged approach represents the flow quite well. The advantage of activating this physical characteristic is to represent the filter where it is dependent on the porosity as well as the permeability of the filter representation.

The third option is sediment scour model that approximates the effects of the flow on the erosion of surfaces and the transport of sediment. The sediment scour model assumes multiple non-cohesive sediment species with different properties including grain size, mass density, critical shear stress,

## **Chapter Three      Theoretical Concept and Numerical Model**

angle of repose and parameters for entrainment and transport. For example, medium sand, coarse sand and fine gravel can be categorized into three different species in a simulation. The advantage of activating this physical characteristic is to represent the sand on the street, which will move and enter into the manhole and filter.

The fourth option is viscosity and turbulence where the viscosity describes the internal friction of a moving fluid. A fluid with large viscosity resists motion because its molecular makeup gives it a lot of internal friction. A fluid with low viscosity flows easily because its molecular makeup results in very little friction when it is in motion as well as the determination of the type of flow it is linear or turbulent where the turbulent flow has several ruler equations used linear flow in the model .

### **3.5.2 Model geometry**

Geometry is structure in FLOW-3D by collecting solid geometric objects to define the flow region for a simulation. The geometry in a simulation can be defined by using one or more components; with each component is composed of one or more subcomponents that are added and subtracted in a sequence to define a complex shape. The construction of the model consists of several segments which represents the street and had the characteristics that represent the solid body as shown in figure (3-1). Made open to represent gully without filter, and the other side is made a porous object to represent gully with filter as each part is used to define all its characteristics.

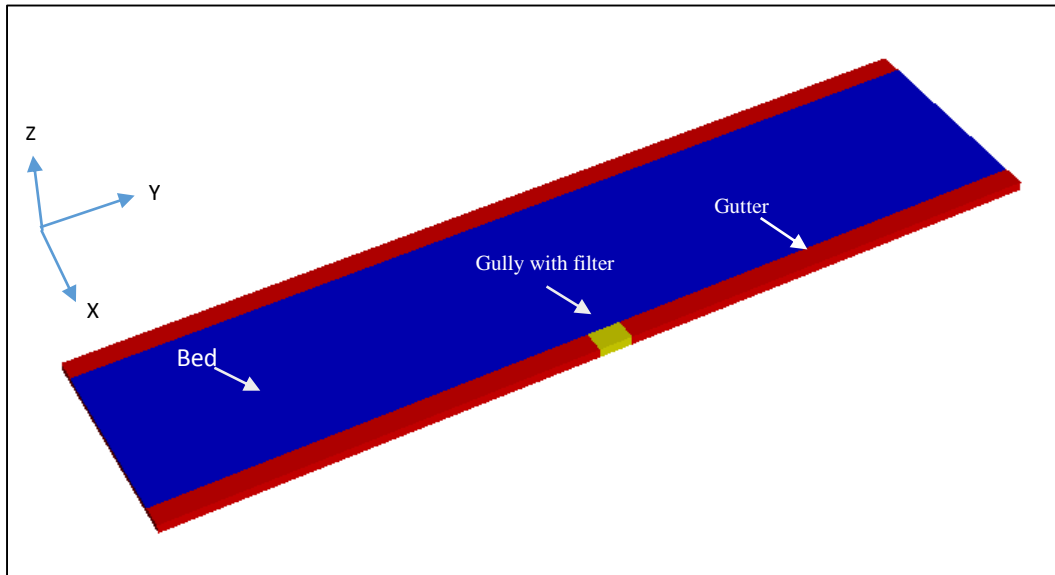


Figure (3-1) Numerical model geometry representation of Flow-3D

### **3.5.3 Meshing**

The grid builds up in Flow-3D is a very important issue for a precise solution. Must be building up a good quality of mesh brought to get actual results from the numerical model. The decisive component of any numerical model simulation is selecting the suitable grid domain along with an appropriate mesh cell size. Cell size and grid can effect both the simulation time and the truth of the results, therefore; it is important to reduce the cells size while calculating the sufficient resolution to take the significant features of the geometry in addition to the important flow detail. The beginning was with a comparatively large mesh of cells thereafter gradually decreases the mesh size is an effective approach to find the critical cell size until the output data no longer changes notably with any furthermore reductions. Specifying excessive cells will increase the calculation progress. Since computations are obtain for all cells, the increasing quantity of cells will increase the time of

## **Chapter Three      Theoretical Concept and Numerical Model**

computation. Thus, the best amount of cells ought to be assigned as shown in figure(3-2). In Flow-3D the count of cells in mesh is the very significant and have direct impact on the accurate solution. These impacts are represented in simulation time and accuracy of the results . Uses small mesh are lead to give good accuracy and longer simulation time. Firstly, the computer may not able to deal with the large amount of data because of the insufficient memory and secondly, there may be a large increase in the time of computation. Anyway, any increase in the ratio of grid size (cell aspect ratios) between two neighboring cells adversely has an impact on the accuracy (Kaatz and James ,2002).

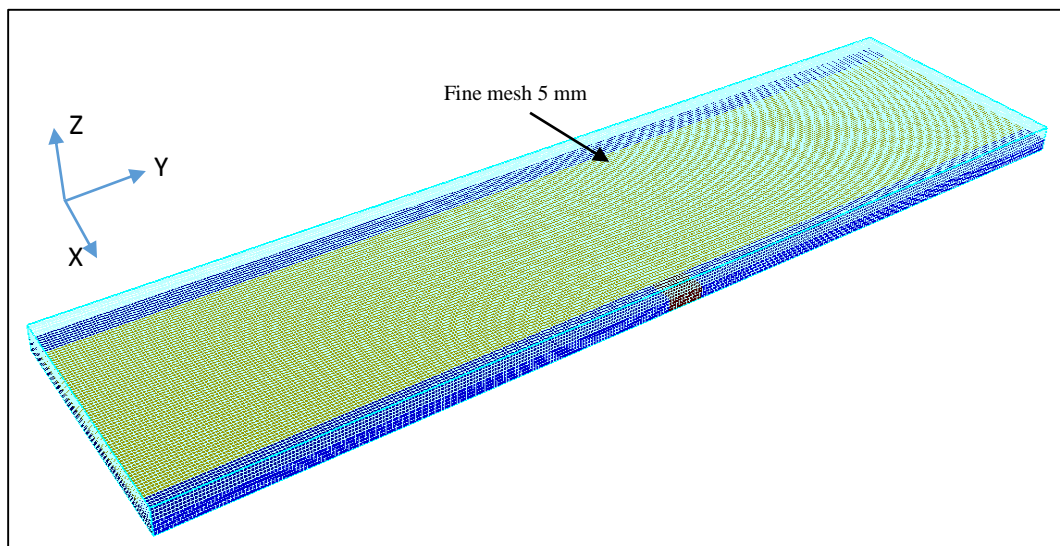


Figure (3-2) Meshing of numerical model (Flow-3d)

FLOW-3D mesh generator uses the Fractional Area Volume Obstacle Representation (FAVOR). This option can be used to determine the optimum amount of cells. Since the cells are orthogonal, it must achieve the best size of cells to generate a system to be nearly the same with the real case.



## **Chapter Three      Theoretical Concept and Numerical Model**

Geometry problems, will occur if cell sizes are not optimum, as shown in figure (3-3). FAVOR option help users to avoid those, problems by obtaining the accurate geometric shapes(FLOW-3D manual,2014)

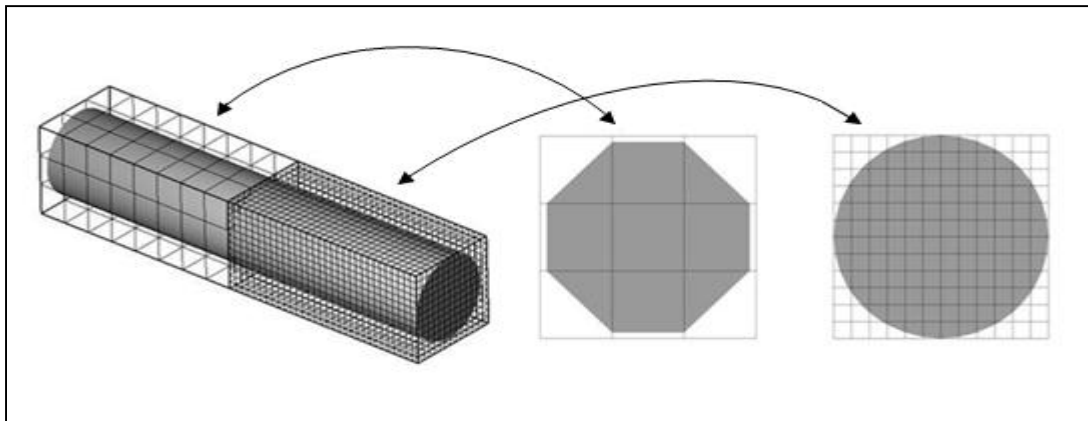


Figure (3-3) FAVOR option with different cell size (FLOW-3D manual,2014)

### **3.5.4 Boundary and Initial Conditions**

Finding of the suitable boundary conditions is very significant phases in the numerical flow analysis. The boundary conditions should correspond with the physical conditions of the problem correctly. Three dimensional flow domain is defined by FLOW3D through using the orthogonal hexahedral meshes in the Cartesian coordinates. Therefore, there are six various boundaries, which are defined on rectangular mesh prism. The boundary conditions have to be carefully defined, as shown in figures (3-4). Upstream boundary (X-min):- velocity condition (v). Downstream boundary (X-max):- an outflow condition (O).Top boundary(Z-max):- symmetry condition (P).

## Chapter Three      Theoretical Concept and Numerical Model

Bottom boundary(Z-min):- an outflow condition (O). Side boundary(Y-min, Y-max):-wall condition (W).

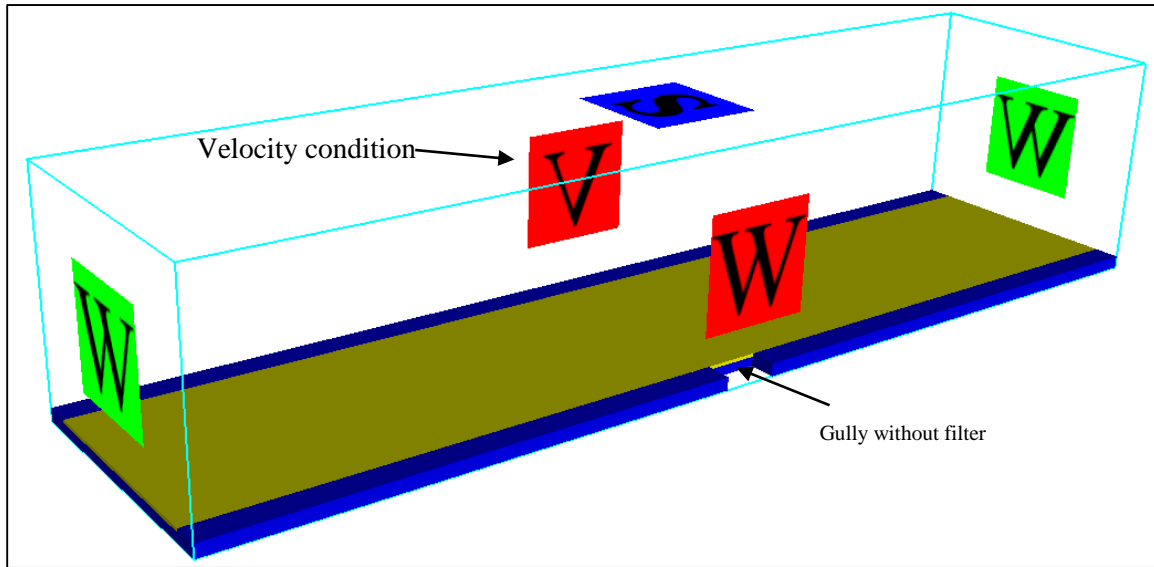


Figure (3-4) Boundary conditions used in this study

The starting conditions in the simulation is defined initial conditions. The initial state of solving transit fluid flow problems should be known in order to discovery a solution, and in a manner similar to that with border conditions. The initial conditions are assumed, and the real state is rounded to the time equal zero. The accuracy of the boundary conditions is more significant than that of the initial conditions because the impact is reduced with time advance(FLOW-3D manual,2014). Because of this effect, it is common to determine the initial geometry of a liquid with rational accuracy but suppose the speed fields and pressure are uniforms. This usually makes better results with a comparatively short period of time where the solution is affected by the initial physical conditions (FLOW-3D manual,2014).

### **3.6 Material Properties**

There are several inputs for the fluid that properties should be defined in numerical model such as viscosity, temperature and density. The fluid is chosen by using fluid database tab and the properties of fluid were specified on the Fluids, tab. In FLOW-3D software, there are a library of familiar, materials to help the user. Each component is defined as solid property by using Geometry and Meshing, tab. Water in 20 °C was adopted in this study.

### **3.7 Solving Options**

Many parameters are affecting, at the time and simulation results. time step size, method of Solution, (explicit or implicit), numerical approximations and convergence settings, are some of the results. The balancing of the accuracy of simulation and run time is a very important point. Selecting the suitable numerical options is very significant to provide efficient and best possible solution of a simulation. In the Numeric's tab the numerical options are specified. There are various options in FLOW-3D to follow fluid interfaces. VOF option chose automatics as advection model to follow fluid interface. It was found that the automatic option is the most efficient and accurate model in FLOW-3D in case of a sharp interface with one fluid free surface flows.

### **3.8 Steps of works in Flow-3D software**

Steps of model work

To create a new simulation follow these steps:-

## **Chapter Three      Theoretical Concept and Numerical Model**

- 1) Go to simulation manager
- 2) Right click on the portfolio part then:-

Select (Add new simulation)

To create a new simulation follow these steps see appendix (A)

### **3.9 Statistical Analysis Model**

Statistical analysis was used to improve a model that links independent variables and dependent variables. The purpose of this part of this study is to explain the appropriate learning of how the parameters affect the dependent variable. In this study, it was decided to use the latest version of statistical products and services solutions (IBM, SPSS) software (Version 20).

#### **3.9.1 The definition around goodness of fit and statistical**

To better realize the representation of any model, one need to realize some model parameters.

Coefficient of Determination ( $R^2$ ): is the square of the relationship between the calculated value and observed of the dependent variable  $0 \leq R^2 \leq 1$ . It is a method of modeling the connection between one or more independent variables and a numerical variable. Simple linear regression is known as the condition of one explanatory variable also, multiple linear regressions the process is known for more than one explanatory variable. The large value of  $R^2$  proposition that the model has been succeeded in illustrate the variability in the response (Holicky, 2013)

The remaining (e) describes the error in the model of the observation. Next, will use the remaining material to supply information about the

## Chapter Three      Theoretical Concept and Numerical Model

sufficiency of the intended model. SPSS can prove the terms of fit goodness of statistical model as: “Root Mean Square Error (RMSE), Mean Absolute Error (MAE), and Mean Absolute Percentage Error (MAPE)”. These are calculated to compare the representation of estimation models. It is significant to assess the accurate of prediction using real projections, and the following terms used for this aim (Hyndman, 2010)

**Root Mean Square Error (RMSE):** is a frequently used measure of the differences between values (sample and population values) predicted by a model or an estimator and the values actually observed and which are on the same scale.

$$RMSE = \sqrt{\frac{\sum_{i=1}^n (y_i - y_i^{\wedge})^2}{n}} \dots\dots\dots(3-9)$$

Where:

$y_i$  : Observation value,  $y_i^{\wedge}$  : Predicted value, n: Number of samples, 1,2,..etc

**Mean Absolute Error (MAE):** is a quantity used to measure the proximity of predictions to final results. The absolute mean error is the same measure of the data being measured. This is known as a precision scale that depends on the scale and therefore cannot be used to make comparisons between series at different levels. It can be used for all forecasts on the same scale. The mathematically challenged usually find this an easier statistic to realize than the RMSE.

$$MAE = \frac{\sum_{i=1}^n |y_i - y_i^{\wedge}|}{n} \dots\dots\dots(3-10)$$

## Chapter Three      Theoretical Concept and Numerical Model

**Mean Absolute Percentage Error (MAPE):** is a measure of accuracy prediction of a forecasting method in statistics, for example in trend estimation". Accuracy is usually expressed as a percentage. Percentage error measures have the disadvantage of being inaccurate or indeterminate if the expected value is zero or close to zero for any observation in the test set. However, if  $y_i$  is close to zero,  $y_i^\wedge$  is also likely to be close to zero

$$MAPE = \frac{1}{n} * \frac{\sum_{T=1}^P |y_i - y_i^\wedge|}{y_i} \dots\dots\dots(3-11)$$

The model is good when MAPE is far from zero (De Myttenaere et al., 2016). Both the MAE and the RMSE they work regularly in typical assessment studies (Chai and, 2014). A small RMSE value means that the error is characterized by a low dispersal (Capozzoli , 2015). It can be guaranteed by the good width of the minimized model MSE (Douglas, 2011).

### **3.10 Dimensional Analysis**

Dimensional analysis is a mathematical tool that shapes the general form of relations that describe natural phenomena. Variables are divided into dependent variables and independent variables (Butterfield, 1999). Choice of repeating variables should be made within the concept's internal variables, and according to the unique number of the system's governing dimensions for best results(Christophea, 2008)

The parameters are classified in terms of mass (M), length (L) and time (T). The variable can be categorized as follows

## Chapter Three      Theoretical Concept and Numerical Model

1. Variables characterizing the fluid; density of water ( $\rho$ ) and viscosity ( $\mu$ )
2. Variables characterizing the flow; intensity (I), duration of intensity (T) acceleration of gravity (g) and bed slope ( $S_0$ ).
3. Variables characterizing filter; length of filter ( $L_f$ ), diameter of sediments ( $D_s$ ) and mass of sediments ( $M_s$ ).
4. Variables characterizing mass of resulting; mass sediments pass through gully with filter( $M_f$ ), and mass sediments pass through gully without filter( $M_g$ ).

Function of all previous variables which can be written in the following formulas:

$$f(M_g, M_f, M_s, I, T, g, D_s, S_0, L_f, \rho, \mu) = 0 \dots\dots\dots(3-12)$$

Since there are eleven variables ( $n = 11$ ) excluding three principal units ( $m = 3$  repeated variable). According to the  $\pi$ - theorem the number of dimensionless parameter is eight, i.e.,  $(n-m) = (11-3) = 8$ . Each term has to contain  $(m+1) = (3+1) = 4$  variables, take repeating variables ( I ,  $M_g$  ,  $L_f$ ) content all fundamental quantities; it can be written the equation from Buckingham -theorem:  $\pi$

$$f(\pi_1, \pi_2, \pi_3, \pi_4, \pi_5, \pi_6, \pi_7, \pi_8) = 0 \dots\dots\dots(3-13)$$

$$\pi_1 = I^{a1} * M_g^{b1} * L_f^{c1} * M_f \dots\dots\dots(3-14)$$

$$\pi_2 = I^{a2} * M_g^{b2} * L_f^{c2} * S_0 \dots\dots\dots(3-15)$$

$$\pi_3 = I^{a3} * M_g^{b3} * L_f^{c3} * T \dots\dots\dots(3-16)$$

## Chapter Three      Theoretical Concept and Numerical Model

$$\pi_4 = I^{a4} * M_g^{b4} * L_f^{c4} * \rho \quad \dots\dots\dots(3-17)$$

$$\pi_5 = I^{a5} * M_g^{b5} * L_f^{c5} * D_s \quad \dots\dots\dots(3-18)$$

$$\pi_6 = I^{a6} * M_g^{b6} * L_f^{c6} * g \quad \dots\dots\dots(3-19)$$

$$\pi_7 = I^{a7} * M_g^{b7} * L_f^{c7} * M_s \quad \dots\dots\dots(3-20)$$

$$\pi_7 = I^{a8} * M_g^{b8} * L_f^{c8} * \mu \quad \dots\dots\dots(3-21)$$

Taking each term and evaluating:

$$\pi_1 = I^{a1} * M_g^{b1} * L_f^{c1} * M_f$$

Expression these in dimension terms we have :

$$M^0 L^0 T^0 = (LT^{-1})^{a1} (M)^{b1} (L)^{c1} M^1$$

For M:       $b1 + 1 = 0 \quad \Leftrightarrow \quad b1 = -1$

For L:       $a1 = c1 = 0$

$$\pi_1 = \frac{M_f}{M_g}$$

By the same way:

$$\pi_2 = S_0 \quad , \quad \pi_3 = \frac{I * T}{L_f} \quad , \quad \pi_4 = \frac{\rho * L_f^3}{M_g}$$

$$\pi_5 = \frac{D_s}{L_f} \quad , \quad \pi_6 = \frac{L_f * g}{I^2} \quad , \quad \pi_7 = \frac{M_s}{M_g} \quad , \quad \pi_8 = \frac{L_f * \mu}{M_g * I}$$



## Chapter Three      Theoretical Concept and Numerical Model

$$f \left( S_0, \frac{I * T}{L_f}, \frac{D_s}{L_f}, \frac{\rho * L_f^3}{M_g}, \frac{M_f}{M_g}, \frac{L_f * g}{I^2}, \frac{M_s}{M_g}, \frac{L_f * \mu}{M_g * I} \right) = 0$$

$$\frac{M_f}{M_g} = \left( S_0, \frac{I * T}{L_f}, \frac{D_s}{L_f}, \frac{\rho * L_f^3}{M_g}, \frac{L_f * g}{I^2}, \frac{M_s}{M_g}, \frac{L_f * \mu}{M_g * I} \right) \dots\dots\dots (3-22)$$

There are several variables of constant magnitude such as acceleration of gravity (g), density of water ( $\rho$ ) and mass of sediments ( $M_s$ ) so it will be dropped.

So the final relationship

$$\frac{M_f}{M_g} = \left( S_0, \frac{I * T}{L_f}, \frac{D_s}{L_f} \right) \dots\dots\dots (3-23)$$

*Chapter Four*  
*Experimental Work*

## ***Chapter Four***

### ***Experimental Work***

#### **4.1 Introduction**

This chapter presents a general overview of the experimental work and the methodology of building model. The model is create at the University of Kerbala, College of Engineering.

#### **4.2 Laboratory model**

The laboratory model consists of several parts connected to each other, and it is a complete system. This system includes a structure that carries all the details of the model, and the rain system in terms of pipes, as well as the land of the street, which in turn contains filters and drainage outlets. This model is a representation of the phenomenon of rain and the transfer of sediments from the street to the outlets of the drainage to enter the system of rain. The laboratory model scale is 1:4 from prototype. All details will be explained in the following sections.

#### **4.3 Materials and Equipments**

##### **4.3.1 Steel frame**

The first part is the steel frame that carries the rain pipe network, as well as carries the street represented by the sandwich, also the gravel filter and all the details of the model. Each iron part of the frame has thickness of 1.5 mm.. The overall dimensions of the structure are (4.1\*2.2\*2)m.

##### **4.3.2 Rain system**

In the second chapter, the researchers explained that there are two types of area in rainfall simulator either less than one square meter or above of one

square meters, so in this study the model used second type. The study relied on the representation of the rain system in a research done by researchers in Italy (Wilson et al., 2014). The rain system consists of two plastic pipes, each pipe has a diameter of 0.5 inches and a length of 4.1 m. Figure(4-1) show the installation process. Each pipe is installed on the upper side of the structural frame, they face each other at a distance of 2.2 m. Each pipe has 12 nozzles with the spacing of 33 cm between them. Directions of nozzle openings were applied by making an angle between the top of nozzle and the horizontal axis ( $48^{\circ}$ - $54^{\circ}$ ) alternate angles of horizontal. The droplets then drop from a height of about 3m. The system also contains valves to control the intensity of rain. Moreover, the water is supplied to the system by a water tank of 500 liters capacity.

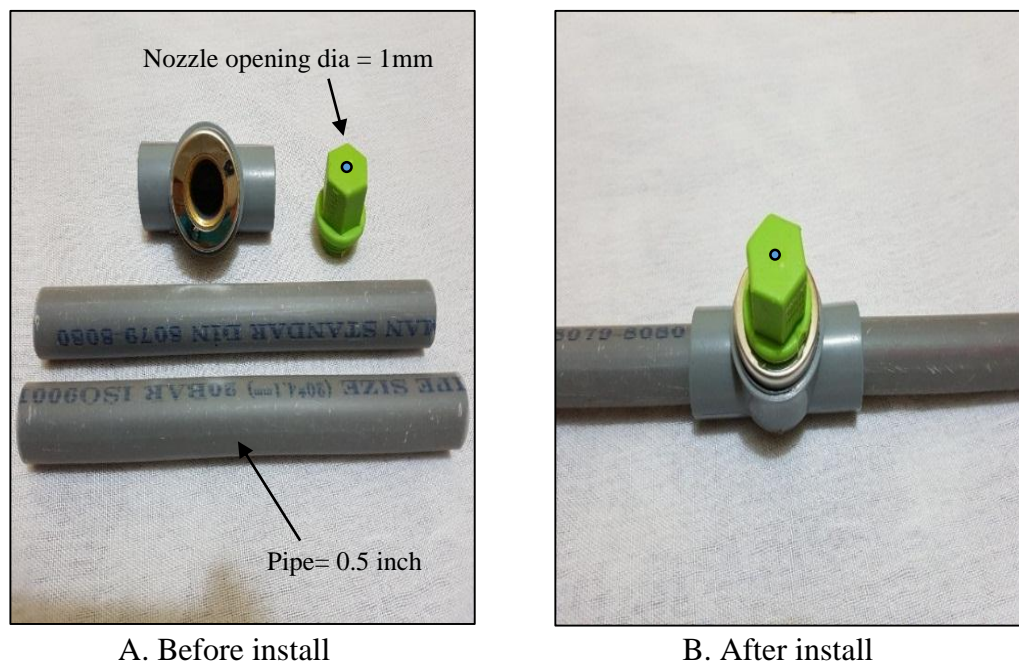
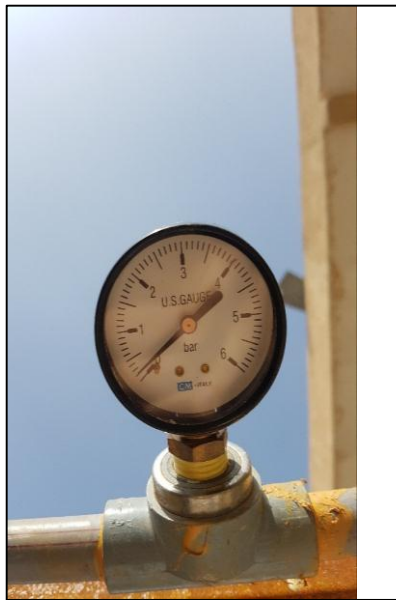


Figure (4-1) Installation process of rain system nozzle

This is positioned at the end of the system and the end of the pipes gauge to measure the pressure of water. The benefit from gauge is to know the pressure of each intensity of the rain, and to make work easy during the change of the intensity ,and the gauge used is (CM-ITALY) as shown in figure (4-2A). The units of measurement of gauge is bar units, and the maximum pressure that the bear gauge is 6 bar, also gauge contains grades less than the bar for easy to read.

ANGCO water pump was used with of 1 HP which has many uses for this pump. It is ideal for lifting water from one point to another in horizontal and vertical mode. The pumping distance is 40 meters and the flow is 50 liters/min, and the figure (4-2B) shows the shape of the water pump.



A. Gauge pressure



B. pump

Figure (4-2) Gauge pressure and pump

The height of pipes on the ground is 2m either the droplets were then dropped from a height of about 3 m. During the operation of rain ,and connect these nozzle at angle ( $48^{\circ}$ - $54^{\circ}$ ) as mentioned earlier in order to obtain more distribution of water drops. In the figure (4-3) the distribution and angle of nozzles are shown

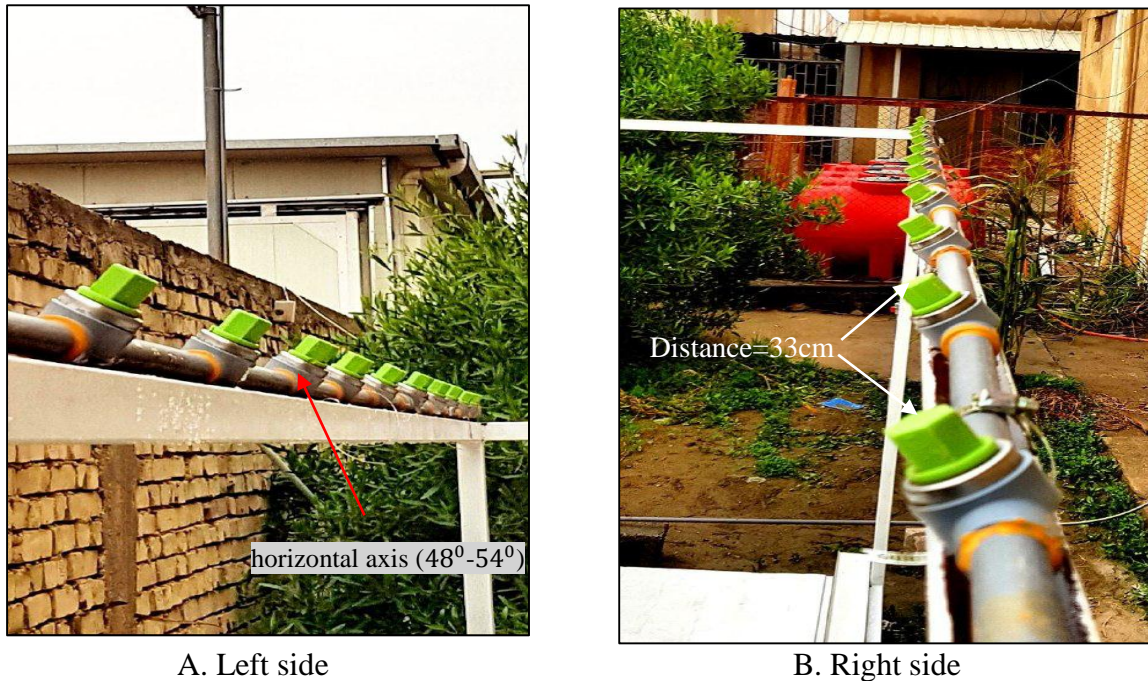


Figure (4-3) Rain water distribution and angle of nozzles of the model

### 4.3.3 Rain collection floor

The rain collection floor consists of several details, including the sandwich available for movement to control the slope representing bed slope, also the curb on the both sides. This rain collection contains the most important segment that will be study is the gully with filter and gully without filter. All rain collection floor and details will be lifted from ground to easily control, and all details will explain as follows section.

### 4.3.3.1 Floor slopping

The sandwich panel is used to represent the surface model because the material is light and easy to move with smooth surfaces. The dimensions of the sandwich were (4\*1)m two pieces were used and put them side to side where the width of the street 2m. Two pieces of the gutter dimensions (4\*0.1)m were used on side of the sandwiches; therefore, The street width with the gutter and sandwiches become (2.2)m, as shown in figure (4-4)



Figure (4-4) Floor slopping

### 4.3.3.2 Gully without filter

The natural street contains two sides, in which each side a gully to drain the rain water. This model will contain one gully without filter in first sides

The natural street contains two sides, in which a gully to drain the rain water. This model will contain one gully without filter in first sides of the street, and the other side will have gully with filter, to compared between the filter and manhole, and how to performance of the filter gravel. The gully without filter were placed in the center of the street, where the dimensions of the manhole is (10\*12) cm as shown in figure (4-5)

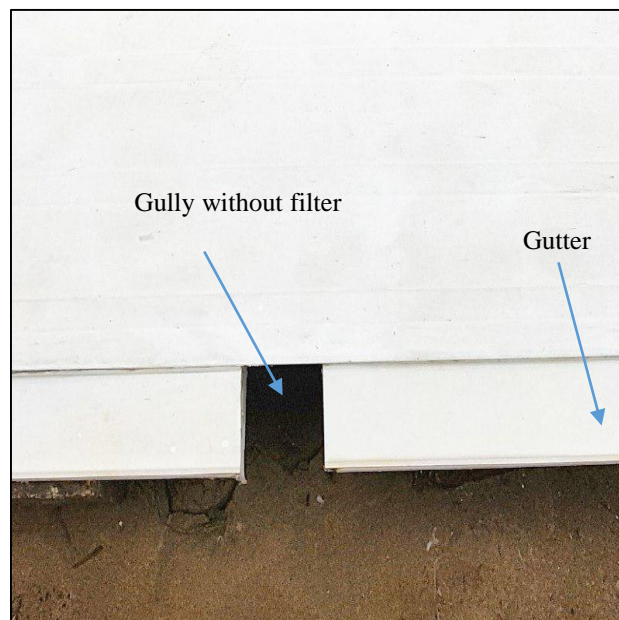


Figure (4-5) Top view of gully without filter

#### 4.3.3.3 Gully with filter

The gravel filter in this study is located on the side of the street and its dimensions are 10 cm width and 5 cm depth, but the length was variable according to the experiments that will be study. The filter width was chosen is 10 cm in order to be equal to the width of the gutter in most streets also the gutter angle was 0.5. The gravel diameter was(1.25-2.5)mm. The effective size of filter particles was 1.5mm, while the uniformity coefficient of filter 1.2.



It is important to mention that, the gravel process where the gravel was placed in the container of filter without a compact. Filter contains a mixture of gravel types, including circular and angular as shown in figure (4-6)



Figure (4-6) Gully with filter

#### **4.3.3.4 Lifting devices and sieves**

There are some tools used in the practical side, and have a great impact that will be explained. One of these tools is the use of lifting device which was placed in the middle of the street ,where the end of each sandwich is on the lifting device, and lifting or lowering this device will control the slope of the street. Two lifting devices were used in model, the lifting device used was an Emirati-made machine, as shown in figure (4-7)



A. Raising

B. Lowering

Figure (4-7) Lifting devices

One of the important things that have been considered is calculating the amount of sediments that will pass through the gully with filter and gully without filter, and how will be controlled by the use of meshes placed at the end or bottom of both gully with filter and gully without filter. The mesh used is No. 200 ,in which its open in this sieve is 0.075mm, and the sediments used in the study the open in the sieve should be of a larger diameter to prevent pass sediments through the sieve as shown in figure (4-8). During the study and the trail this method has given results. Calculating weights of sediments remaining on the sieve is to find the difference between the weight of the sieve with sediments and without sediments.



A. Gully without filter

B. Gully with filter

Figure (4-8) Both gully details at top view

After the completion of the process of building the model, as shown in figures (4-9,4-10) the laboratory experiments started. There are a set of variables that are studied by a dimensional analysis. There are steps to be taken in each experiment. In the beginning, the slope of the ground is fixed in each experiment by using lifting device, the intensity of the rain is also fixed through the valve; the length of filter is fixed as well. A quantity of sediments is distributed regularly on the model ground, after that, the rainfall is done during a fixed period of time, then of the end of the process, the weight of the passing sediments is measured in both the manhole and the filter by using sieves 200.

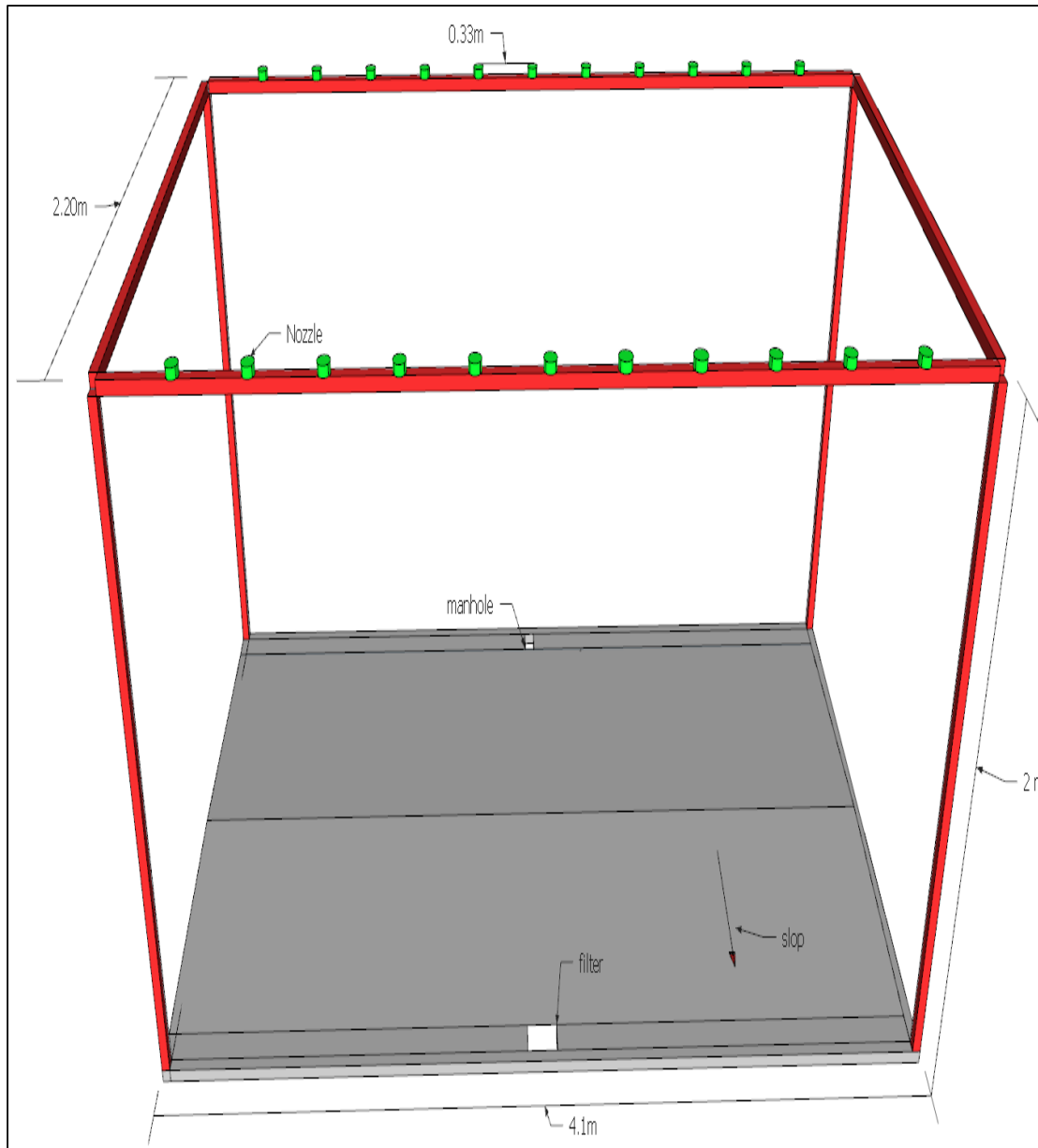


Figure (4-9) Sketch of the frame, nozzle for experimental work



Figure (4-10) Shape of the frame, nozzle for experimental work

#### 4.4 Laboratory tests

There are several laboratory tests in both practical and the theoretical sides, which are related to the rain system of the intensity of rainfall and its integration; the gravel filter and permeability tests and porosity of the filter are also available.

#### 4.4.1 Uniformity and intensity rainfall

There are several tests to assess the level of simulations of rain. These tests are checking the uniformity of rain and checking the intensity of rain as this test assesses the level of the distribution of rain . This test was discovered by Christiansen, as mentioned in(Aksoy *et al.*, 2012). This test depends on statistical equivalence. The inspection consists of a collection of container with fixed diameter, and equal distances in the form of a mathematical matrix, where the distance between the center of the container and the other is 50 cm. Also there are three lines of container each line contains 8 containers this makes the number of containers 24 as shown in figure(4-11). After the completion of the distribution process, the rain is run during a period of time, and the height of the water is calculated in each container and the application of the equation of coefficient of uniformity (CuC)as mention in equation(2-1)

$$(\text{CuC}) = \left( 1 - \frac{\sum_1^N |X_i - \bar{X}|}{N\bar{X}} \right) 100 \quad \dots\dots\dots(2-1)$$

where  $X_i$  is amount of rainfall at location  $i$ ,  $N$  is points number where measuring container are placed on the ground to collect rain and  $\bar{X}$  is average amount of precipitation. The CuC is a useful indicator of spatial uniformity of precipitation. The uniformity of rainfall is well when it reaches 70 % as mentioned in (Wilson *et al.*, 2014a).

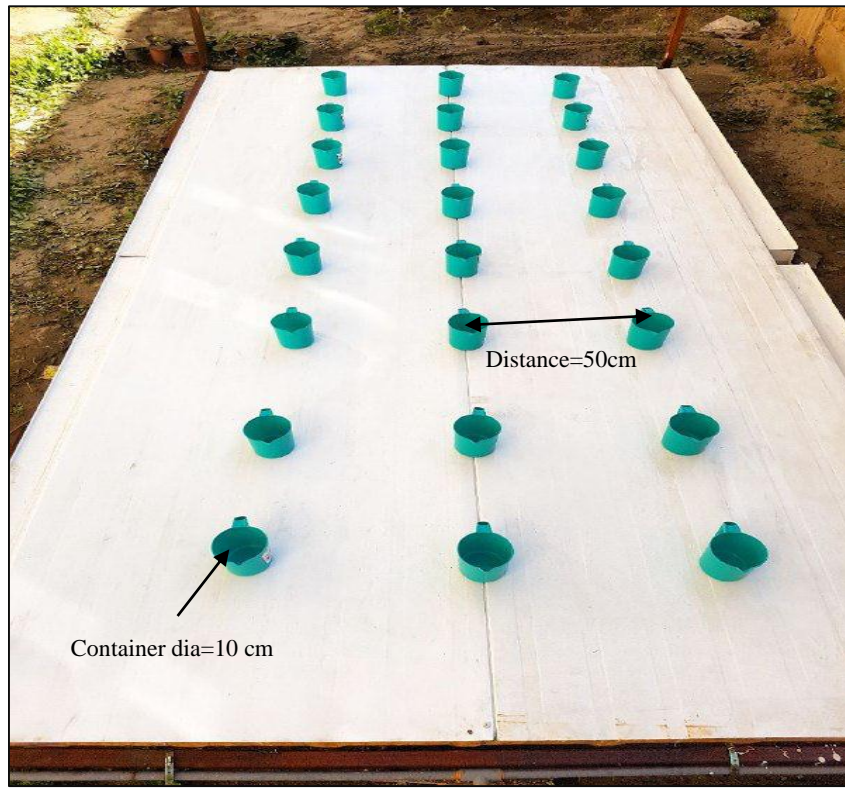


Figure (4-11) Distribution of container according to Christiansen theory

### 4.4.2 Permeability Test

Fixed head permeability testing is a common laboratory testing method used to find the permeability of granular soils, such as sand and gravel with little or no clay, (ASTM, 2006). This test method is designed to test reconstituted or disturbed granular soil specimen. The flow of water through a column of a cylindrical soil sample under constant pressure differential represents a fixed head permeability test. The test is done in the permeability cell, or permeameter, which can differ in size based on the grain size of the material tested, as shown in figure (4-12).

$$V = K * i \dots\dots\dots(4-1)$$

material tested, as shown in figure (4-12).

$$V = K * i \dots\dots\dots(4-1)$$

Where

V= velocity , k= permeability coefficient , i= hydraulic gradient



Figure (4-12) Permeability devices

The advantage of this experience is to know how much the permeability, to be used in numerical model FLOW-3D. The result of permeability of 1.139 cm/s

### 4.4.3 Porosity test

The amount of empty space in a rock or other earth substance is tested;



this empty space is known as pore space. Porosity is how much water a substance can hold. Porosity is usually stated as a percentage of the material's total volume (ASTM, 2010). From result of test the obtain porosity of filter obtained is 0.27 will used in numerical model as shown in table(4-1).

$$\text{Porosity} = \text{void volume}/\text{total volume} \dots\dots\dots(4-2)$$

#### **4.4.4 Sieve analysis**

A local sandy soil was used in this study as a sediment on the floor. This soil is provided from local materials in Karbala governorate, and soil samples were sieved, according to(ASTM, 2007). After conducting the analysis, the sand was transferred from the sieve # 8 and the remaining sieve # 16 where the sand used as the filter. As for the sand used to represent the sand, the street is the remaining sieve # 100

#### **4.4.5 Density**

The density of the sediments is used in accordance with the specifications (ASTM Standard D7263-09, 2009) , where the sample was taken from the sand in dry state after that divide the weight of sample on the volume of this sample. The result given density of sediments is 1780 kg/m<sup>3</sup>

Table (4-1) list of laboratory tests

Case	Laboratory tests	Results	Notes
Filter materials	Permeability Test	Darcy (k) =1.139cm/s	Effective size (D10) =1.5 mm Uniformity coefficient U.C=1.2
	Porosity test	n= 0.27	
Rainfall distribution	Uniformity of rainfall	(CuC) = 81%	The uniformity of rainfall is well when it reaches 70 %
Sediment used on floor	Density	$\rho = 1780 \text{ kg/m}^3$	The sediment is insoluble
	Sieve analysis	Used the sediment remaining on sieve # 100 =0.2mm	

### 4.5 Testing procedure

In the previous chapter, the dimensional analysis was explained and the variables that will be worked on have been selected. The variables that will be worked on in the practical side are the rainfall intensity, the duration of the

intensity, the bed slope and the length of the filter also the remaining variables will be installed in the practical side. In each experiment that will be conducted a fixed amount of sediments (150g) will be put on the floor, after that run the rainfall showers. In the end of each experiment calculate the amount of sediments passing from both the gully with filter and gully without filter. The filter is washed after the end of each experiment to be clean for each test. The variables that will be installed in the practical side are ( diameter of gravel filter , diameter of sediments , mass of sediments). The tables (4-1) illustrate the variables will be experiment.

Table (4-2) Variable in experimental work

Run	Slope	Intensity $mmh^{-1}$	Length filter(mm)	Duration(min)
1	1	30	100	5
2	1.5	37	150	10
3	2	44	200	15
4	2.5	51	250	20
5	3	58	300	25

#### 4.6 Methodology of laboratory test

As mentioned previously, the main aim of this study is improving the efficiency of storm network by using a new gully filter. Figure (4-13) summarizes the study methodology of laboratory test.

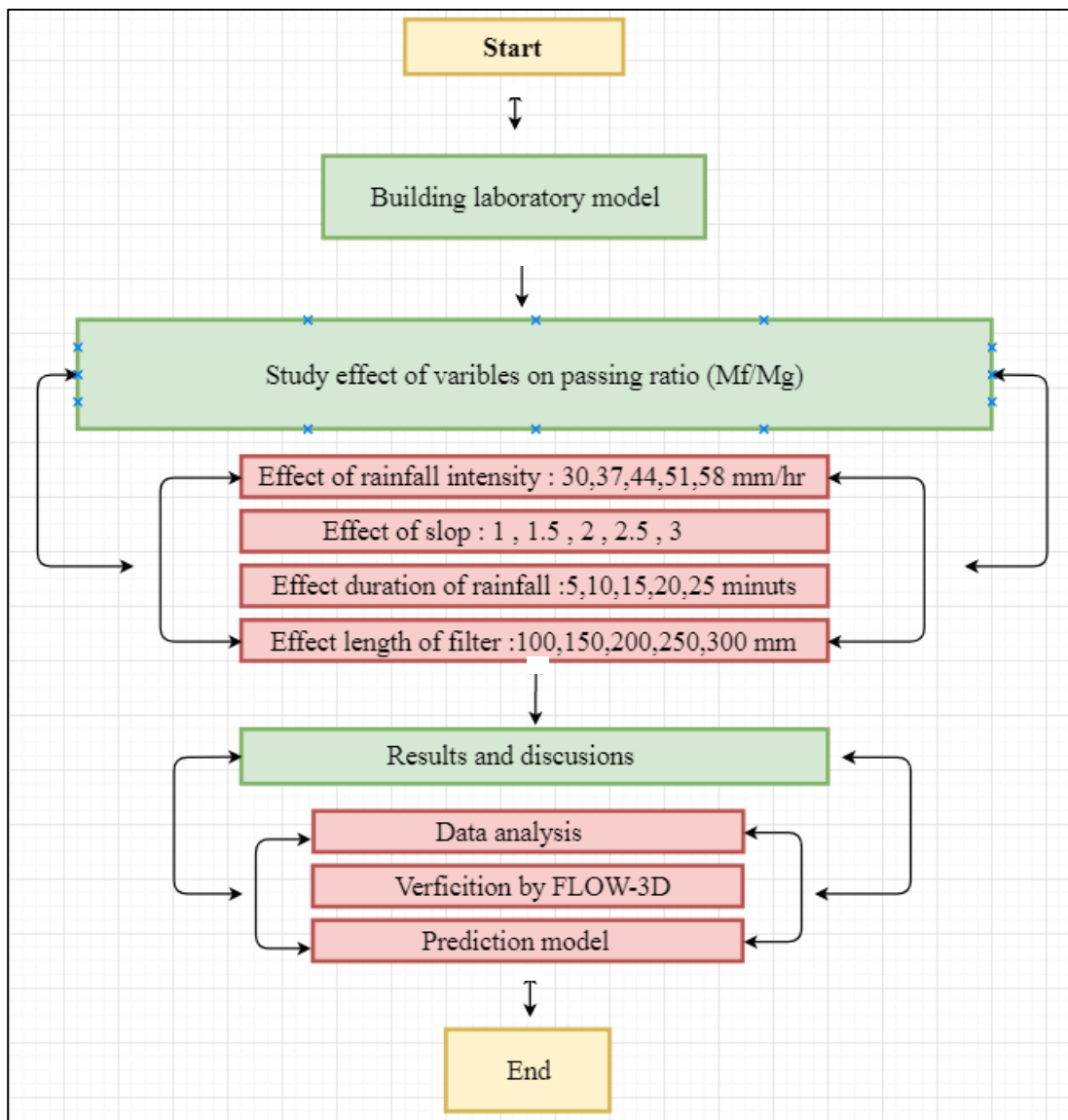


Figure (4-13) Methodology of laboratory test

### **4.7 Summery**

The laboratory storm network and filter model consisted of several separate parts attached to form a complete system as follow:

1. The first part was a steel frame that carries the rain pipe network, as well as carrying the floor, the gravel filter, and all other model segments. Each part of the frame had a thickness of 1.5 mm. The dimensions of the structure were 4.1\*2.2\*2 m.
2. The second part was the rainfall system, which consists of two plastic pipes, each with a diameter of 0.5 inches and a length of 4.1 m. Each pipe was installed on the upper side of the structural frame, and they faced each other at a distance of 2.2 m. Each pipe had 12 nozzles with spacing's of 33 cm between them.
3. The third part the gravel filter, was installed on one side of the two-sided floor model. The gravel filter dimensions were 10 cm width and 5 cm depth with varied lengths. The gravel particle sizes were(1.25-2.5 mm), the effective size=1.5mm and uniformity coefficient=1.2.
4. There are several laboratory tests in both practical and the theoretical sides such as uniformity of rainfall, permeability of filter, porosity of filter, density of sediment used and sieve analysis.

*Chapter Five*  
*Results and Discussion*

## ***Chapter Five***

### ***Results and Discussion***

#### **5.1 Introduction**

This chapter presents analysis and discussion of the data, which were obtained from the experimental work and numerical model. It is divided into many sections to discuss the results according to the categories. The main categories included are based on the study program. The first includes the presentation and discussion of the effects of intensity of rain, length of filter, slope of ground, duration of intensity, and diameter of sediment on the passing ratio. The second category deals with the results obtained from the numerical model that will be discussed and compared with the experimental results. The last categories include the prediction equation.

#### **5.2 Experimental results**

As mentioned in the previous chapter, a set of variables that are studied. These variables will show the effect on the passing ratio from gully with to gully without filter ( $M_f/M_g$ ). The relationship between efficiency of filter and passing ratio ( $M_f/M_g$ ) is inversely related.

##### **5.2.1 Effect of rain storm intensity**

The passing ratio ( $M_f/M_g$ ) is affected by the change in the intensity of rainfall. Five different intensities of rainfall were used 30, 37, 44, 51 and  $58\text{mmh}^{-1}$ . Each intensity is runoff on the floor with five slopes 1, 1.5, 2, 2.5 and 3. The duration for all intensities is 15min, the diameter of sediments

was 0.2 mm and the length of filter is 200mm. The passing ratio ( $Mf/Mg$ ) for each intensity is shown in figure (5-1). The effective size and uniformity coefficient of filter for each experiment were 1.5mm and 1.2 respectively. At the beginning of each experiment the weight of the sediments distribution on the floor is 300 g. In the end of each experiment calculate the weight of sediment passing from both gully with and gully without filter.

As observed, increasing the intensity of the rainfall yield decreasing of the passing ratio( $Mf/Mg$ ), so will be increase efficiency of filter. The reason of changing the passing ratio is increasing the rainfall intensity, and this will increase the velocity of water on the ground ,and thus the amount of sediments transported is greater. The amount of the decrease in the passing ratio ( $Mf/Mg$ ) between the intensities 30-58  $mmh^{-1}$  for all slopes is non-uniform. There are many reasons for the non-uniform of the passing ratio( $Mf/Mg$ ), first is the uniformity of rainfall (81%) is not ideal. Therefore, the drag force for each sediment is different from the each other. The second causes of the difference the passing ratio ( $Mf/Mg$ ) is the distribution of sediments on the surface of the street is irregular, so will gives a difference in the results. It is noted that increasing both intensity and slope giving results showing more efficiency for filter, because the amount of sediments enter the filter is large, so the quantity of sediments caught is big as shown in figure(5-2).



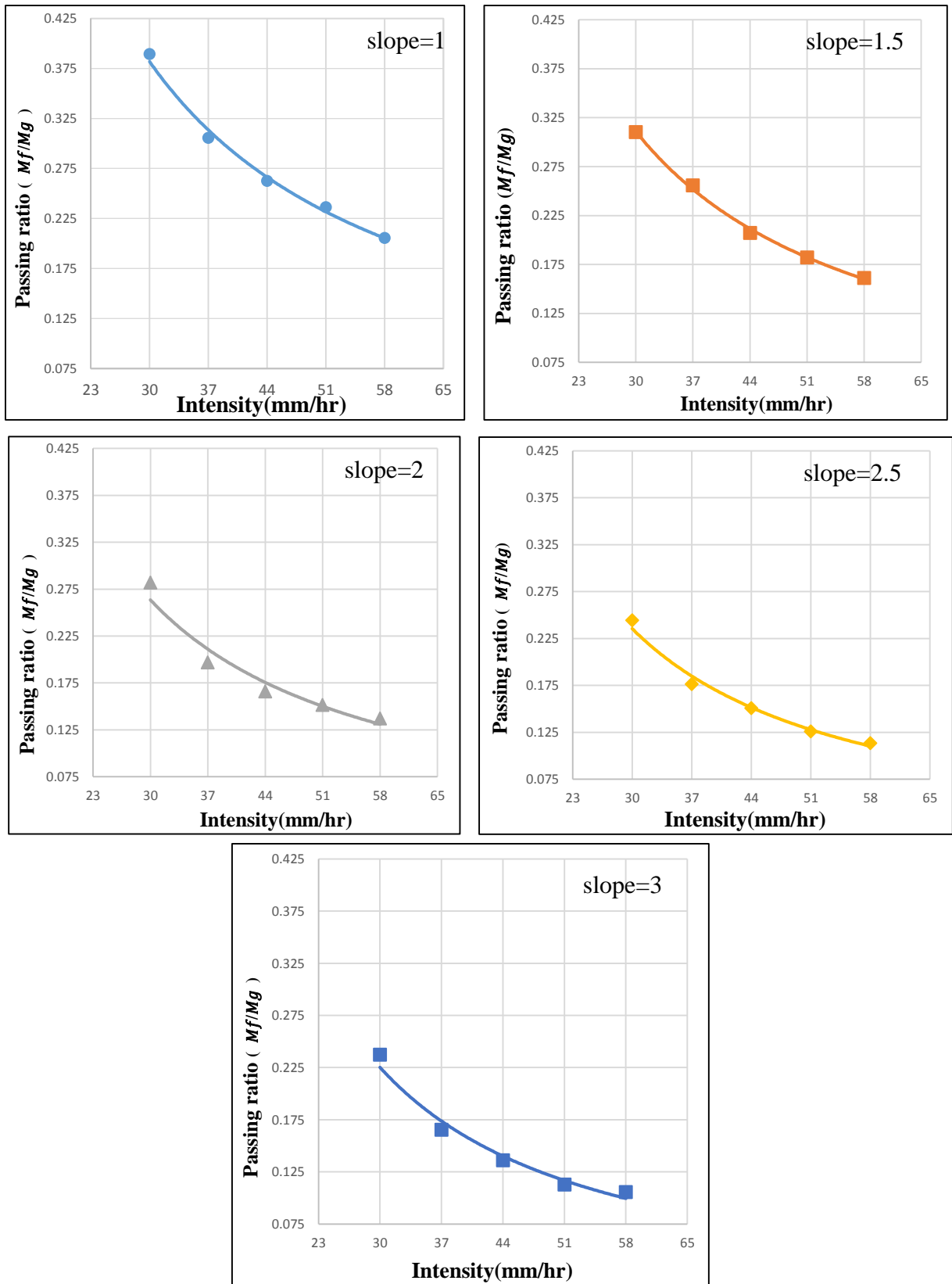
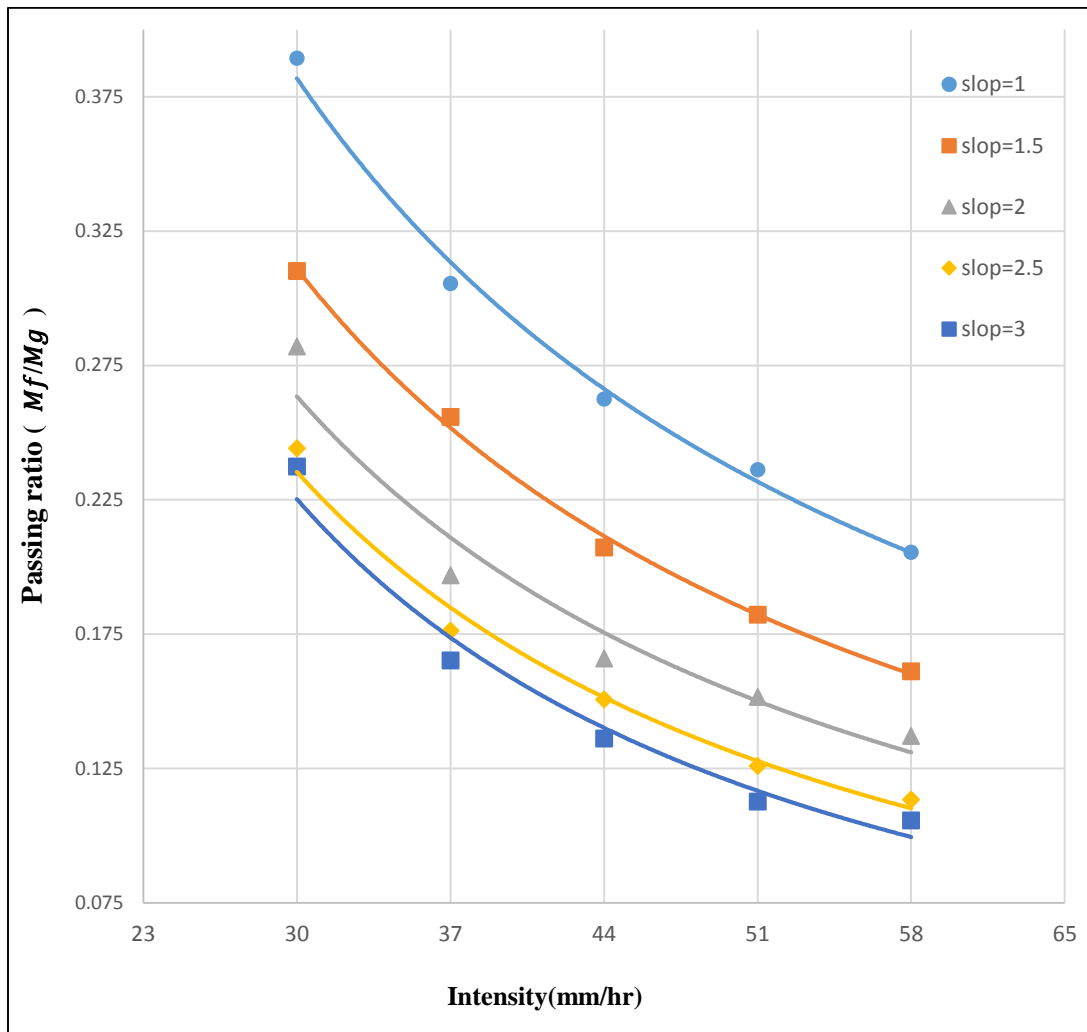


Figure (5-1).Relation between intensity and passing ratio ( $Mf/Mg$ )



Figure(5-2). Relation between intensity and passing ratio for different slopes

### 5.2.2 Effect of the length of filter

The amount of sediments passing form filter is greatly affected by the length of the filter. Therefore, length of the filter is controlled to study behavior of passing sediments. Five sizes of length of filter were used: 100,150,200,250 and 300mm. For each length of filter, the run was done with intensity of rainfall  $44 \text{ mmh}^{-1}$ , and the dimeter of sediments was 0.2 mm,

also the duration of intensity is 15min. The weight of the sediments distribution on the ground is 300g. Figure (5-3) show the passing ratio ( $Mf/Mg$ ) for each length of filter.

It is clear from the results that length of filter has a crucial effect on the amount of the passing ratio( $Mf/Mg$ ). The passing ratio observed decreases with increase the length of filter, due to increase surface area of filter to catch the sediments ,as well as increasing the length of the path in the filter made the sediments need a high velocity and energy to pass from the filter. It was observed that the difference in the passing ratio( $Mf/Mg$ ) not more than 0.015 for each length of filter. The difference in the passing ratio( $Mf/Mg$ ) beginning to increase with the decrease of the slope, this is because the difference in the velocity of the runoff was increased by increasing the slope. It is note that the efficiency of filter increases by increasing the length of the filter, because the filter is catch the largest amount of sediments with increasing the length. Figure(5-4) shown assembly figure of all slopes, where it is noted by increase the slope decrease the passing ratio( $Mf/Mg$ ) but will be increase efficiency of filter.

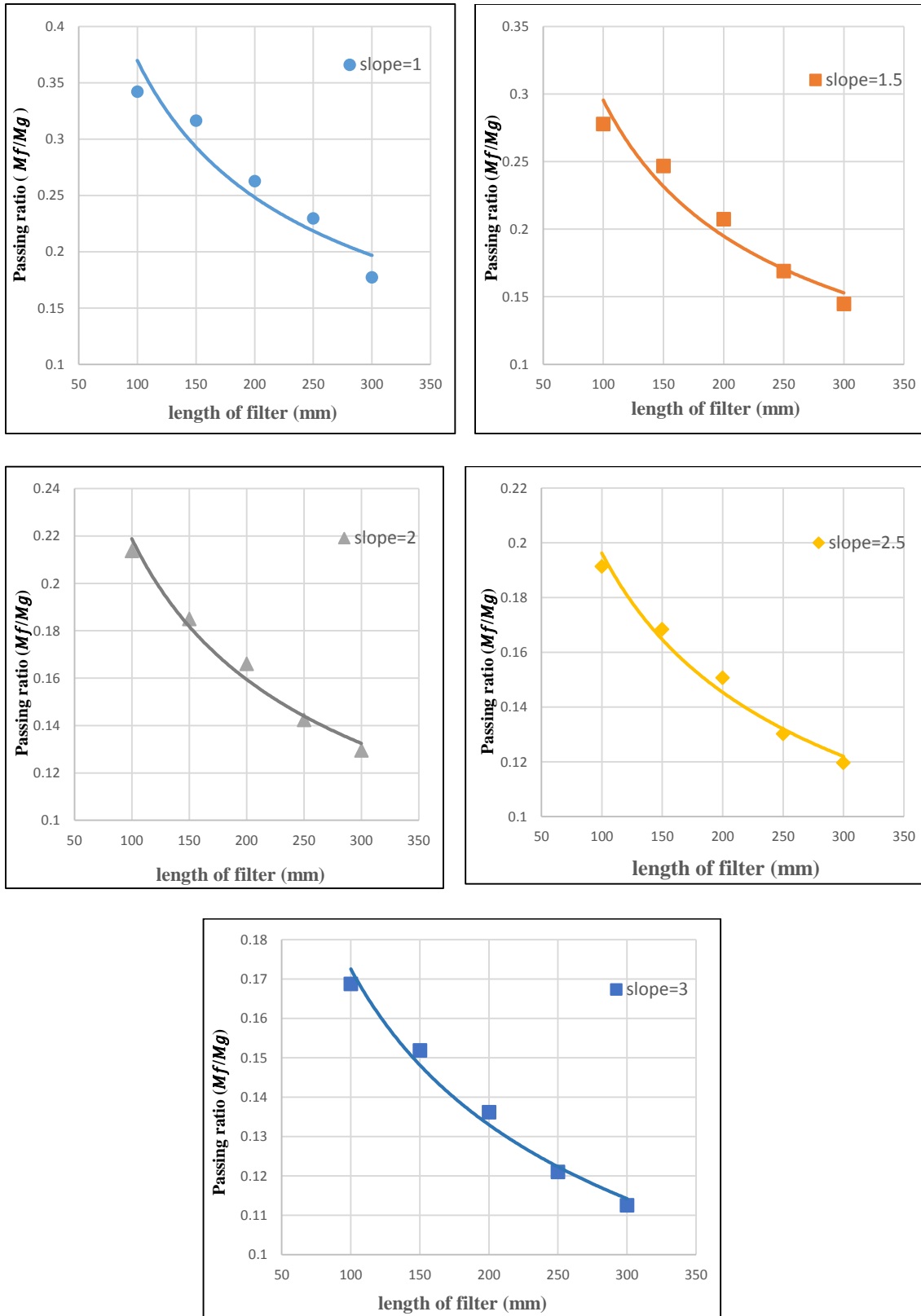


Figure (5-3).Relation between length of filter and passing ratio( $M_f/M_g$ )

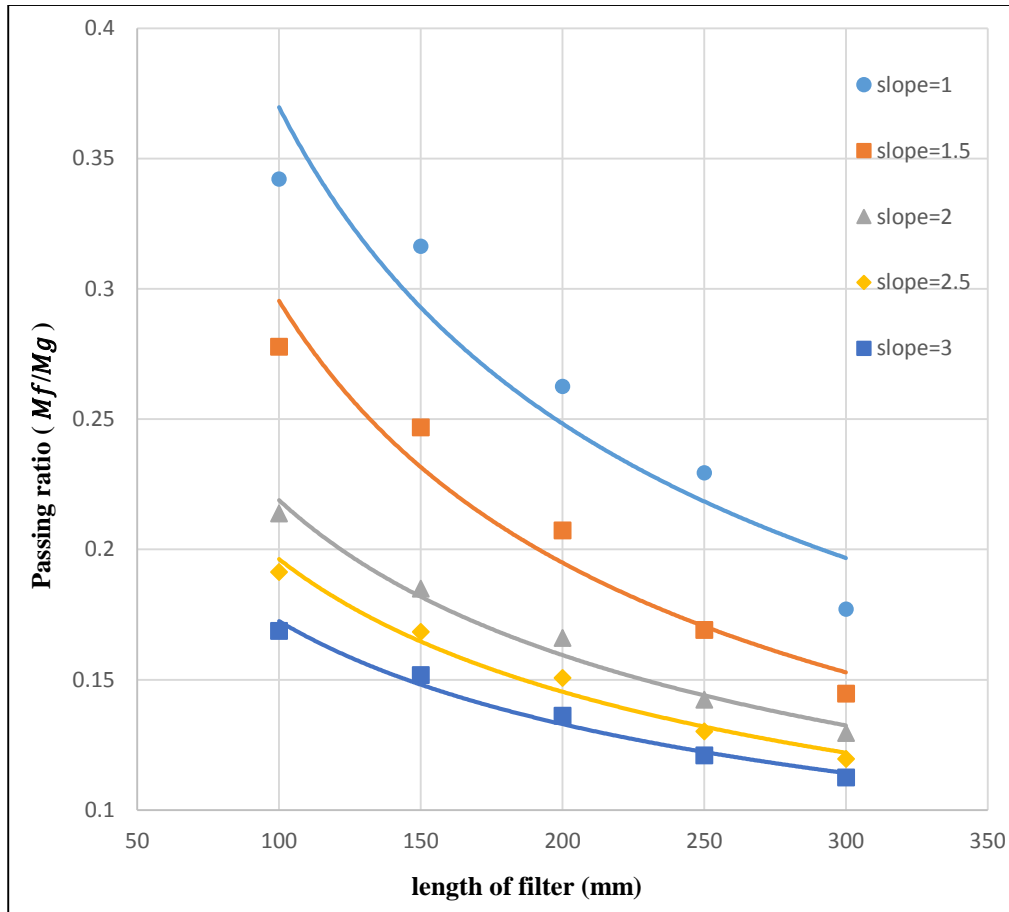


Figure (5-4).Relation between length of filter and passing ratio for different slopes

### 5.2.3 Effect the duration of intensity

The duration of the rainfall intensity affects significantly on the amount of the transported sediments. To test the effect duration of intensity on passing ratio ( $Mf/Mg$ ). Five different durations of rainfall intensities were used: 5, 10, 15, 20 and 25 minutes, and each duration is runoff on the ground with five slopes: 1, 1.5, 2, 2.5 and 3. The rainfall intensity is  $44 \text{ mmh}^{-1}$ , the diameter of sediments was 0.2 mm and the length of filter is 200mm. The weight of the sediments distribution on the ground is 150 g for each lane. The results shown in the figures (5-5,5-6) the passing ratio ( $Mf/Mg$ ) for each duration of intensity and slopes.

The results show that the amount of the passing ratio ( $Mf/Mg$ ) is decreasing with the increase of the value of duration of intensity. In case the slope 3 for each duration the difference between passing ratio does not exceed 0.015, also in slope 1 for each duration the difference does not exceed 0.03. It was observed from the results that the quantities of passing ( $Mf/Mg$ ) is near to uniform, this is because the constant rainfall intensity, where the runoff has a stable velocity. Therefore the amount of sediments transported increases uniformly with the increase of duration of intensity.

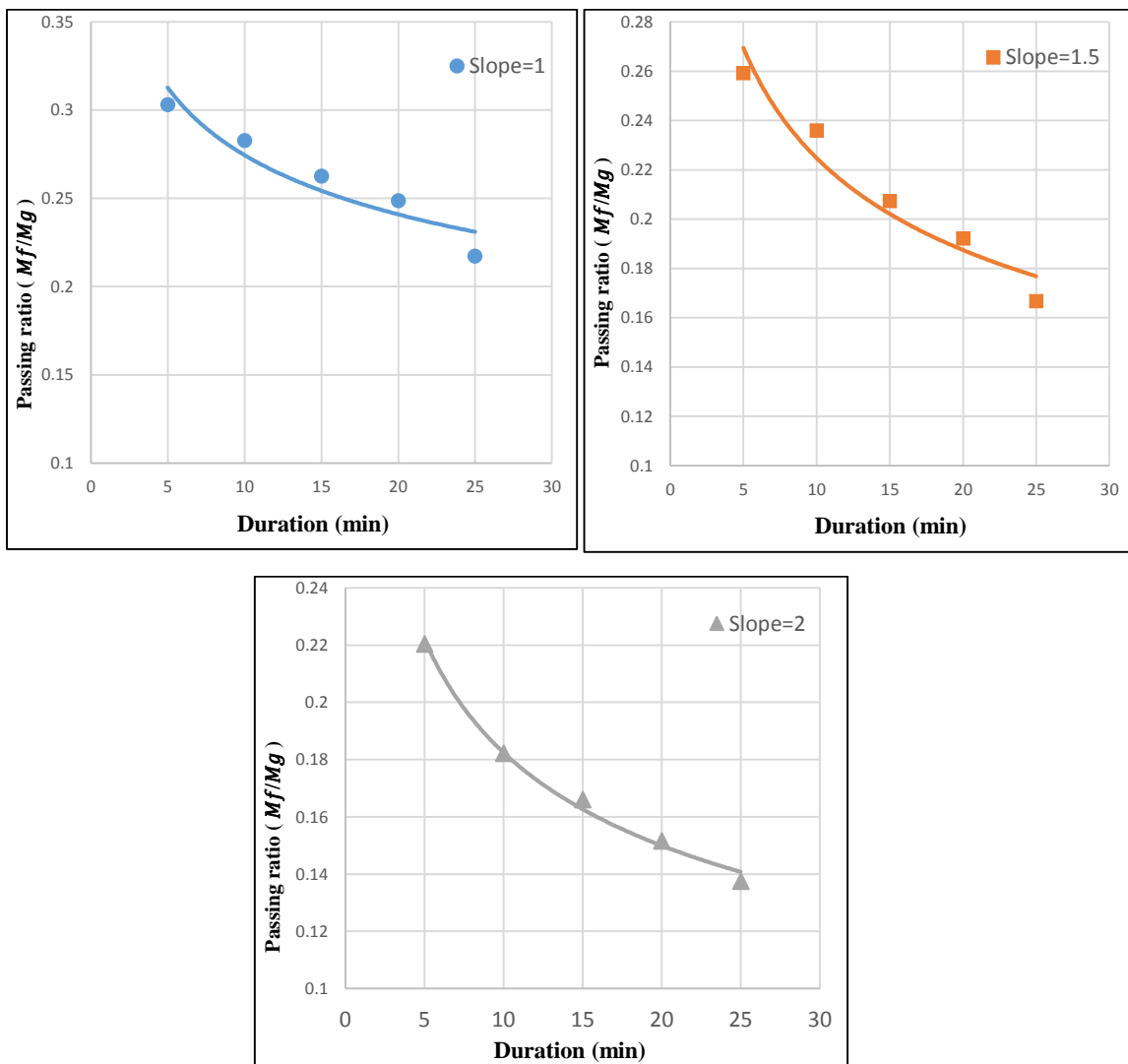
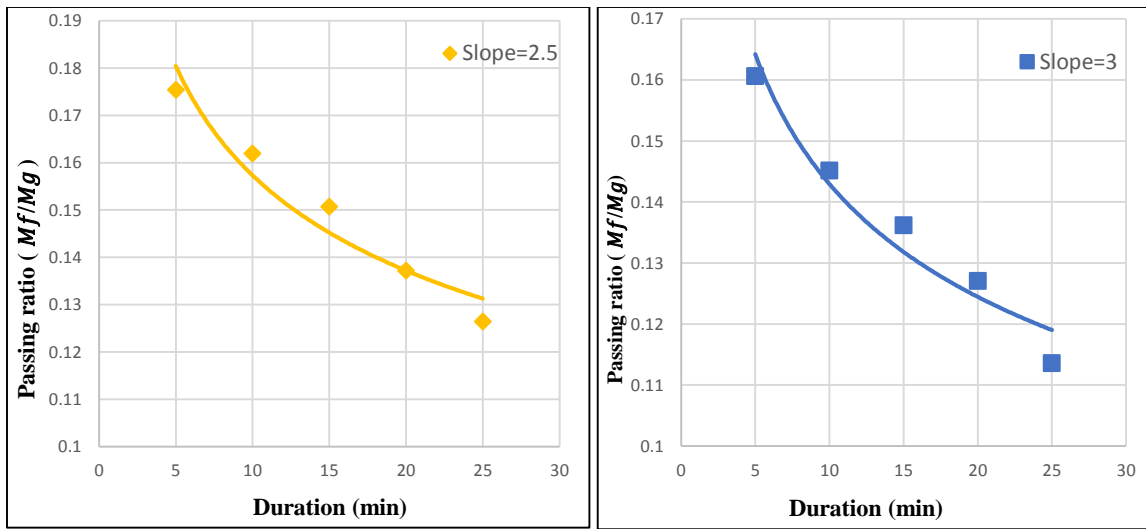


Figure (5-5).Relation between duration of intensity and passing ratio ( $Mf/Mg$ ) at intensity  $44 \text{ mmh}^{-1}$



Figure(5-5).continue

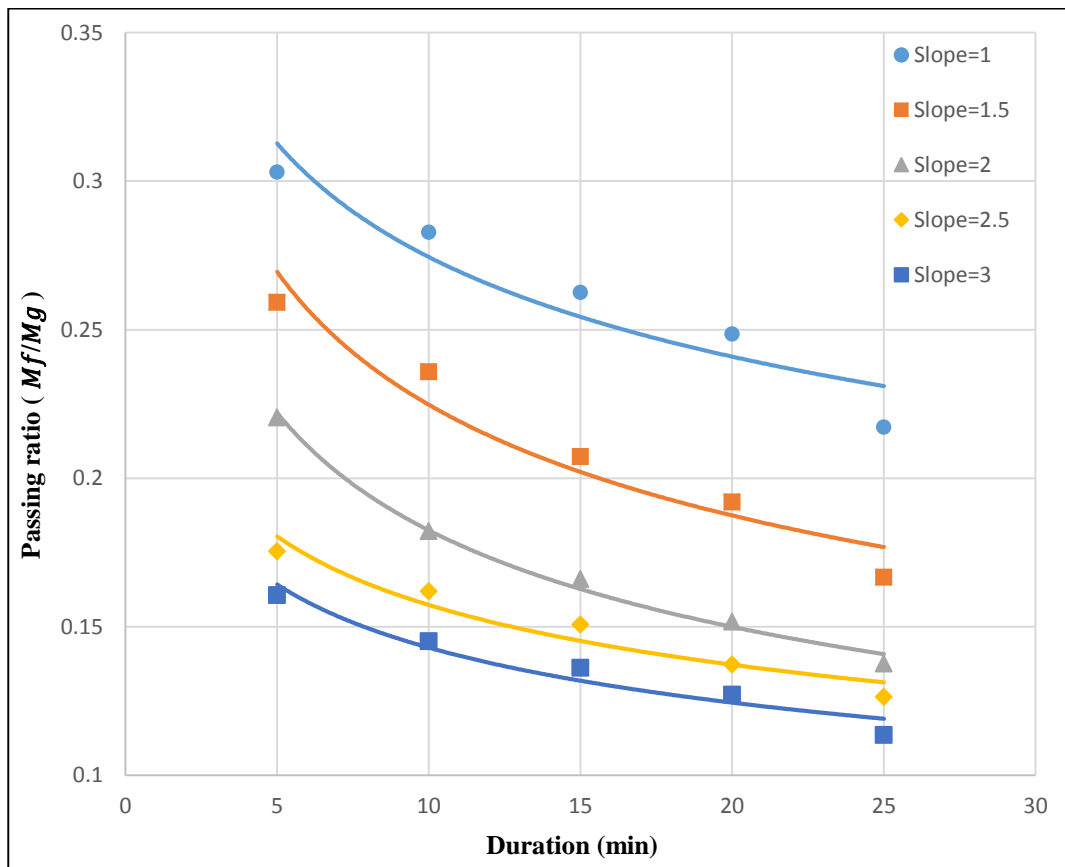


Figure (5-6).Relation between duration of intensity and passing ratio for different slopes

### 5.2.4 Effect of the slope

The slope of ground is one of the most important things affecting the transmission and velocity of both runoff and sediments, and it is very significant in discharge runoff. Twenty five runs were conducted to determine the effect slope of ground had on the passing ratio from gully with filter to gully without filter. The rainfall intensity is  $44 \text{ mmh}^{-1}$  and the diameter of sediments was 0.2 mm also, the weight of sediments distribution on the ground was 150 gram for each lane. For every slope used (1,1.5,2,2.5 and 3) the duration change five times. The figure (5-4) has shown the relation between passing ratio with slope

The results give indicator that the increase in the slope of floor decreases the passing ratio ( $Mf/Mg$ ). The reason for the change in the passing ratio is the velocity of runoff will be unstable; therefore, the velocity of the transmission sediments depends on the velocity of the runoff. It was observed the change in results passing ratio( $Mf/Mg$ ) with slopes for all duration reach is near to uniform. This is because the rainfall intensity is constant and the increase in the intensity duration is regular, so the change in passing ratio( $Mf/Mg$ ) is close to uniform. From the result shown that the slopes has a large effect on the efficiency of the filter. Figure(5-8) shown assembly figure of all duration, where it is noted by increase the duration decrease the passing ratio( $Mf/Mg$ ) will be increase efficiency of filter.



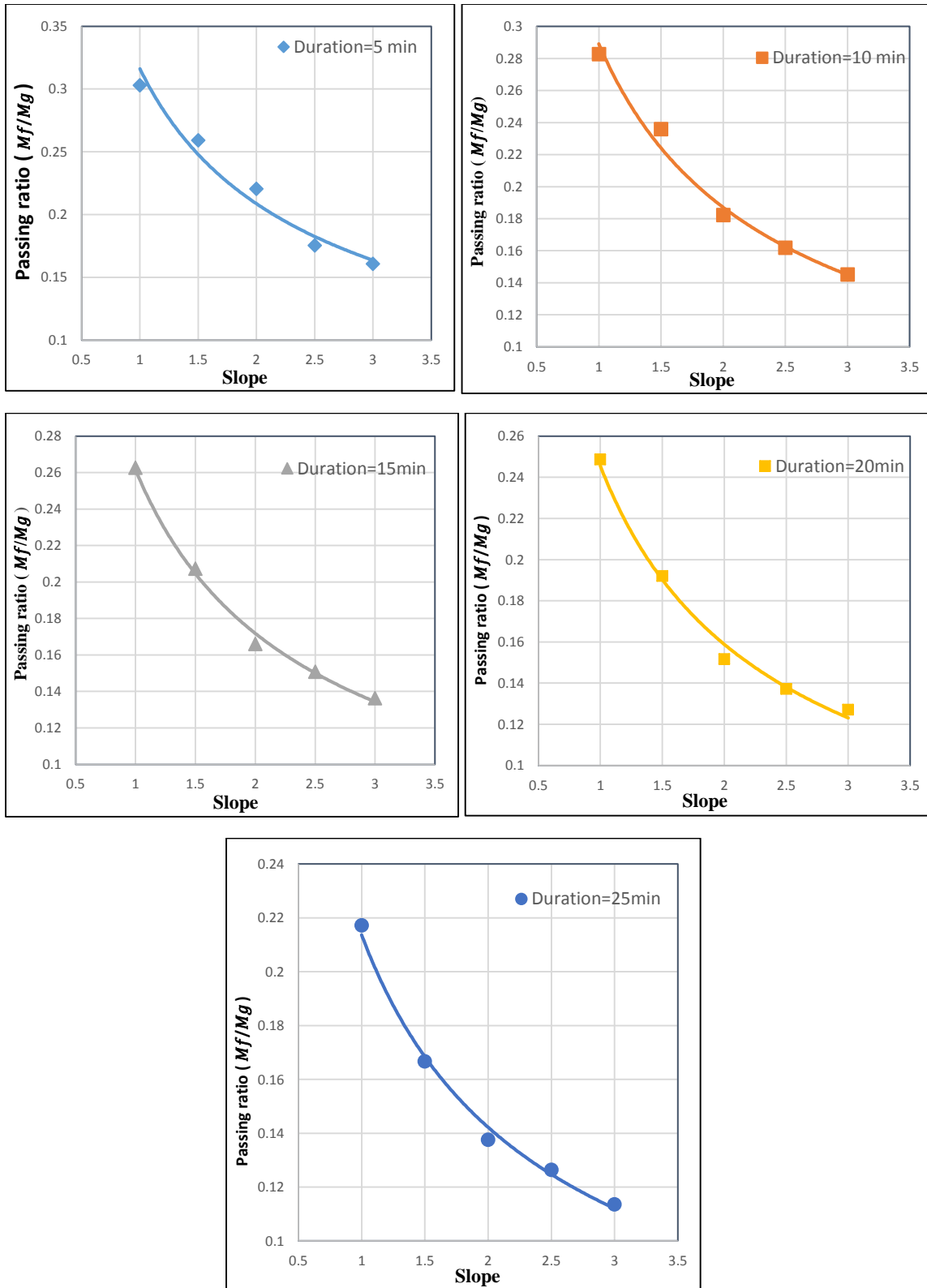


Figure (5-7).Relation between slope and passing ratio( $Mf/Mg$ ) at intensity  $44 \text{ mmh}^{-1}$

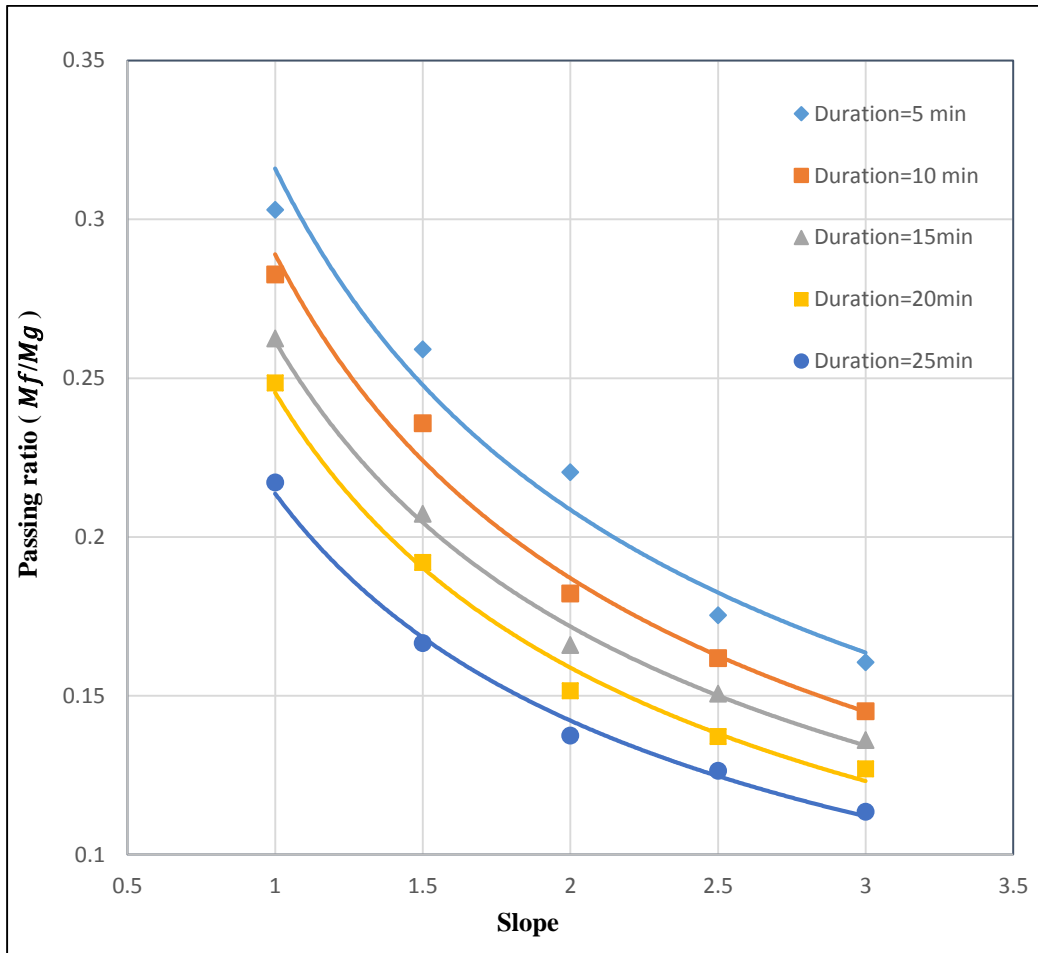


Figure (5-8).Relation between slope and passing ratio for difference durations

### 5.3 Numerical model Flow-3D

In this study the results of FLOW-3D to determine the passing ratio (Mf/Mg) gives good agreement with the result obtain from experimental work. As mentioned in chapter three the result of FLOW-3D was effected mainly by the grid size (mesh). The grid size was not only significant for the reducing precise of the governing equations but also for drawn the solid shapes. Different grid sizes have been used to obtain the optimum one, where 15 mm grid size lead to the details of the model has not clarified accurately.

When using a uniform mesh size of 1.5 mm in all directions leads to another problem is the difficulty of operating because of the large number of cells that reaches millions of cells and needs a very long time. To predict rapid changes in passing ratio characteristics, the grid sizes should be used as best as possible therefore, different sizes of cells such as (15, 10, 5, and 2) mm are selected to determine the best size is the minimum cell size that meets this phenomenon conditions. For this target, four runs were achieved to find the best grid as shown in figure (5-9) also, the result is presented in table (5-1). The results of the numerical analysis show that the reduced grid size leads to a change in the numerical results compared to the experimental result of approaching the real value. The grid size (5 mm) was used in this study as the suggested mesh size in the result compared to the experimental result. Also, use an 5 mm mesh to accurately capture details and reduce potential calculation time. However, when using a (2 mm) grid size, the model will run more time and there will be no significant change in the results.

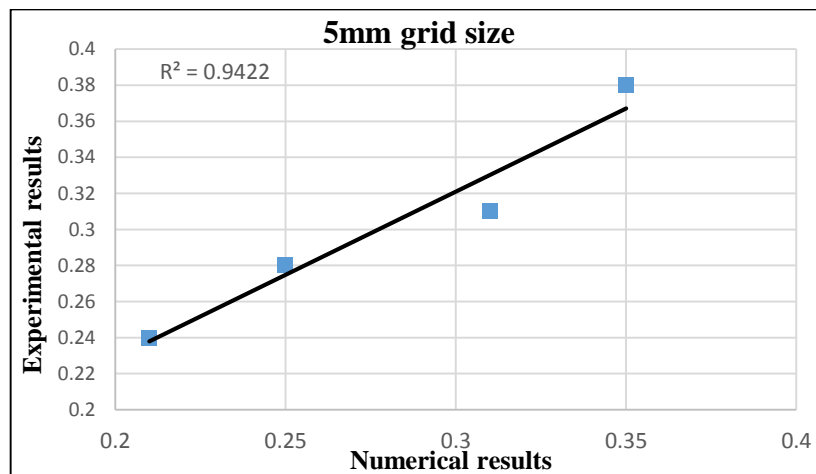


Figure (5-9) Relationship between passing ratio in experimental and numerical (FLOW-3D) for 5 mm grid size

Table (5-1): The correlation coefficient for different grid size

Grid Size(mm)	% Av. error	$R^2$
15	17.2	0.83
10	15.1	0.85
5	5.22	0.94
2	4.7	0.95

### 5.3.1 Validation of the Results of Numerical and Experimental Models

FLOW-3D used to predict changes in model characteristics in parameters of rainfall intensity, bed slope, duration of intensity, length of filter and diameter of sediments. FLOW-3D is a powerful numerical model that can be the key to achieving acceptance results with less time and less money. In order to ensure Flow-3D work and to verify the effectiveness of the numerical model program, the current numerical model was applied in the same physical model conditions. For low simulation errors important parameters that have a large effect on the numerical result such as the size of the grid must be calibrate, and the boundary conditions were applied to the numerical were selected accurately. Then after checking the percent conformity of the laboratory results with the numerical results. The results show that the average percentage error was 7 % ,but maximum percentage error was 16 % (see appendix B). The reason for the difference between the measured and

computed passing ratio ( $Mf/Mg$ ) is due to the size of cell in model. Also the numerical work is more accurate and perfect than experimental work, where in the experimental work some errors occur and are out of control. As in the figures(5-10,-5-11,5-12,5-13) shows us the curves resulting from program FLOW-3D

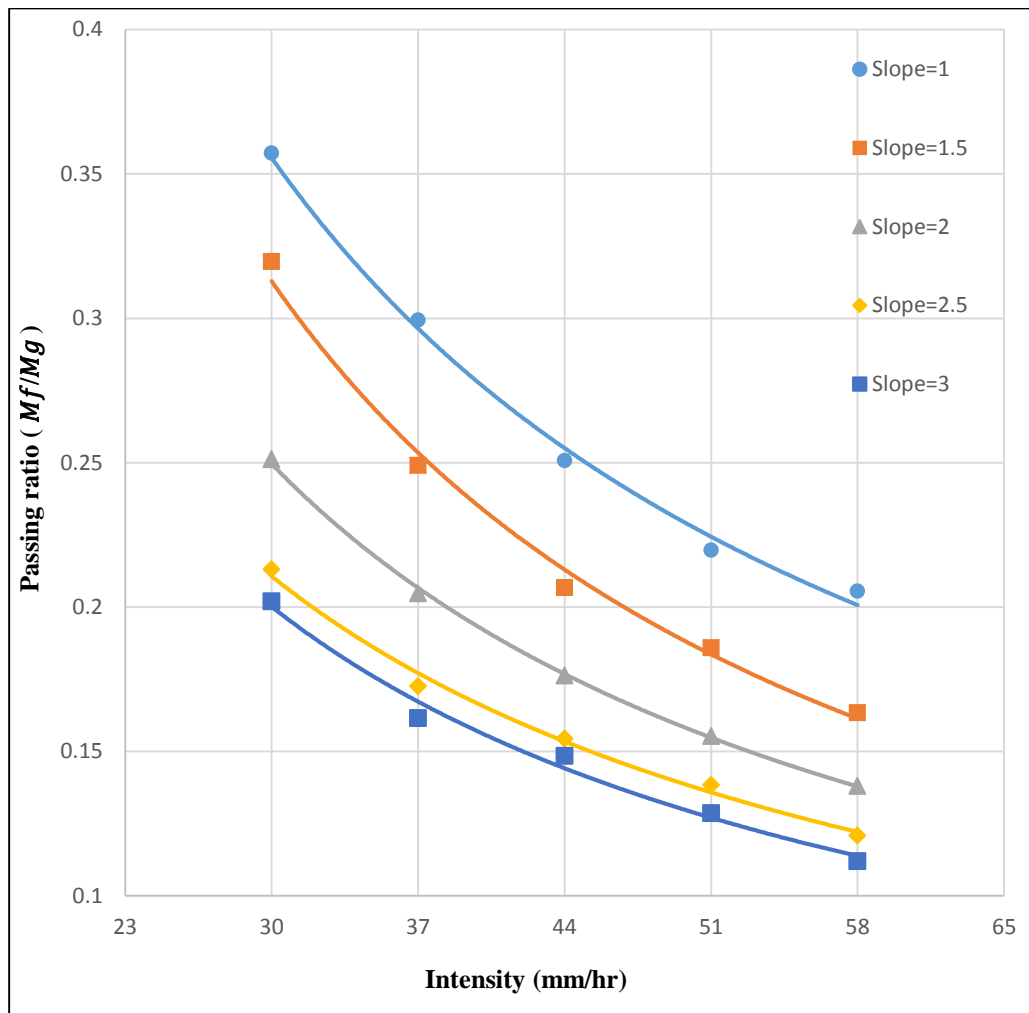


Figure (5-10) Relation between intensity and passing ratio (FLOW-3D)

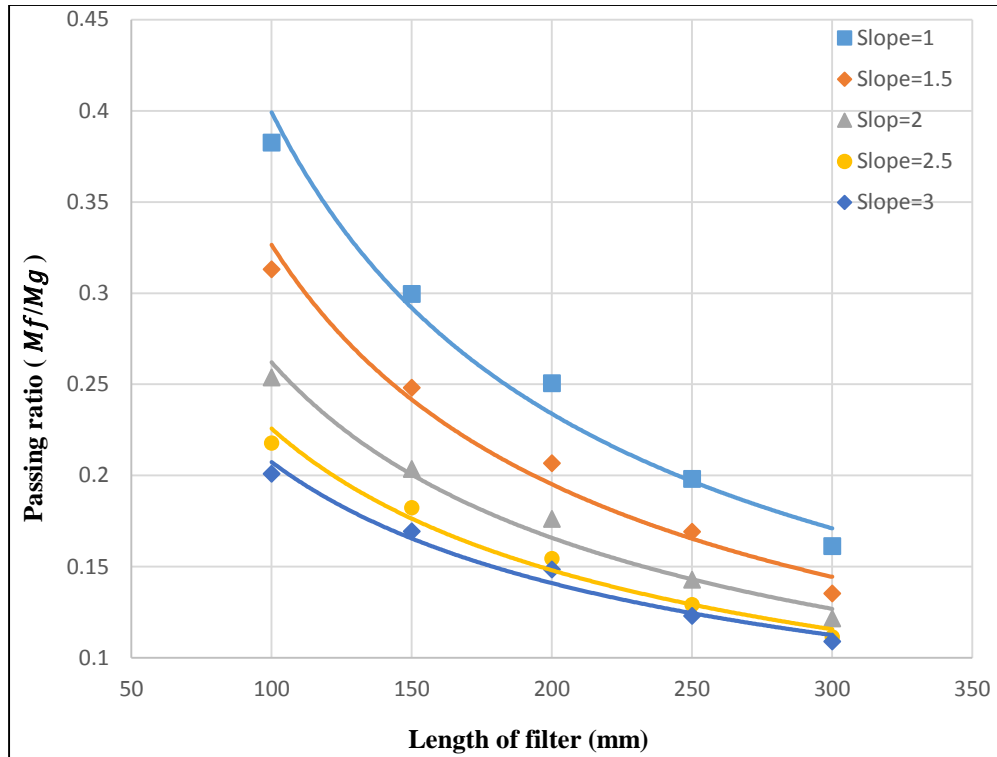


Figure (5-11) Relation between length of filter and passing ratio (FLOW-3D)

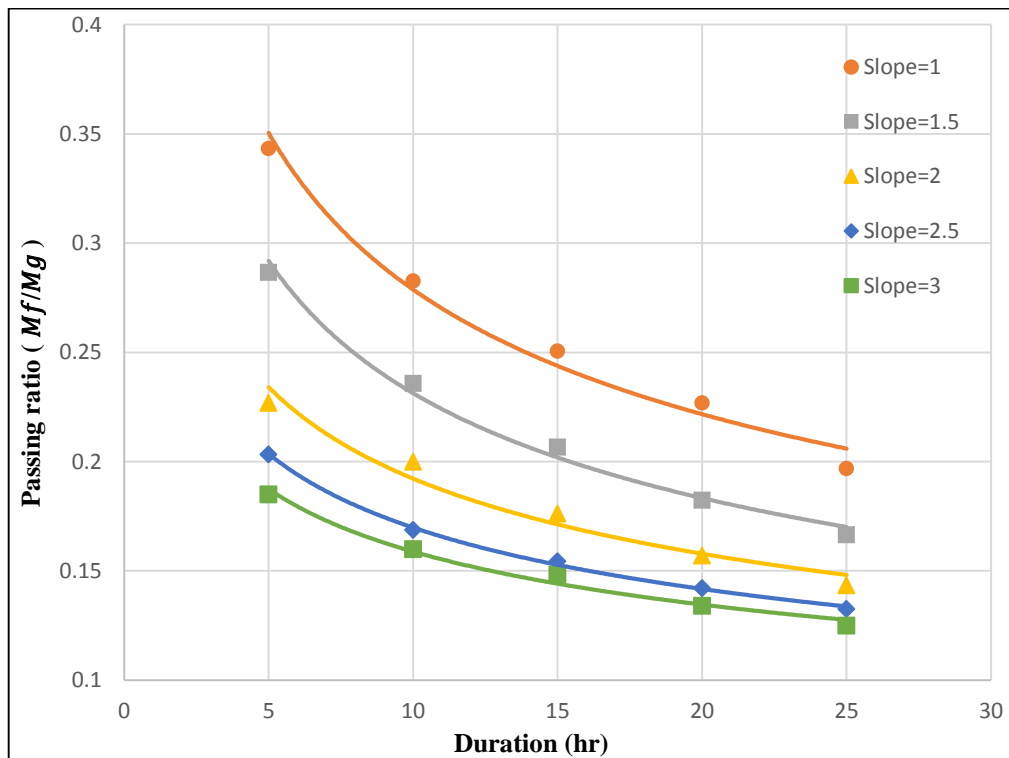


Figure (5-12) Relation between intensity duration and passing ratio (FLOW-3D)

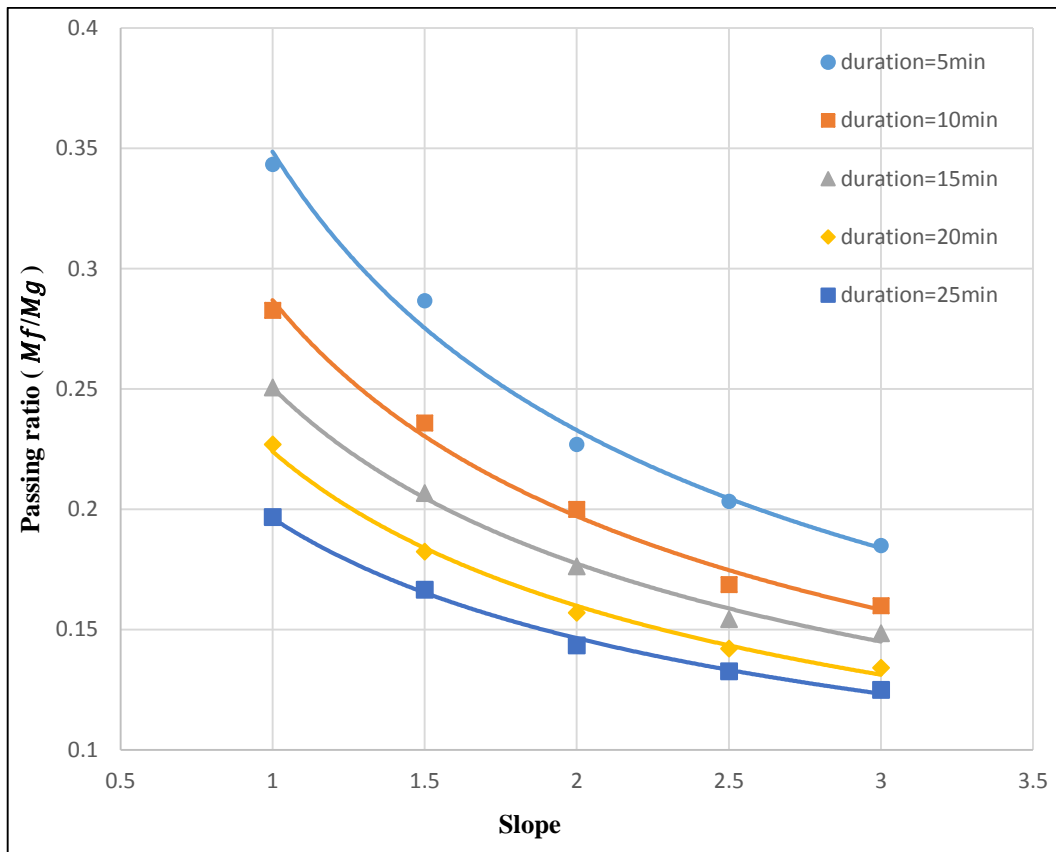


Figure (5-13) Relation between slope and passing ratio (FLOW-3D)

The correlation coefficient ( $R$ ) is the overall measure of usefulness of regression, the height correlation, the better the variance that depended on variable is explained by the independent variables (rainfall intensity, bed slope, duration of intensity and length of filter) as shown in figure(5-14). The value of  $R^2$  is 0.92, it is given to indicate that the result is almost acceptable.

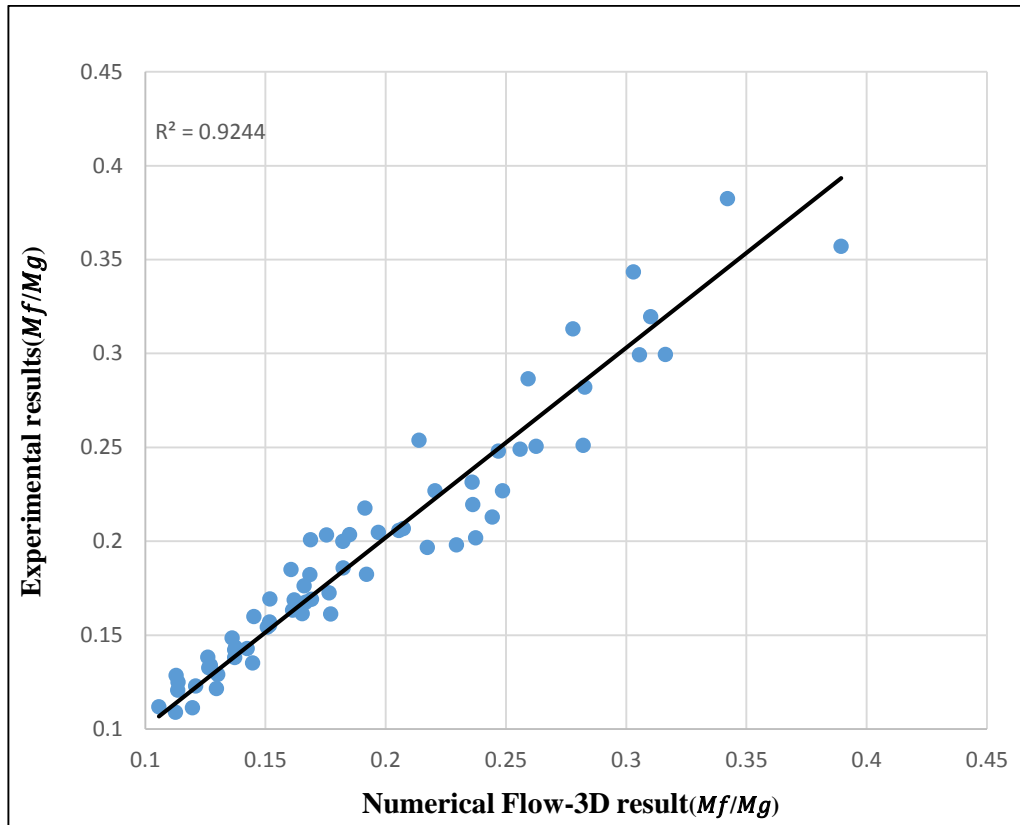


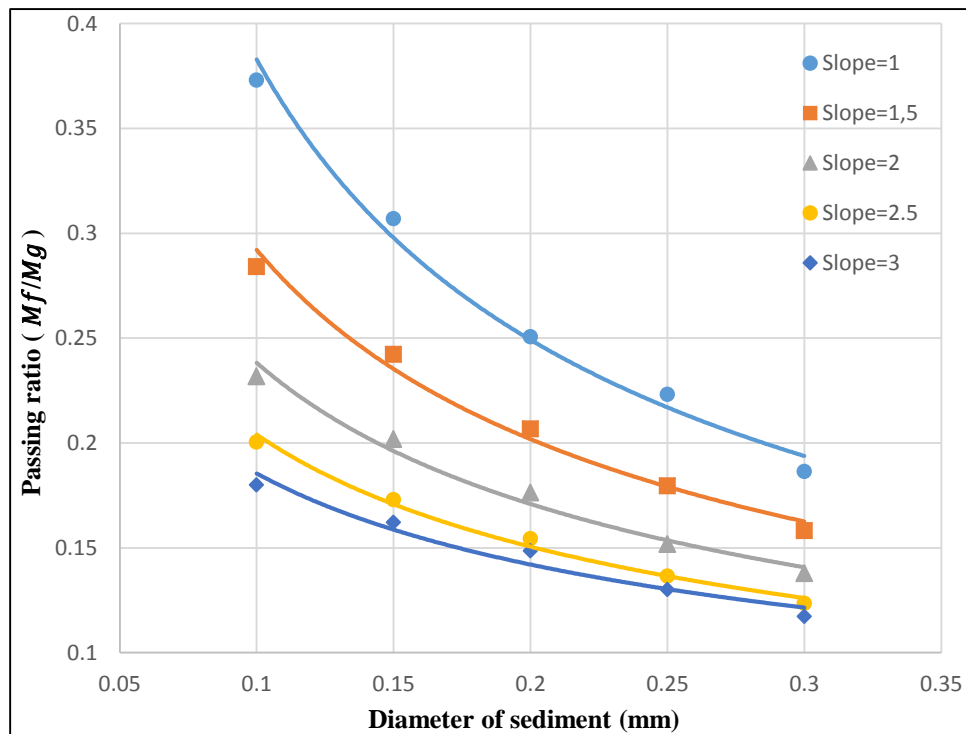
Figure (5-14) Comparison between the result for numerical and experimental work

### 5.3.2 Effect the diameter of sediments

After the completion of the experimental work and comparing the results using the program FLOW-3D was taken a new variable is the diameter of sediments that distributed on the floor. The diameter of sediments is one of the important variables in this types study, where there are in fact regions that have different sediments types. Five different diameter of sediments were used 0.1, 0.15, 0.2, 0.25 and 0.3 mm, each diameter of sediments on the ground run with five slopes 1,1.5,2, 2.5 and 3.The duration of intensity is 15min, the rainfall intensity is  $44 \text{ mmh}^{-1}$  and the length of filter is 200mm. The passing ratio ( $Mf/Mg$ ) for each diameter is shown in figure (5-15).



It can be observed that when increase the diameter of the sediments will decreasing the passing ratio ( $Mf/Mg$ ). It is noted from the results at diameter 0.1 mm that the rate of decreases passing ratio with increase slope is greater than from other diameter, where slope 1 the passing ratio was 0.37, while at slop 3 the passing ratio 0.18. The causes of decrease passing ratio at the diameter 0.1 mm is the size of the sediments is small so it is easy to move and erosion with runoff. It is observed at diameter 0.3 mm and slope 1 the passing ratio was 0.18, while at slop 3 the passing ratio was 0.11, Where the difference is less than the with previous diameter of sediments, because the increase of the diameter will be the difficult passing sediments through the filter, so this will decrease the passing ratio.



Figure(5-15) Effect diameter of sediments on passing ratio from (FLOW-3D)

### 5.4 Dimensional Analysis and Predicted Model

Since the dependent variable is the passing ratio from ( $Mf/Mg$ ), and the other independent variable is dimensionless group. The data was correlated using Pearson correlation and analyzed using SPSS. The results shows that the slope of ground has the largest impact on the passing ( $Mf/Mg$ ) as shown in table (5-2).

Table (5-2): The correlation coefficient for different variables

Dependent variable	Independent variable	Pearson correlation
Passing ratio	Rainfall intensity	-0.36
Passing ratio	Slope	-0.43
Passing ratio	Duration of intensity	-0.24
Passing ratio	Length of filter	-0.4
Passing ratio	Diameter of sediments	-0.31

Figure. (5-16) shows the negative relationship between the passing ratio ( $Mf/Mg$ ), and the slope (S), the correlation value is 0.43. The passing ratio( $Mf/Mg$ ) decreases with the increase of the slope of ground, where there are increases of the velocity of water on the ground ,and thus the amount of sediments transported is greater. A negative sign indicates that the relationship is inversely.

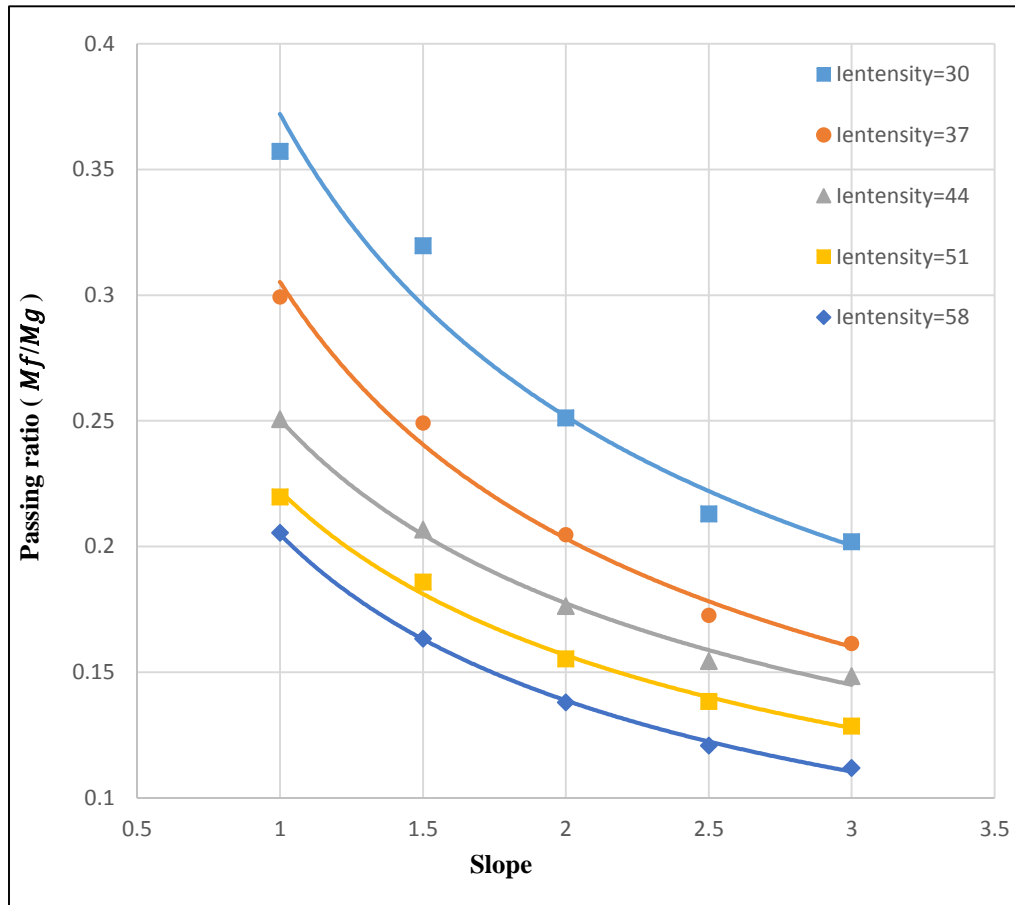


Figure (5-16) Effect slope on passing ratio ( $Mf/Mg$ )

Figure. (5-17) shows the effect of the ratio between the ( $(I * T)/Lf$ ) and the passing ratio ( $Mf/Mg$ ), where the negative relationship between the passing ratio and intensity, where the correlation value is -0.36. This was observed with the increasing of the intensity of the rain decrease the passing ratio ( $Mf/Mg$ ).

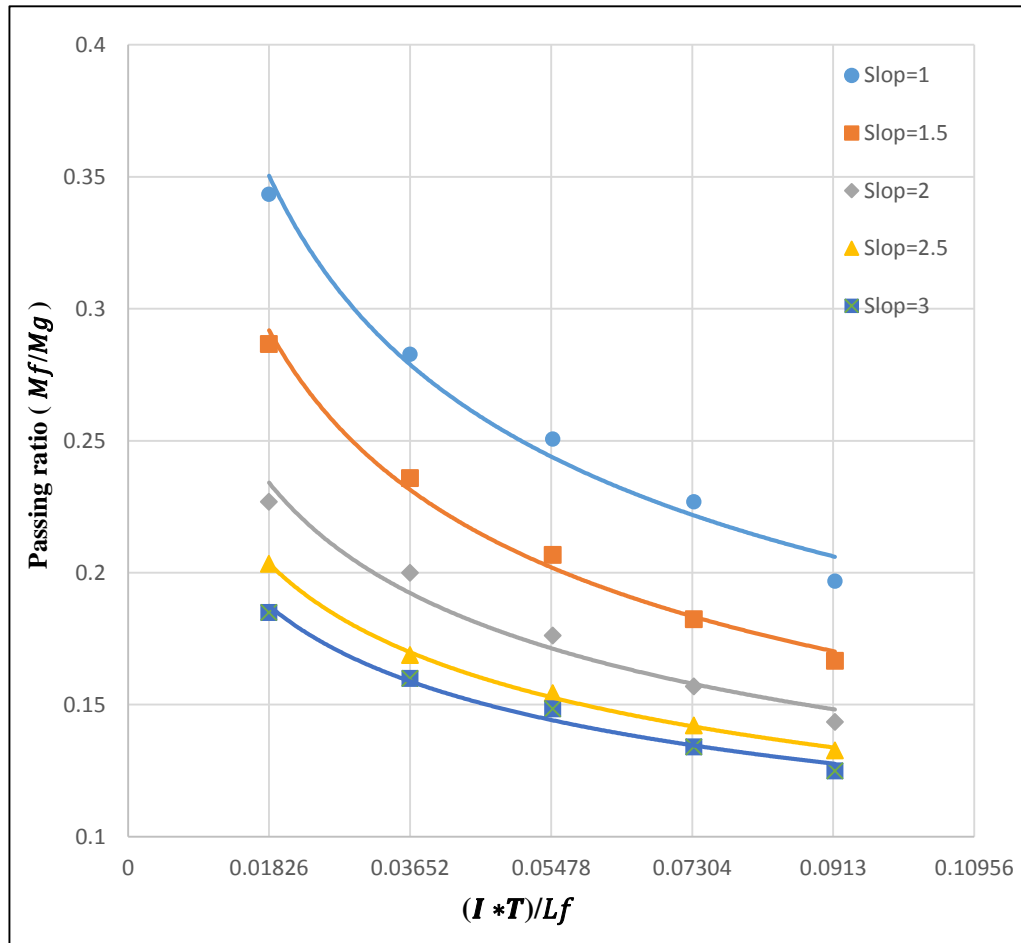


Figure (5-17) Relationship between passing ratio and  $(I * T)/Lf$

Figure (5-18) shows the effect of different diameter of sediments on the passing ratio ( $Mf/Mg$ ). Also negative relationship between the passing ratio and length of filter where the correlation value is -0.40. It is observed that when increasing the diameter of the sediments passing will decrease.

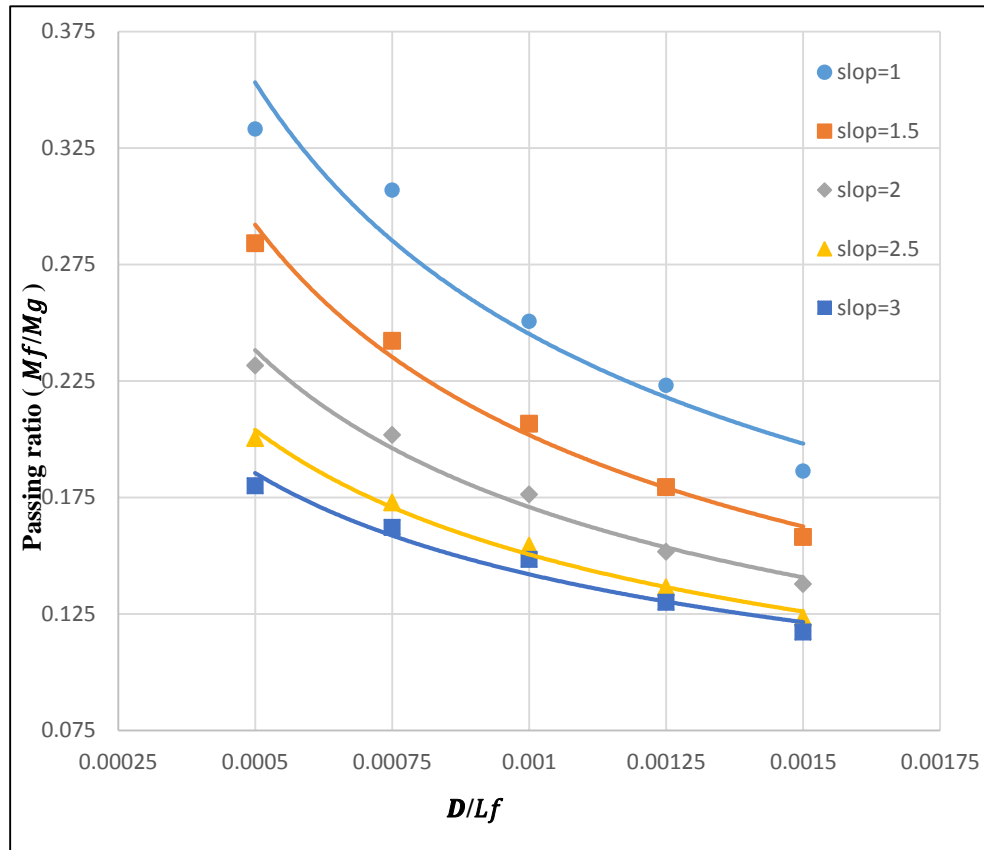


Figure (5-18) Relationship between passing ratio and  $D/Lf$

SPSS was implemented to achieve analysis and build the required model. The prediction model was non-linear, the data used to build and validated prediction model (see appendix C), 65 data to build the module where used while the other 20 data used to validate the equation. Figure (5-19) presents the comparison between the experimental data and the estimated values of the passing ratio from gully with filter to gully without filter. Value of coefficient of determination for equation was of ( $R^2 = 0.88$ ). It can be concluded that the passing ratio under similar conditions can be reasonably estimated using the dimensional analysis.

Prediction equation

$$\frac{M_f}{M_g} = 0.095 + 866 * A + 7240 * A * B + 9.07 * B^2 + 0.018 * C^2 - 0.118 * C - 9.39 * B - 7240 * A^2 \dots (5-1)$$

where

$$A = \frac{D_s}{L_f}, \quad B = \frac{I * T}{L_f}, \quad C = S$$

$$R^2 = 0.88$$

Mean Absolute Error (MAE) = 0.013

Root Mean Square Error (RMSE) = 0.05

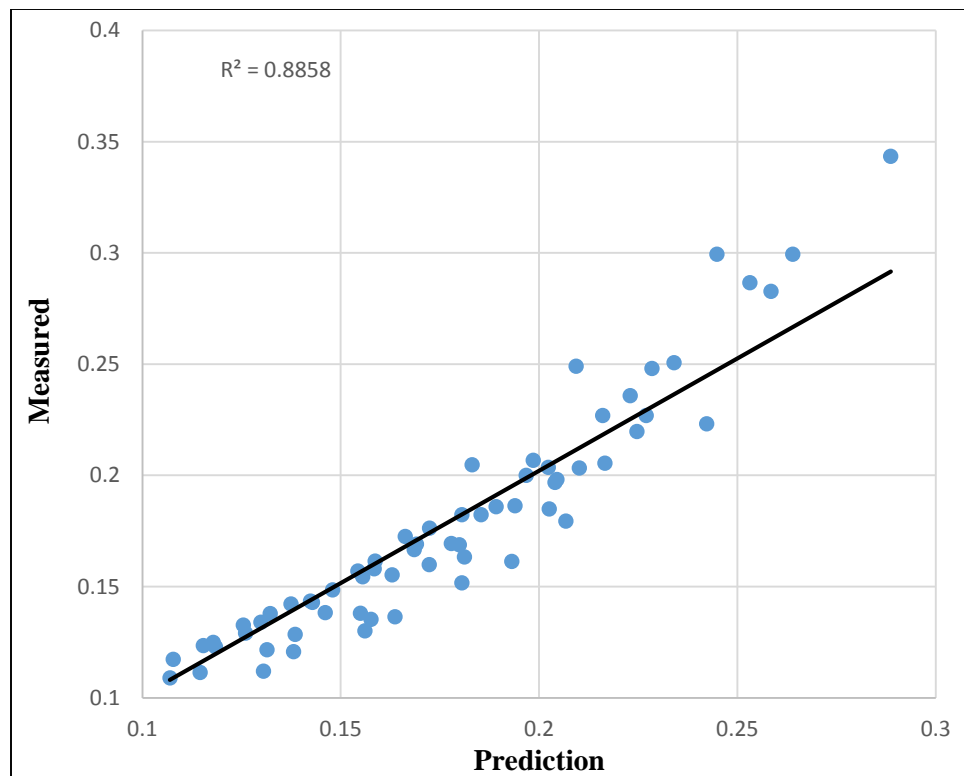


Figure (5-19) Comparisons between the observed and predicted passing ratio  $\left(\frac{M_f}{M_g}\right)$

*Chapter Six*  
*Conclusions and Recommendations*

## *Chapter Six*

### *Conclusions and Recommendations*

#### **6.1 Introduction**

The conclusions of the study are presented in this chapter. The conclusions depend on the results shown in the previous chapter. The present study was to investigate the mechanisms of passing sediments from gully with filter and gully without filter during raining.

#### **6.2 Conclusions**

Depending on the results extracted from the current research and the limit of the variable considered, the following points summarize the most significant results and conclusions.

- 1- It was observed that the bed slope had significant effects on the amount of the passing ratio ( $Mf/Mg$ ). The passing ratio ( $Mf/Mg$ ) was 35% for minimum slope of ground and 11% for maximum slope.
- 2- The results showed that the importance of the length of filter, where the passing ratio decreases when the length of filter in filed is more than 400mm.
- 3- The change in diameter of sediments is directly commensurate to the efficiency of filter, where the passing ratio at 0.1mm and 0.3mm diameter of sediments is 12% and 37% respectively.
- 4- The duration of intensity have the minimum correlation with the passing ratio ( $Mf/Mg$ ) from other variables, while the maximum correlation with passing ratio ( $Mf/Mg$ ) occurred in bed slope.



- 5- The results show that the passing ratio from ( $Mf/Mg$ ) is 35% for minimum rainfall intensity of  $30 \text{ mmh}^{-1}$  and 12.5% for maximum rainfall intensity  $58 \text{ mmh}^{-1}$ .
- 6- A comparison between the results of the physical model and the numerical model indicates that the FLOW-3D model was able to simulate the success rate with an error rate of less than 16%.
- 7- The using of SPSS model to estimate the passing ratio gives result that agree with ( $R^2 = 0.88$ ).

## **6.2 Recommendations**

The following suggested for future researchers and recommendations:

- 1- This study is limited to this filter (effective size=1.5mm , uniformity coefficient=1.2 , porosity=0.27 , permeability=1.13 cm/sec)
- 2- Experimental work can be extended to study the effect of new variables such as the type of grade gravel used in the filter.
- 3- To apply this study in the storm networks, it must be kept in mind that made the gully without filter containing two basins for the process of washing to prevent clogging the filter are used.
- 4- New variables can be used to simulate rainfall, such as the effect of wind and rainfall angle.

## **References**

Hafzullah Aksoy.H ,Erdem.U and Sevket.C ., (2012) ‘A rainfall simulator for laboratory-scale assessment of rainfall-runoff-sediment transport processes over a two-dimensional flume’, *Catena*. Elsevier B.V., 98, pp. 63–72. doi: 10.1016/j.catena.2012.06.009.

Alavinia, M., Saleh, F. N. and Asadi, H. (2018) ‘Effects of rainfall patterns on runoff and rainfall-induced erosion’, international journal of sediment research. Elsevier b.v., pp. 1–9. doi: 10.1016/j.ijsrc.2018.11.001.

Astm (2007) *D422–63 (2007)* standard test method for particle-size analysis of soils, astm international, west Conshohocken. doi.

ASTM (2006) ‘Standard test method for permeability of granular soils (constant head) using water picnometer’, ASTM international, west Conshohocken, pa. doi: 10.1520/c0577-07r14.2.

ASTM (2010) ‘D4404. Standard test method for determination of pore volume and pore volume distribution of soil and rock by mercury intrusion porosimetry’, Astm International. doi: 10.1520/D4404-10.tion.

ASTM Standard D7263-09 (2009) ‘Standard test methods for laboratory determination of density (unit weight) of soil specimens’, *ASTM International*. doi: 10.1520/D7263-09.2.

Butterfield, R. (1999) ‘Dimensional analysis for geotechnical engineers’, *Geotechnique*. Thomas Telford Ltd, 49(3), pp. 357–366.

Capozzoli, A., Grassi, D. and Causone, F. (2015) ‘Estimation models of heating energy consumption in schools for local authorities planning’, *Energy and Buildings*. Elsevier, 105, pp. 302–313.

Cerdà, A., Ibáñez, S. and Calvo, A. (1997) ‘Design and operation of a small and portable rainfall simulator for rugged terrain’, *Soil Technology*. doi: 10.1016/S0933-3630(96)00135-3.

Chai, T. and Draxler, R. R. (2014) ‘Root mean square error (RMSE) or mean absolute error (MAE)?–Arguments against avoiding RMSE in the literature’, *Geoscientific model development*. Copernicus GmbH, 7(3), pp. 1247–1250.

## **References**

Charles R. Fleischmann (2005) , United states patent ( 10 ) patent no .:street curb drain filter’, 2(12). doi: 10.1016/j.(73).

Christophe, F., Sell, R. and Coatanéaa, E. (2008) ‘Conceptual design framework supported by dimensional analysis and system modelling language.’, *Estonian journal of engineering*, 14(4).

Chughtai, F. and Zayed, T. (2008) ‘Infrastructure condition prediction models for sustainable sewer pipelines’, *journal of performance of constructed facilities*. doi: 10.1061/(asce)0887-3828(2008)22:5(333).

D. Moore, I., C. Hirschi, M. and J. Barfield, B. (1983) ‘Kentucky rainfall Simulator’, *Transactions of the ASAE*. St. Joseph, MI: ASAE, 26(4), pp. 1085–1089. doi: <https://doi.org/10.13031/2013.34081>.

Defersha, M. B. and Melesse, A. M. (2012) ‘Effect of rainfall intensity, slope and antecedent moisture content on sediment concentration and sediment enrichment ratio’, *Catena*. Elsevier B.V., 90, pp. 47–52. doi: 10.1016/j.catena.2011.11.002.

Douglas C. Montgomery, G.C.R., N. F. H. (2011) *Engineering statistics*. fifth edit. arizona state university.

Earl Roger Singleton (2004), United states patent,curb inlet filter’, 1(12). doi: 10.1038/incomms1464.

Earl Roger Singleton, O. (2006), United States Patent cellular libraries of peptide ( 10 ) Patent N0 .: ( 45 ) Date of Patent ’:, 2(12).

Fernández-Gálvez, J., Barahona, E. and Mingorance, M. D. (2008) ‘Measurement of infiltration in small field plots by a portable rainfall simulator: Application to trace-element mobility’, *water, air, and soil pollution*. doi: 10.1007/s11270-008-9622-2.

Fister, W. *et al.* (2012) ‘A portable wind and rainfall simulator for in situ soil erosion measurements’, *Catena*. doi: 10.1016/j.catena.2011.03.002.

FLOW3D user’s manual (2014) ‘User Manual’.

Foster, I. D. L. *et al.* (2000) ‘Drip-screen rainfall simulators for hydro- and pedo-geomorphological research: The coventry experience’, in *Earth Surface Processes and Landforms*. doi: 10.1002/1096-9837(200007)25:7<691::AID

## **References**

George W. Murfae (1992) ‘United states patent (19) 54’, 96(19), pp. 62–66. doi: us005485919a.

Grant R. Emery (1995) ‘United States Patent (19) 54,Curb inlet gravel sediment filter’, 96(19), pp. 62–66. doi: US005485919A.

Grierson, I. T. and Oades, J. M. (1977) ‘A rainfall simulator for field studies of run-off and soil erosion’, *Journal of agricultural engineering research*. doi: 10.1016/0021-8634(77)90091-9.

Grismer, M. E. (2011) ‘Rainfall simulation studies – a review of designs , performance and erosion measurement variability’, TSC Rainsim workshop, p. 110.

Guy, B., WT, D. and Rudra, R. (1987) ‘The Roles of Rainfall and Runoff in the Sediment Transport Capacity of Interrill Flow’, *Transactions of the American Society of Agricultural Engineers*, 30(5), pp. 1378–1386. doi: 10.1039/c5py00012b.

Happel, H. (2004)‘United States Patent applit is , \* cited by examiner,catch basin filter for stormwater runoff’, 2(12).

Hatt, B. E., Fletcher, T. D. and Deletic, A. (2007) ‘Treatment performance of gravel filter media: Implications for design and application of stormwater infiltration systems’, *Water Research*, 41(12), pp. 2513–2524. doi: 10.1016/j.watres.2007.03.014.

Hirt, C. W. and Nichols, B. D. (1981) ‘Volume of fluid (VOF) method for the dynamics of free boundaries’, *Journal of Computational Physics*. doi: 10.1016/0021-9991(81)90145-5.

Holický, M. (2013) *Introduction to probability and statistics for engineers, Introduction to Probability and Statistics for Engineers*. doi: 10.1007/978-3-642-38300-7.

Hyndman, R. J. (2010) ‘Measuring forecast accuracy’, *Journal of business forecasting methods & systems*. doi: 10.1007/s11336-007-9039-7.

Kaatz, K. J. and James, W. P. (2002) ‘Analysis of Alternatives for Computing Backwater at Bridges’, *Journal of Hydraulic Engineering*. doi: 10.1061/(asce)0733-9429(1997)123:9(784).

## **References**

Kincaid, D., Solomon, K. and Oliphant, J. C. (1996) ‘Drop size distributions for irrigation sprinklers’, *Transactions of the ASAE*. doi: 10.13031/2013.32550.

Larry James Allen; Bridgette Lyniece Allen (2000) ‘United States Patent ( 19 FIG-2),PLASTIC SELF-RELIEVING CURB INLET FILTER’, (19).

Montagu T. Chinn and Geralde M. Chinn,. (1997) ‘United States Patent (19)’, (19).

Myttenaere, A., Grand, C., and Golden, B,. (2016) ‘Mean absolute percentage error for regression models’, *Neurocomputing*. Elsevier, 192, pp. 38–48.

Proce-, C. U. H. and Method, R. H. (2001) ‘Ethod for’, (1), pp. 352–356.

Siriwardene, N. R., Deletic, A. and Fletcher, T. D. (2007) ‘Clogging of stormwater gravel infiltration systems and filters: Insights from a laboratory study’, *Water Research*, 41(7), pp. 1433–1440. doi: 10.1016/j.watres.2006.12.040.

Siriwardene, Nilmini R., Deletic, A. and Fletcher, T. D. (2007) ‘Modeling of sediment transport through stormwater gravel filters over their lifespan’, *Environmental science and technology*, 41(23), pp. 8099–8103. doi: 10.1021/es062821v.

Thomas E. Hegemier (1993) ‘Stormwater inlet filter’. United States Patent (19)., doi: US005485919A.


Wilson, T. G.,Cortis. C and Montaldo. N,. (2014) ‘Development and testing of a large, transportable rainfall simulator for plot-scale runoff and parameter estimation’, *Hydrology and Earth System Sciences*, 18(10), pp. 4169–4183. doi: 10.5194/hess-18-4169-2014.


# Appendix

## Steps of model work

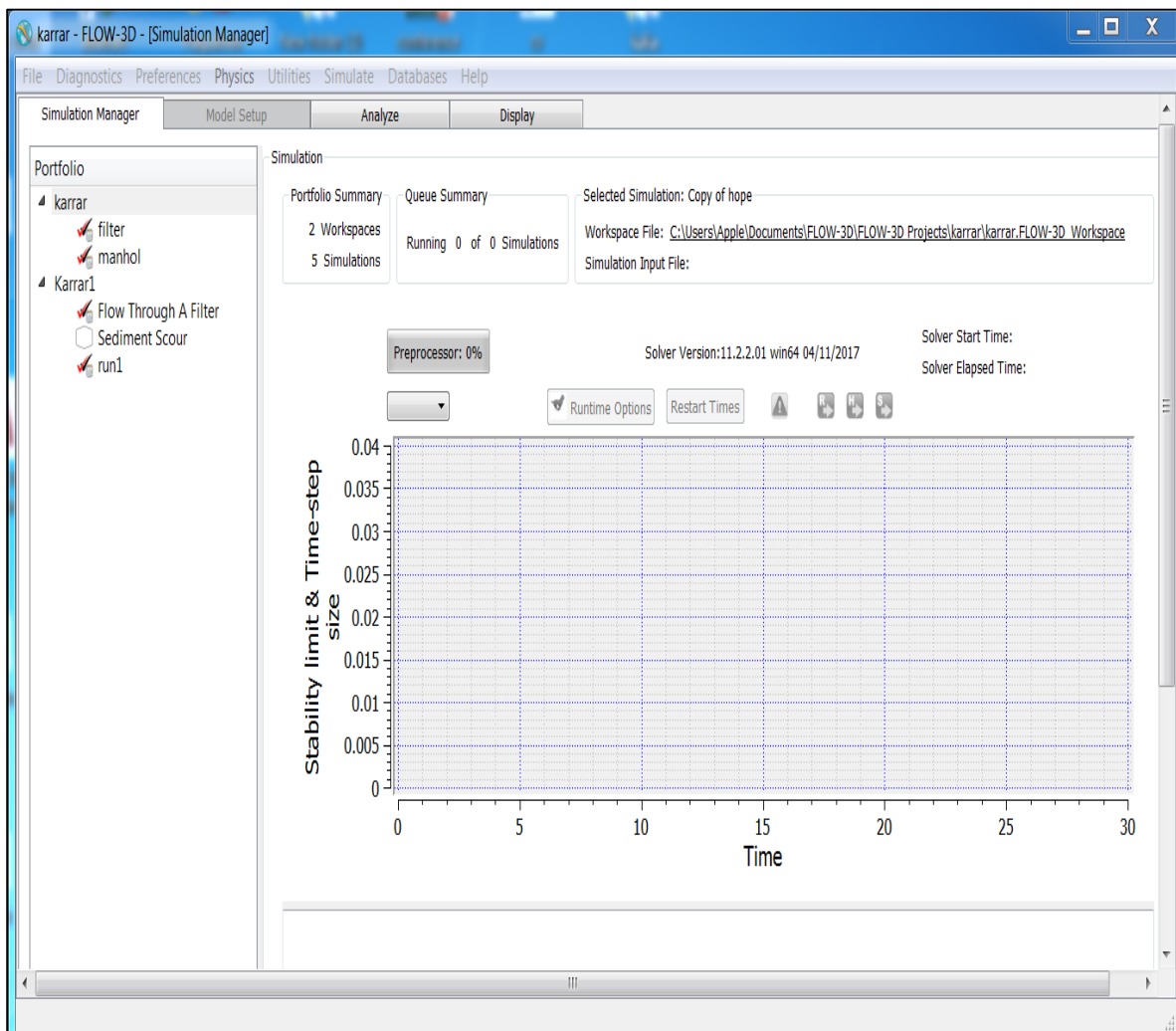
To create a new simulation follow these steps:-

- 1) Go to simulation manager
- 2) Right click on the portfolio part then:-

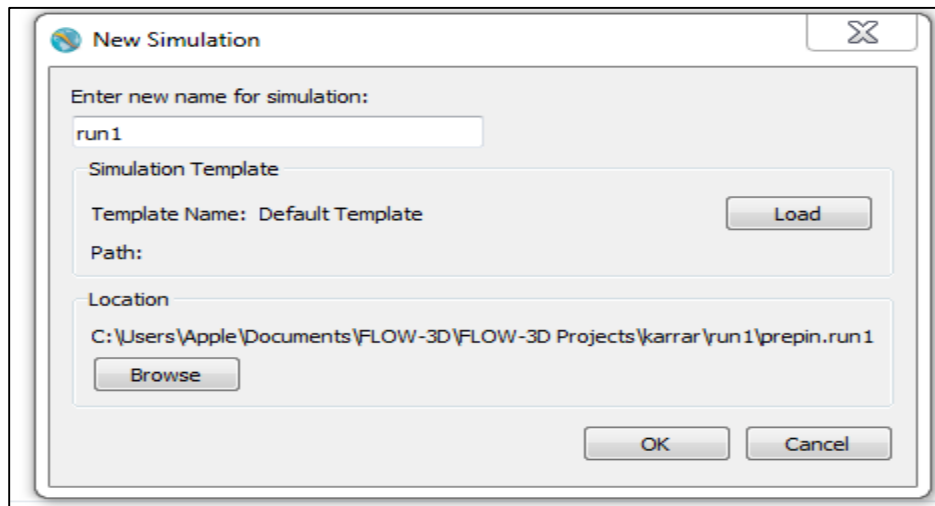
select  Add new simulation, then



Enter the name of the new simulation  Run1 then click ok

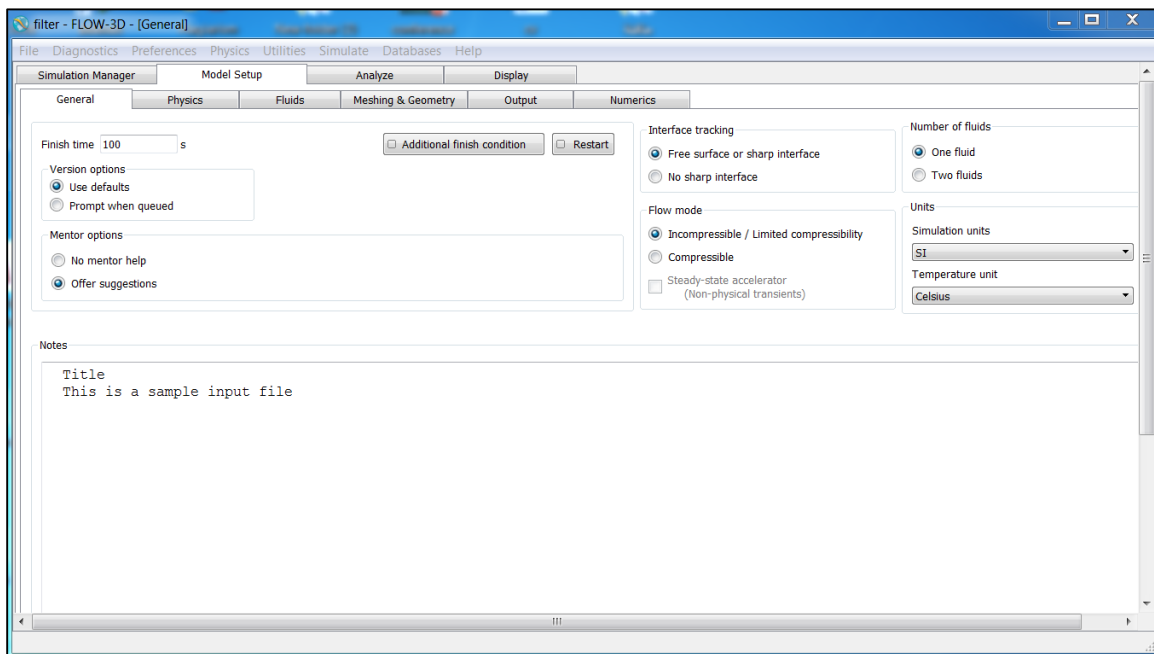
From the browse icon select the location save of file in hard



# Appendix



After that go to  model setup  General  
and adjust the following parameter



Finish time  unstable

Flow mode  Incompressible

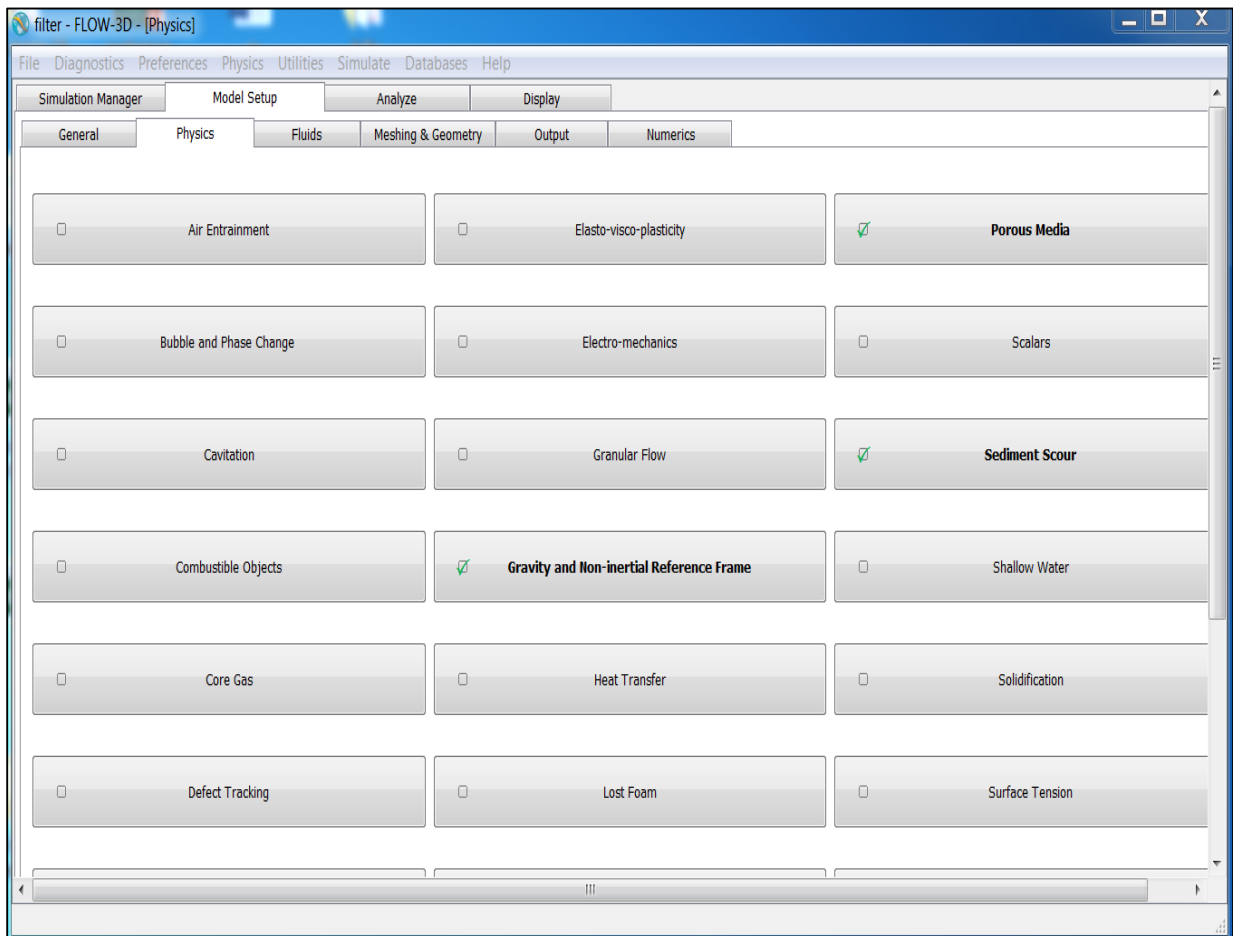
# Appendix

Number of fluids  $\longrightarrow$  one fluid

Simulation units  $\longrightarrow$  SI

Temperature unit  $\longrightarrow$  Celsius

After that from same choice go to  $\longrightarrow$  Physics and active the following characteristic

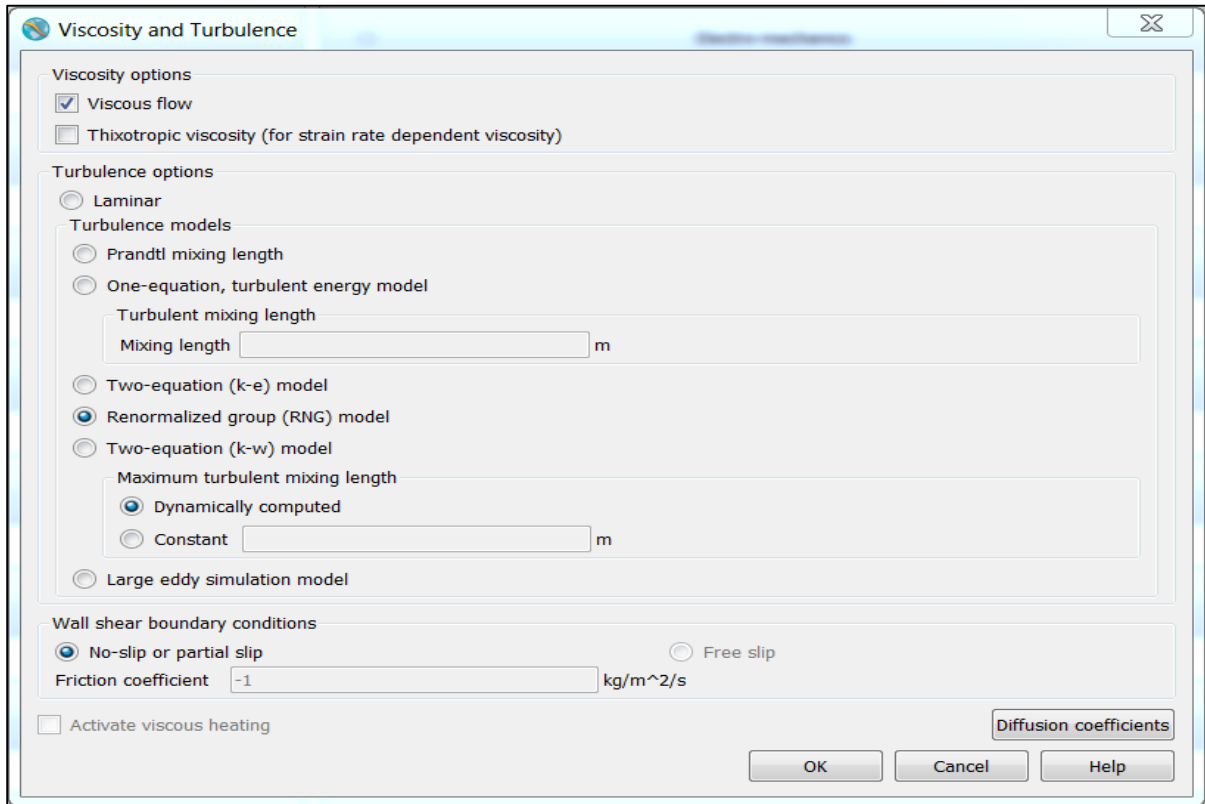


Gravity and non-inertial references frame  $\longrightarrow$  -9.81 in **Z** component

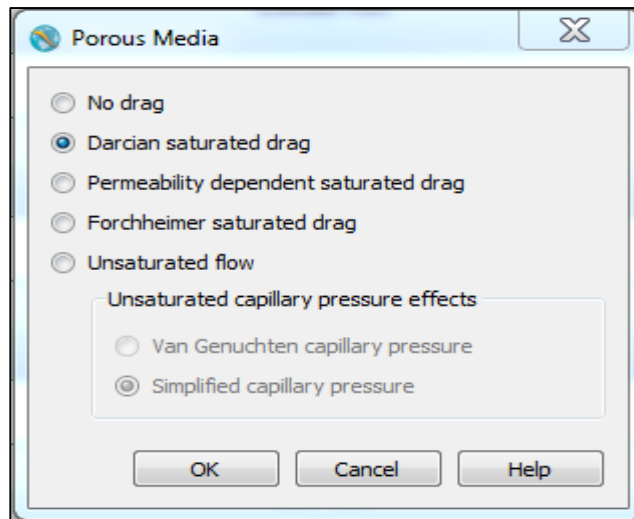
Viscosity and turbulence  $\longrightarrow$  Renormalized group (RNG) model



# Appendix

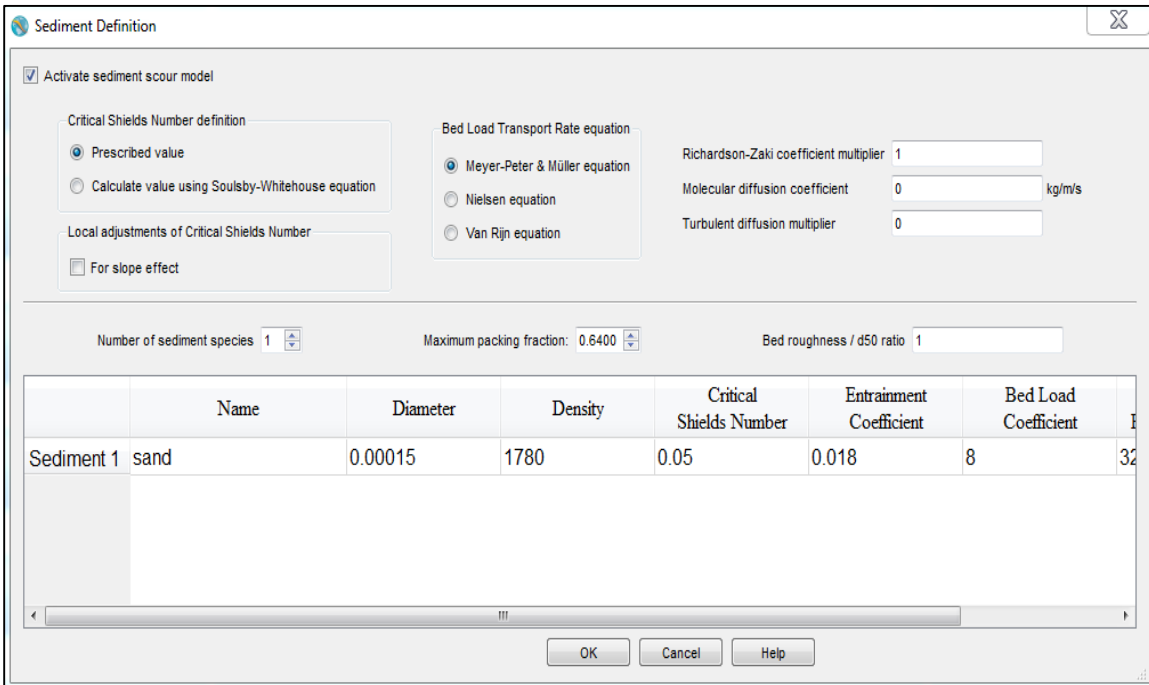


Porous media  $\longrightarrow$  Darcian saturated drg



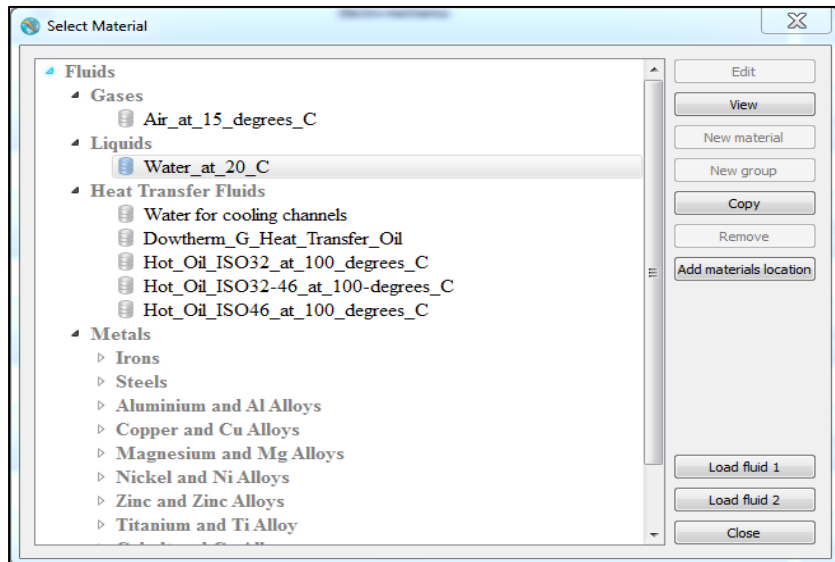
# Appendix

Sediments scour  $\longrightarrow$  Activate sediments scour



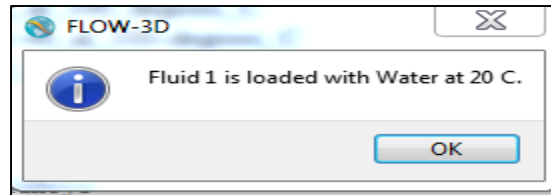
Then go to the fluid  $\longrightarrow$  Materials  $\longrightarrow$  Materials Fluids database  $\longrightarrow$  Overwrite existing material parameters  $\longrightarrow$


press ok  $\longrightarrow$  Select water at 20 C  $\longrightarrow$  Load fluid

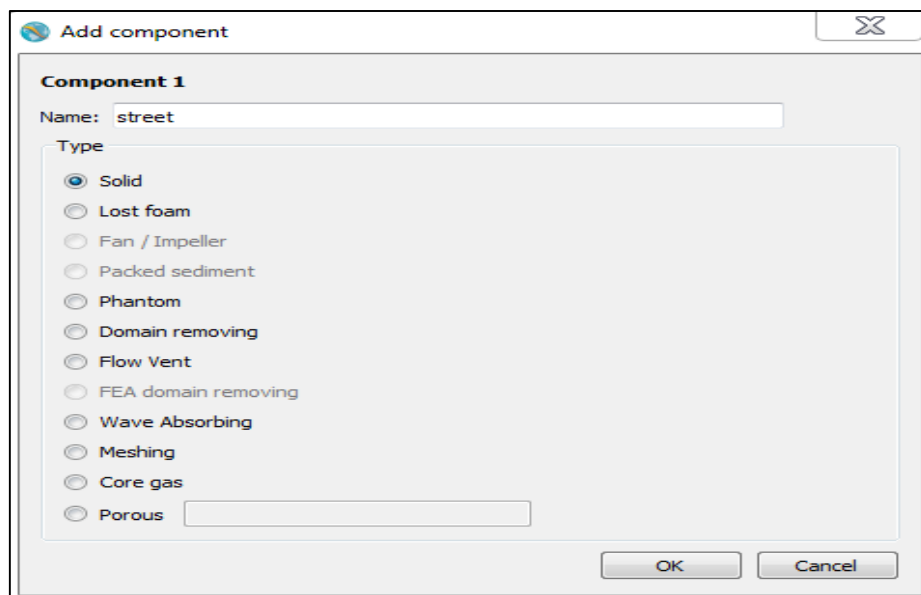


## Appendix

After that a message will appear show that the fluid 1 is loaded

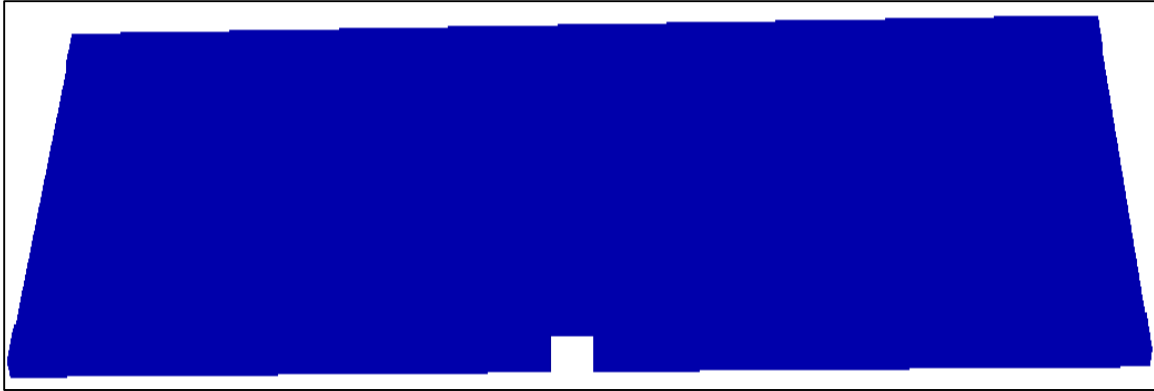


After that go to  Meshing & Geometry Then create the subcomponent of the street, the type of component was selected as solid

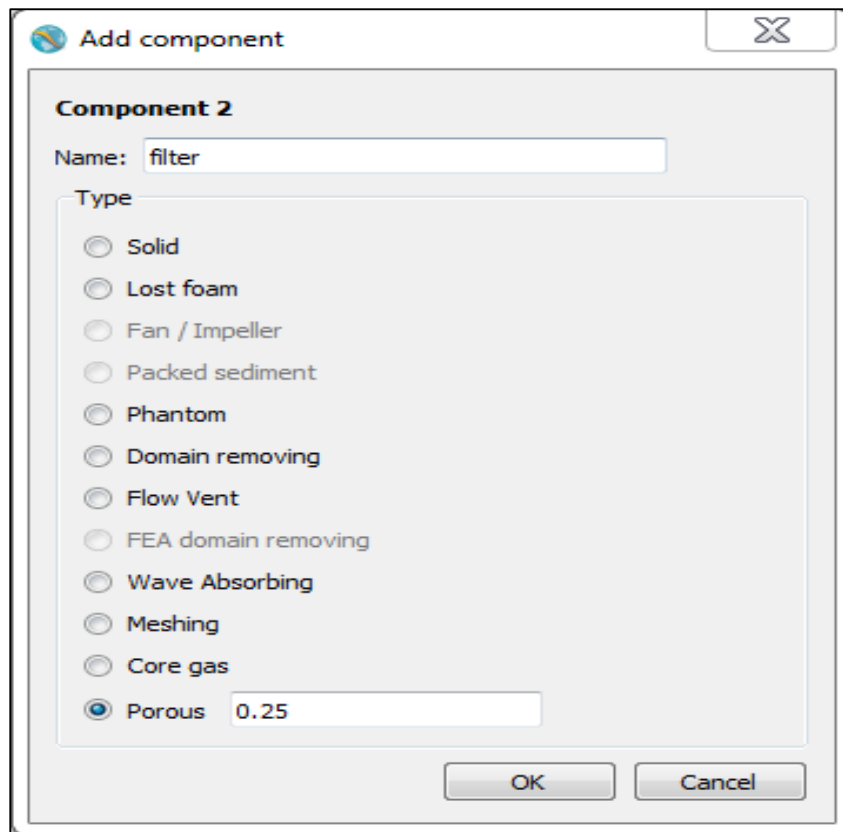


After the particle is installed, the shape of the street in lane that contain the manhole is as follows

## Appendix

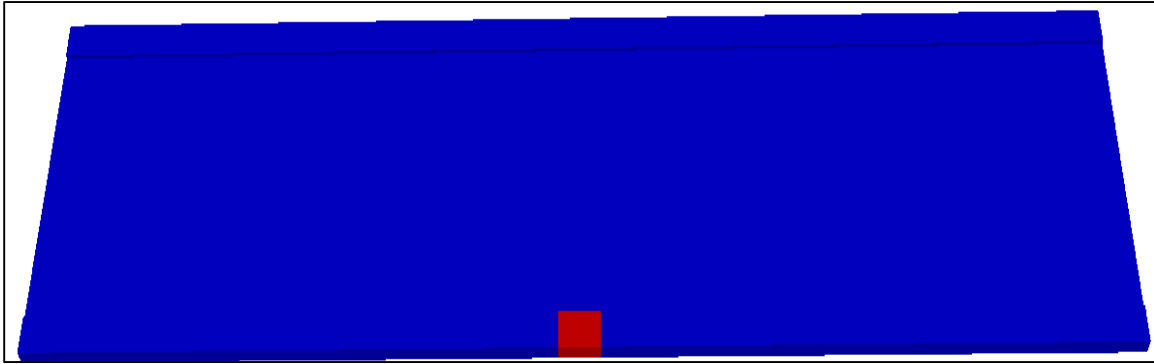


Then create the subcomponent of the filter, the type of component was selected as porous

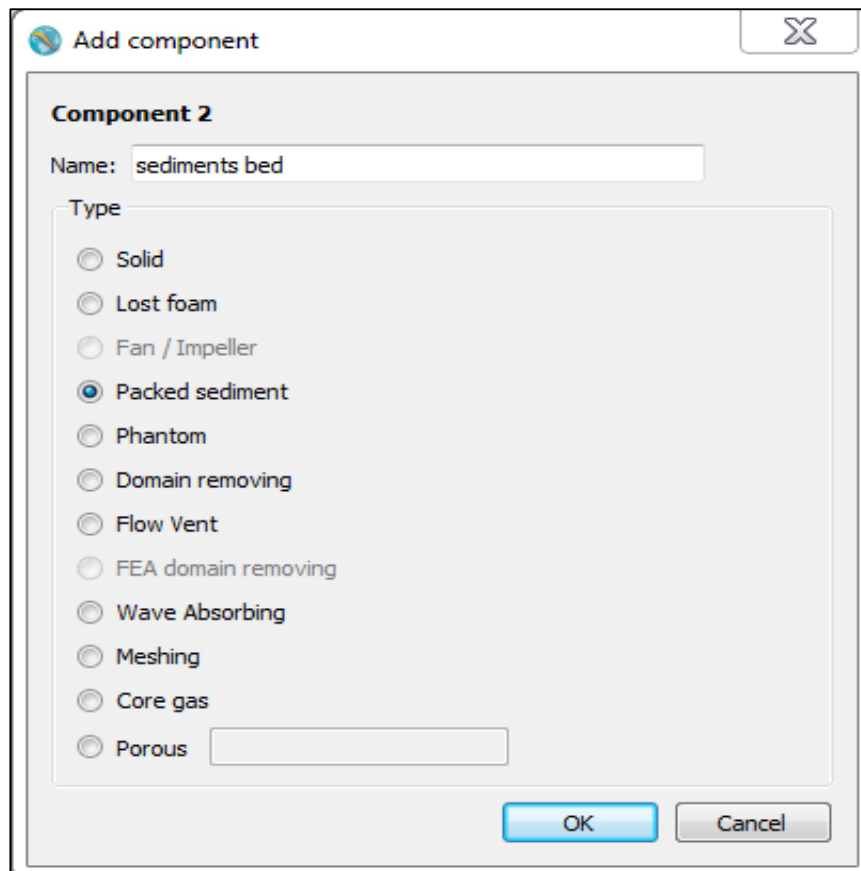


After the filter is installed, the shape of the street in lane that contain the filter is as follow

## Appendix

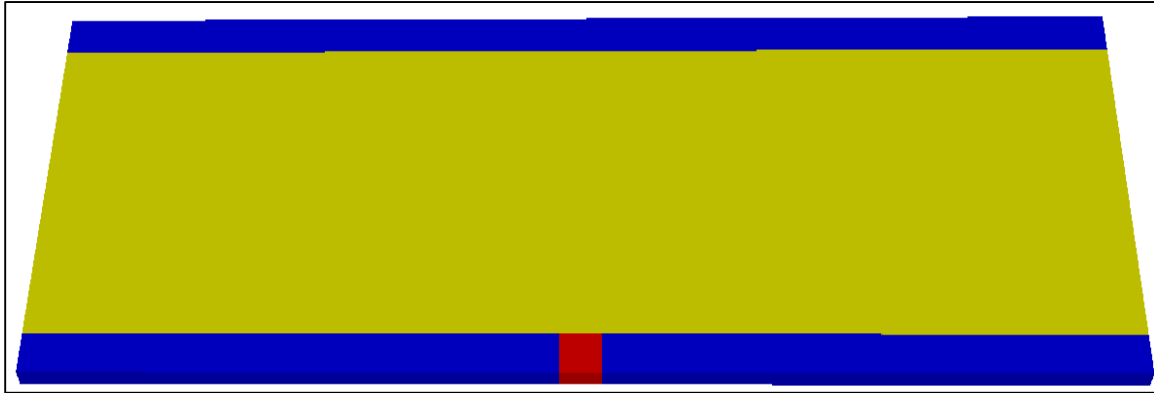


Then create the subcomponent of the sediments bed, the type of component was selected as packed sediments

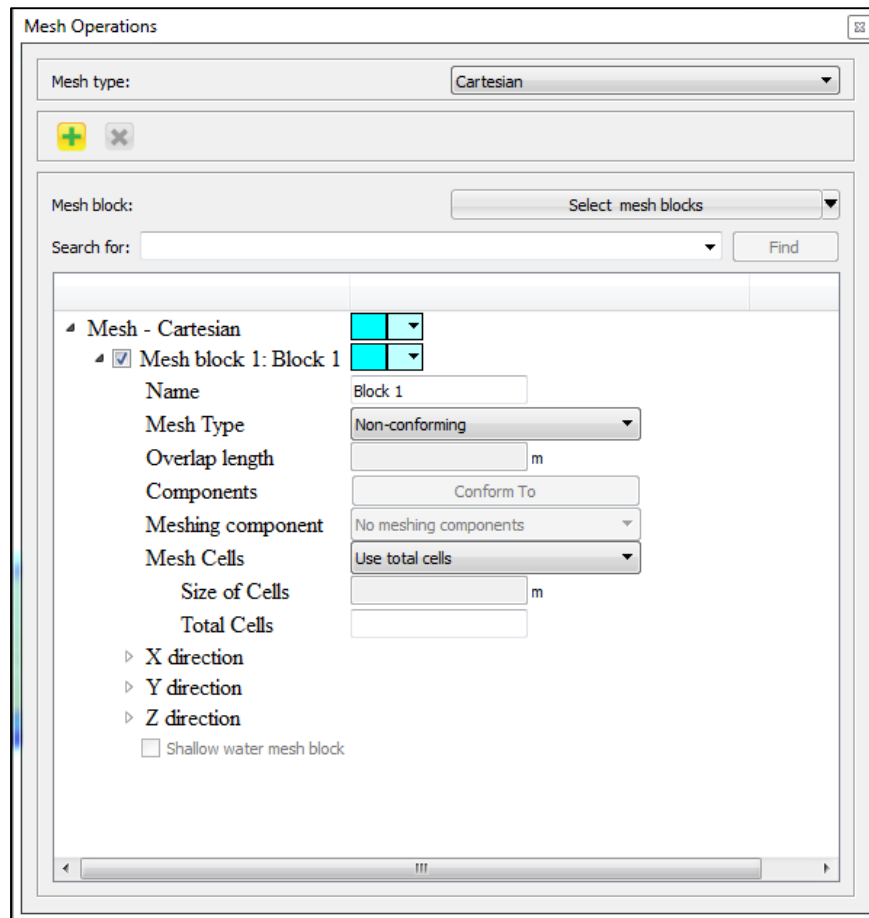


Place the sediments layer above the street as shown below

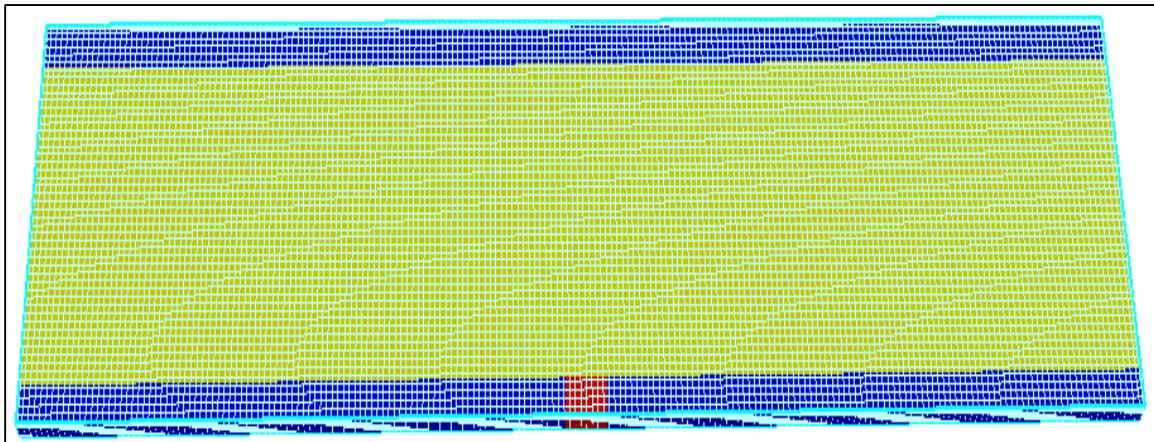
# Appendix



Then create mesh block by using snap to geometry and set the grid size 5mm



# Appendix



Then define the boundary condition in case of (Y min , Y max , X max ) define as wall while Z max define as (symmetry), Z min define as outflow and ,X min define as velocity flow .

Mesh block 1: Block 1 [X Min Boundary]

Boundary type

Symmetry     Continutive     Specified pressure     Grid overlay     Wave  
 Wall     Periodic     Specified velocity     Outflow     Volume flow rate

Velocity  
 X Velocity: 0.0587 m/s  
 Y Velocity: m/s  
 Z Velocity: m/s

Pressure Pa  
 Stagnation pressure  
 Wave absorbing layer  
 Length: m  
 Damping coefficient at wave approach face: 0 1/s  
 Damping coefficient at boundary: 1 1/s  
 Background stream velocity: User prescribed  
 Stream velocity in X: 0 m/s  
 Stream velocity in Y: 0 m/s  
 Stream velocity in Z: 0 m/s  
 Time scale: Code calculated s

Density kg/m<sup>3</sup>  
 Volume fraction of entrained air  
 Alloy solute concentration kg/m<sup>3</sup>  
 Dissolved solute concentration kg/m<sup>3</sup>  
 Dispersed phase drop diameter m

Non-condensable gas volume fraction 0  
 Relative saturation 0

Sediment  
 Scalars

Use fluid elevation  
 Fluid fraction 1  
 Fluid elevation 0.0003 m  
 Rating Curve m  
 Natural inlet, automatic flow regime  
 Natural inlet, sub-critical flow  
 Natural inlet, super-critical flow  
 Natural inlet, critical flow  
 Min. elevation:  
 Max. elevation:

Electric Charge Coul/m<sup>3</sup>  
 Specified potential boundary  
 Electric potential kg-m<sup>2</sup>/Coul/s<sup>-2</sup>

Turbulence quantities    Thermal information

OK    Cancel

# Appendix

Mesh block 1: Block 1 [Y Min Boundary]

Boundary type

Symmetry     Continuitive     Specified pressure     Grid overlay     Wave  
 Wall     Periodic     Specified velocity     Outflow     Volume flow rate

Velocity

X Velocity:  m/s  
 Y Velocity:  m/s  
 Z Velocity:  m/s

Pressure  Pa  
 Stagnation pressure

Wave absorbing layer

Length  m  
 Damping coefficient at wave approach face  1/s  
 Damping coefficient at boundary  1/s  
 Background stream velocity  User prescribed

Stream velocity in X  m/s  
 Stream velocity in Y  m/s  
 Stream velocity in Z  m/s  
 Time scale  Code calculated  s

Density  kg/m<sup>3</sup>  
 Volume fraction of entrained air   
 Alloy solute concentration  kg/m<sup>3</sup>  
 Dissolved solute concentration  kg/m<sup>3</sup>  
 Dispersed phase drop diameter  m

Non-condensable gas volume fraction  0

Sediment   
 Scalars

Relative saturation  0

Use fluid fraction     
 Fluid fraction  1  
 Fluid elevation  -1.0e+10 m  
 Rating Curve  m  
 Natural inlet, automatic flow regime  
 Natural inlet, sub-critical flow  
 Natural inlet, super-critical flow  
 Natural inlet, critical flow  
 Min. elevation:   
 Max. elevation:

Electric Charge  Coul/m<sup>3</sup>  
 Specified potential boundary  
 Electric potential  kg-m<sup>2</sup>/Coul/s<sup>2</sup>

Turbulence quantities Thermal information

OK Cancel

Mesh block 1: Block 1 [Z Min Boundary]

Boundary type

Symmetry     Continuitive     Specified pressure     Grid overlay     Wave  
 Wall     Periodic     Specified velocity     Outflow     Volume flow rate

Allow fluid to enter at outflow boundary

Pressure  Pa  
 Stagnation pressure

Wave absorbing layer

Length  m  
 Damping coefficient at wave approach face  1/s  
 Damping coefficient at boundary  1/s  
 Background stream velocity  User prescribed

Stream velocity in X  m/s  
 Stream velocity in Y  m/s  
 Stream velocity in Z  m/s  
 Time scale  Code calculated  s

Density  kg/m<sup>3</sup>  
 Volume fraction of entrained air   
 Alloy solute concentration  kg/m<sup>3</sup>  
 Dissolved solute concentration  kg/m<sup>3</sup>  
 Dispersed phase drop diameter  m

Non-condensable gas volume fraction  0

Sediment   
 Scalars

Relative saturation  0

Use fluid fraction     
 Fluid fraction  1  
 Fluid elevation  -1.0e+10 m  
 Rating Curve  m  
 Natural inlet, automatic flow regime  
 Natural inlet, sub-critical flow  
 Natural inlet, super-critical flow  
 Natural inlet, critical flow  
 Min. elevation:   
 Max. elevation:

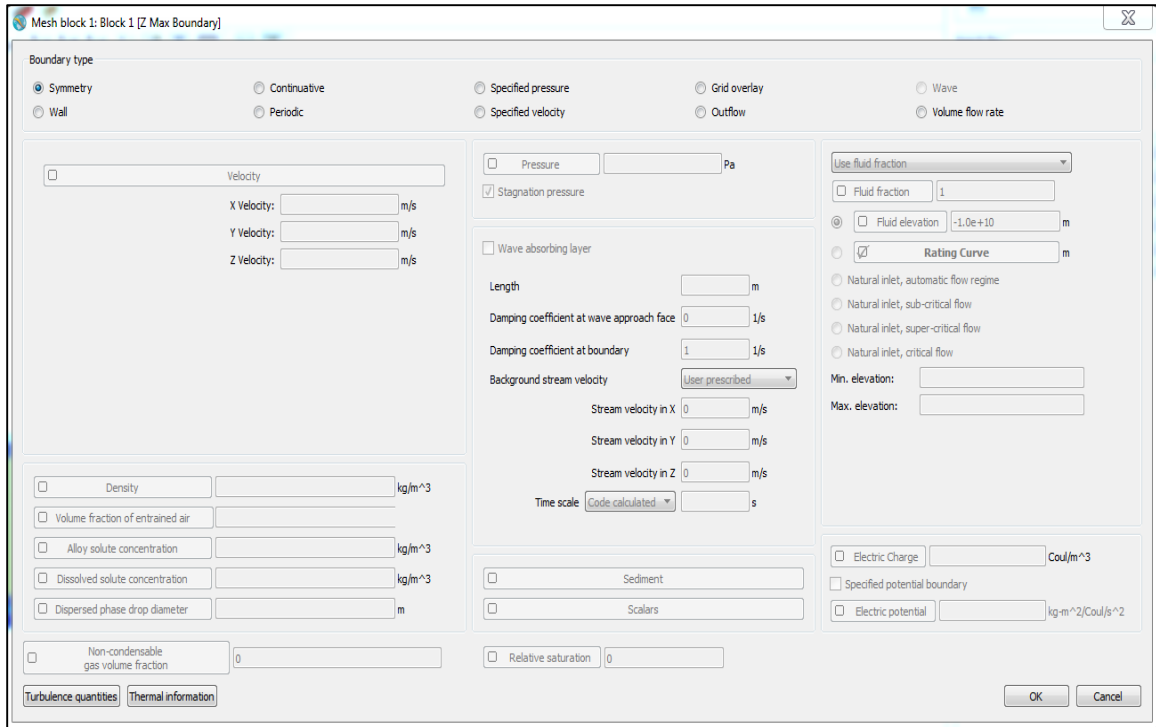
Electric Charge  Coul/m<sup>3</sup>  
 Specified potential boundary  
 Electric potential  kg-m<sup>2</sup>/Coul/s<sup>2</sup>

Turbulence quantities Thermal information

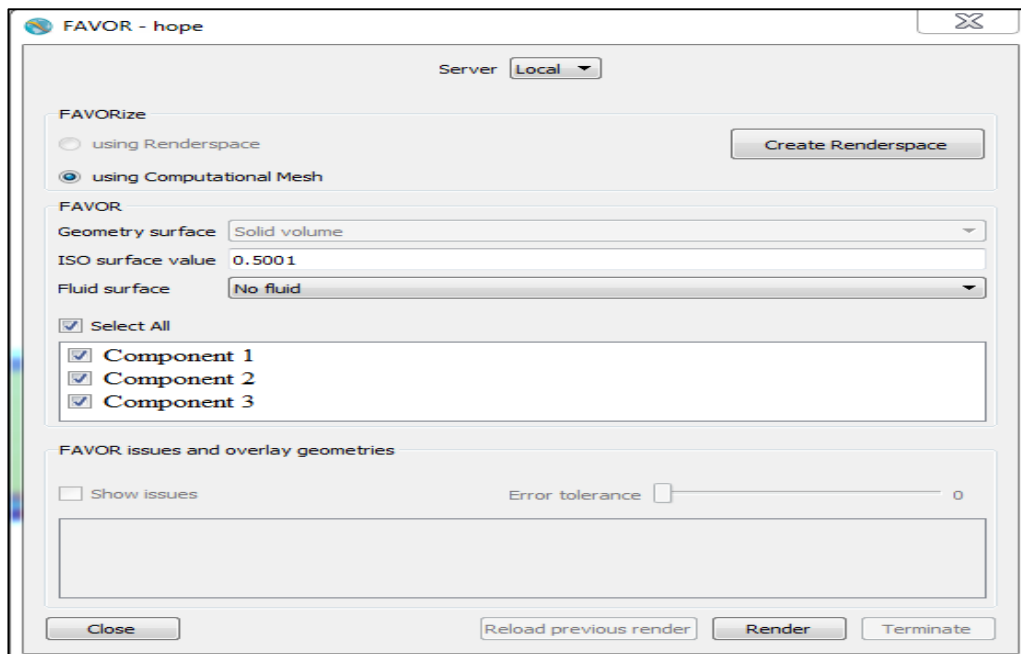
OK Cancel



# Appendix

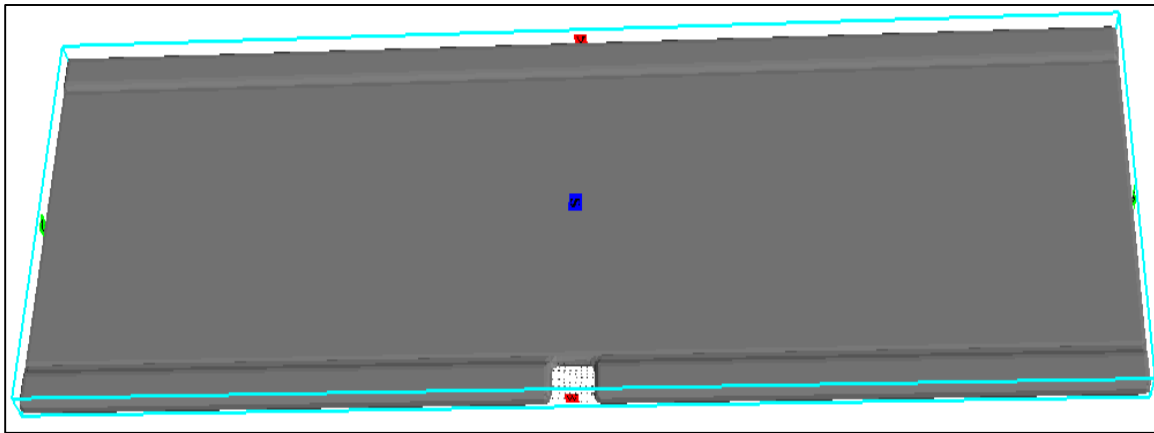


Then to test the effective of the creative mesh use the FAVOUR option to show what the mesh capture for the plan

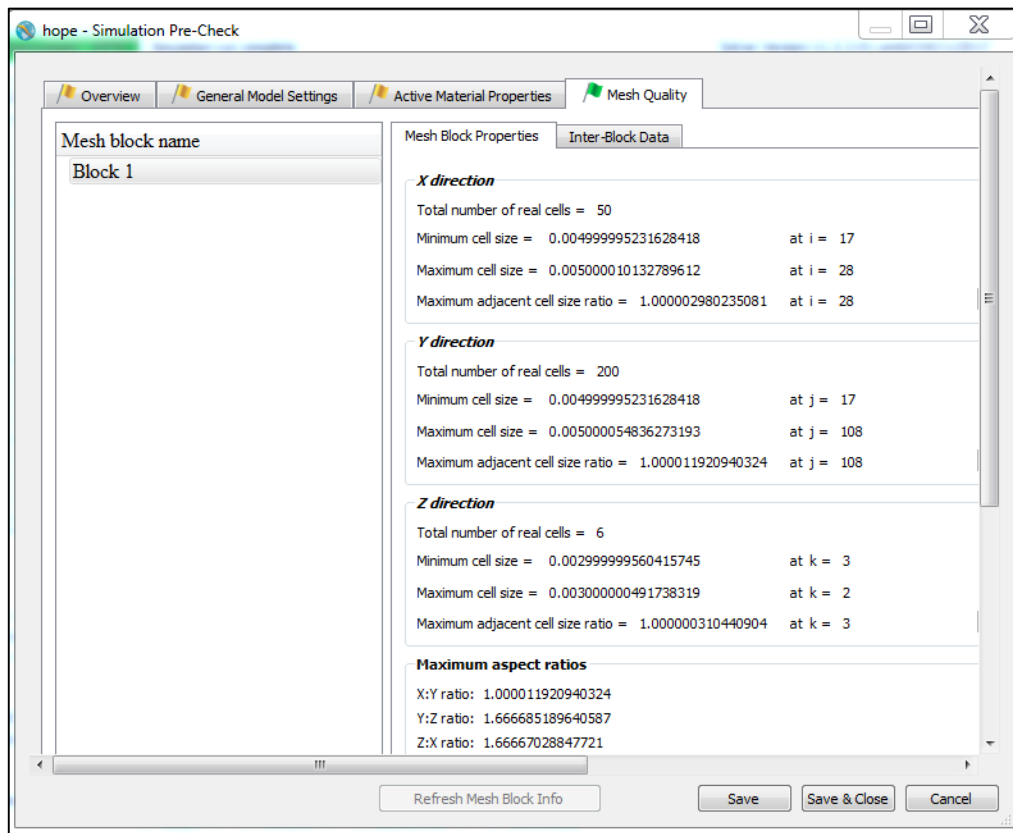


# Appendix

When render the favor give

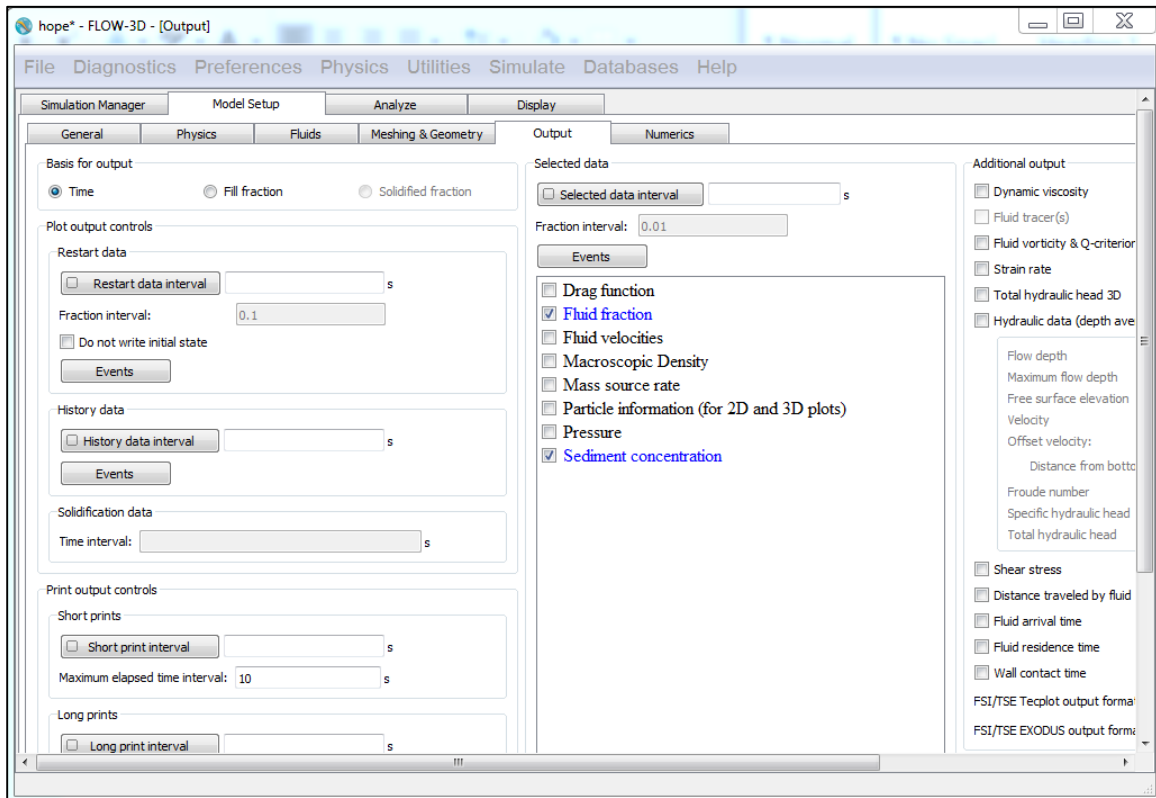


Also, from (the simulate pre-check) the cell aspect ratio could use to validation from the creative mesh as well as the closer the number to 1 the best of the accuracy.

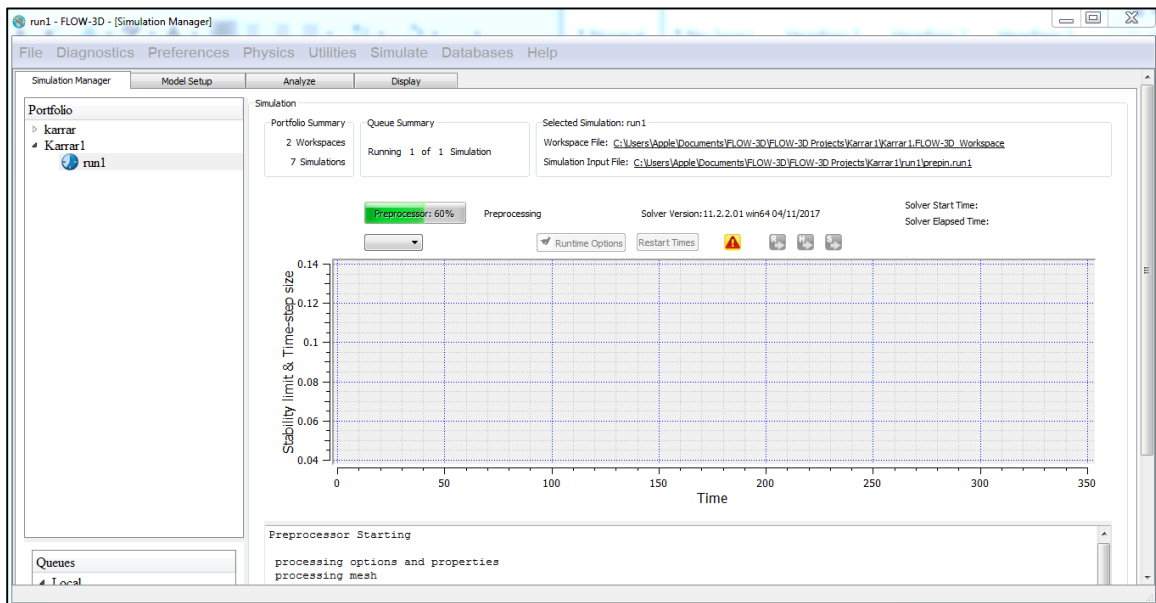


# Appendix


Then active the required out put

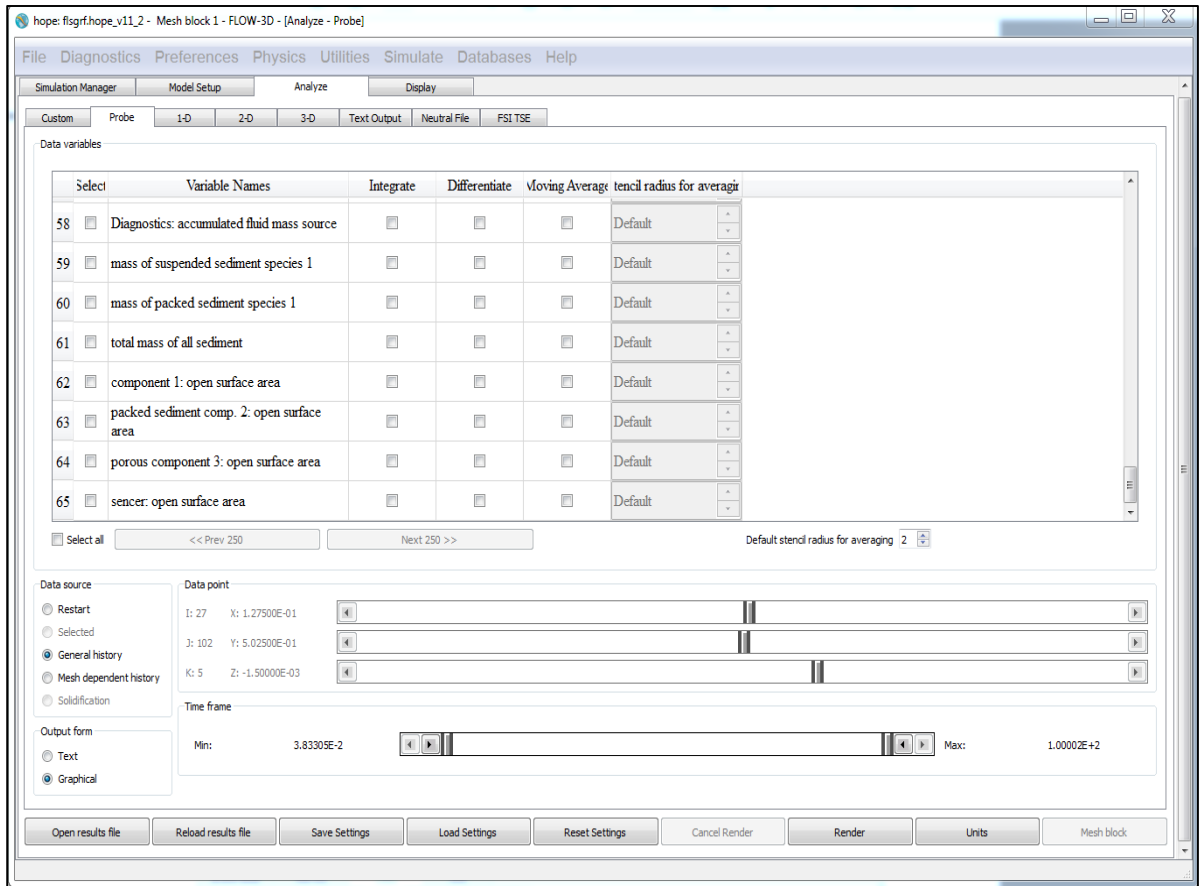


Then right click on the Run1 and press on the run simulate Local



# Appendix

In the end of run simulation can show any result by press  probe



## Appendix

### FLOW-3D passing ratio results versus measured in experimental work

<b>Run</b>	<b>Measured</b>	<b>Flow-3D</b>	<b>% Error</b>
1	0.389380531	0.357200322	-9.009009
2	0.310175439	0.319723183	2.986253
3	0.282111437	0.251217637	-12.29762
4	0.244259893	0.213037921	-14.65559
5	0.237442922	0.201930502	-17.58646
6	0.305555556	0.299363057	-2.068558
7	0.255877897	0.249103024	-2.719707
8	0.196927803	0.204792332	3.840246
9	0.176380368	0.172619048	-2.178972
10	0.165249607	0.161499143	-2.322281
11	0.262564103	0.250691244	-4.736049
12	0.207317073	0.206766917	-0.266075
13	0.166019417	0.176291793	5.826917
14	0.150704225	0.15443038	2.412838
15	0.136159601	0.148491879	8.305018
16	0.236220472	0.21969697	-7.521042
17	0.182261506	0.185918927	1.967213
18	0.151658768	0.155339806	2.369668
19	0.12596707	0.138401157	8.984092
20	0.112784588	0.128623853	12.31441
21	0.205498473	0.205749847	0.122175
22	0.161220044	0.163398693	1.333333
23	0.137184116	0.138086643	0.653595
24	0.113468907	0.120837017	6.09756
25	0.105665349	0.11198946	5.647059
26	0.342105263	0.382488479	10.55802
27	0.277777778	0.313157895	11.29785
28	0.213782051	0.253799392	15.76731
29	0.191374663	0.217721519	12.10117
30	0.168691589	0.200928074	16.04379
31	0.316315789	0.299539171	5.600809
32	0.246808511	0.248120301	0.528691
33	0.184952978	0.203647416	9.179806
34	0.168432491	0.182278481	7.596064
35	0.151807229	0.16937355	10.37135
36	0.229444444	0.198156682	15.78941

# Appendix

<b>37</b>	<b>0.169067797</b>	<b>0.169172932</b>	<b>0.062146</b>
<b>38</b>	0.142394822	0.142857143	0.323625
<b>39</b>	0.130193906	0.129113924	0.836457
<b>40</b>	0.120987654	0.122969838	1.611927
<b>41</b>	0.177142857	0.161290323	9.828571
<b>42</b>	0.144628099	0.135338346	6.864095
<b>43</b>	0.129568106	0.121580547	6.569767
<b>44</b>	0.11965812	0.111392405	7.420358
<b>45</b>	0.1125	0.109048724	3.164894
<b>46</b>	0.303030303	0.343434343	11.76471
<b>47</b>	0.259166667	0.286666667	9.593023
<b>48</b>	0.220422535	0.226973684	2.886303
<b>49</b>	0.175409836	0.203389831	13.75683
<b>50</b>	0.160633484	0.185	13.17109
<b>51</b>	0.282758621	0.282175862	0.206523
<b>52</b>	0.235882353	0.231588235	1.854204
<b>53</b>	0.182222222	0.2	8.888889
<b>54</b>	0.161923077	0.1688	4.074007
<b>55</b>	0.14516129	0.16	9.274194
<b>56</b>	0.248571429	0.226956522	9.52381
<b>57</b>	0.192028986	0.182432432	5.260333
<b>58</b>	0.151648352	0.157024793	3.423944
<b>59</b>	0.137209302	0.142191142	3.503622
<b>60</b>	0.127083333	0.134095634	5.229328
<b>61</b>	0.217241379	0.196875	10.34483
<b>62</b>	0.166666667	0.167666667	0.596421
<b>63</b>	0.137577002	0.143468951	4.106776
<b>64</b>	0.126415094	0.132692308	4.730654
<b>65</b>	0.113576271	0.125	9.138983

## Appendix C

Data used to building and validated prediction model

<b>Run</b>	<b><math>S_0</math></b>	<b><math>\frac{I * T}{L_f}</math></b>	<b><math>\frac{D_s}{L_f}</math></b>	<b><math>\frac{M_f}{M_g}</math></b>
1	1	0.0375	0.001	0.3572
2	1.5	0.0375	0.001	0.3197
3	2	0.0375	0.001	0.2512
4	2.5	0.0375	0.001	0.213
5	3	0.0375	0.001	0.2019
6	1	0.04625	0.001	0.2994
7	1.5	0.04625	0.001	0.2491
8	2	0.04625	0.001	0.2048
9	2.5	0.04625	0.001	0.1726
10	3	0.04625	0.001	0.1615
11	1	0.055	0.001	0.2507
12	1.5	0.055	0.001	0.2068
13	2	0.055	0.001	0.1763
14	2.5	0.055	0.001	0.1544
15	3	0.055	0.001	0.1485
16	1	0.06375	0.001	0.2197
17	1.5	0.06375	0.001	0.1859
18	2	0.06375	0.001	0.1553
19	2.5	0.06375	0.001	0.1384
20	3	0.06375	0.001	0.1286
21	1	0.0725	0.001	0.2055
22	1.5	0.0725	0.001	0.1634
23	2	0.0725	0.001	0.1381
24	2.5	0.0725	0.001	0.1208
25	3	0.0725	0.001	0.112
26	1	0.11	0.002	0.3825
27	1.5	0.11	0.002	0.3132
28	2	0.11	0.002	0.2538
29	2.5	0.11	0.002	0.2177
30	3	0.11	0.002	0.2009
31	1	0.07333	0.0013	0.2995
32	1.5	0.07333	0.0013	0.2481
33	2	0.07333	0.0013	0.2036
34	2.5	0.07333	0.0013	0.1823
35	3	0.07333	0.0013	0.1694
36	1	0.044	0.0008	0.1982

## Appendix C

<b>37</b>	<b>1.5</b>	<b>0.044</b>	<b>0.0008</b>	<b>0.1692</b>
<b>38</b>	2	0.044	0.0008	0.1429
<b>39</b>	2.5	0.044	0.0008	0.1291
<b>40</b>	3	0.044	0.0008	0.123
<b>41</b>	1	0.03667	0.0007	0.1613
<b>42</b>	1.5	0.03667	0.0007	0.1353
<b>43</b>	2	0.03667	0.0007	0.1216
<b>44</b>	2.5	0.03667	0.0007	0.1114
<b>45</b>	3	0.03667	0.0007	0.109
<b>46</b>	1	0.055	0.0005	0.3332
<b>47</b>	1.5	0.055	0.0005	0.2841
<b>48</b>	2	0.055	0.0005	0.2318
<b>49</b>	2.5	0.055	0.0005	0.2005
<b>50</b>	3	0.055	0.0005	0.18
<b>51</b>	1	0.055	0.0008	0.3069
<b>52</b>	1.5	0.055	0.0008	0.2423
<b>53</b>	2	0.055	0.0008	0.2019
<b>54</b>	2.5	0.055	0.0008	0.173
<b>55</b>	3	0.055	0.0008	0.1622
<b>56</b>	1	0.055	0.0013	0.2232
<b>57</b>	1.5	0.055	0.0013	0.1795
<b>58</b>	2	0.055	0.0013	0.1517
<b>59</b>	2.5	0.055	0.0013	0.1365
<b>60</b>	3	0.055	0.0013	0.1301
<b>61</b>	1	0.055	0.0015	0.1864
<b>62</b>	1.5	0.055	0.0015	0.1581
<b>63</b>	2	0.055	0.0015	0.1379
<b>64</b>	2.5	0.055	0.0015	0.1235
<b>65</b>	3	0.055	0.0015	0.1173
<b>66</b>	1	0.01826	0.001	0.3434
<b>67</b>	1.5	0.01826	0.001	0.2867
<b>68</b>	2	0.01826	0.001	0.227
<b>69</b>	2.5	0.01826	0.001	0.2034
<b>70</b>	3	0.01826	0.001	0.185
<b>71</b>	1	0.03652	0.001	0.2828
<b>72</b>	1.5	0.03652	0.001	0.2359
<b>73</b>	2	0.03652	0.001	0.2
<b>74</b>	2.5	0.03652	0.001	0.1688
<b>75</b>	3	0.03652	0.001	0.16
<b>76</b>	1	0.07326	0.001	0.227



## Appendix C

<b>77</b>	<b>1.5</b>	<b>0.07326</b>	<b>0.001</b>	<b>0.1824</b>
<b>78</b>	2	0.07326	0.001	0.157
<b>79</b>	2.5	0.07326	0.001	0.1422
<b>80</b>	3	0.07326	0.001	0.1341
<b>81</b>	1	0.09152	0.001	0.1969
<b>82</b>	1.5	0.09152	0.001	0.1667
<b>83</b>	2	0.09152	0.001	0.1435
<b>84</b>	2.5	0.09152	0.001	0.1327
<b>85</b>	3	0.09152	0.001	0.125

## المستخلص

تعد شبكات الامطار في البنية التحتية الحضرية من العناصر مهمة في المجتمع. واحدة من أهم المشاكل التي تواجه مثل هذه الشبكات هي انسداد الأنابيب بسبب دخول الرواسب في شبكات صرف الامطار ، والتي يمكن أن تسبب الفيضانات أثناء هطول الأمطار الغزيرة. الهدف من هذه الدراسة هو تحسين كفاءة شبكة الامطار باستخدام مرشح جديد يقلل من نفاذ الرواسب. تقدم هذه الدراسة نموذجًا مختبريًا يحتوي النموذج على شبكة من الأنابيب لمحاكاة المطر بالإضافة إلى شارع من الجانبين ، في الجانب الأول يحتوي على اخدود مع مرشح ، بينما يحتوي الجانب الآخر على اخدود بدون مرشح. تمت دراسة العديد من المتغيرات المؤثرة على نسبة العابر من اخدود مع المرشح إلى اخدود بدون مرشح ، مثل كثافة هطول الأمطار وطول المرشح وزمن الشدة المطرية ومنحدر الأرض.

تم التحقق من العمل المختبري باستخدام نموذج عددي FLOW-3D, الغرض من النموذج العددي هو دراسة متغير جديد لم يدرس في العمل المختبري مثل قطر الرواسب. تم استخدام خمس شدات مختلفة من هطول الأمطار 30 و 37 و 44 و 51 و 58 (مم / ساعة) ، كل شدة تستخدم على الأرض مع خمسة منحدرات 1 و 1.5 و 2 و 2.5 و 3. كانت اطول المرشح 100 و 150 و 200 و 250 و 300 مم, بينما كانت الفترة الزمنية للشدة المطرية 5 و 10 و 15 و 20 و 25 دقيقة أوضحت النتائج أن ميل الأرض وطول المرشح كانا أكثر العوامل تأثيرا على نسبة العابر من اخدود مع المرشح إلى اخدود بدون مرشح. ان نسبة العابر كانت 35% لأدنى ميل من الأرض ، و 11% لأقصى ميل للأرض. لوحظ انخفاض نسبة العابر عندما يزيد طول المرشح الموجود في الحقل عن 400 ملمتر. ان مدة الشدة المطرية لها تأثير أقل أهمية على نسبة العابر من المتغيرات الأخرى. أظهرت النتائج أن النسبة العابر من اخدود مع مرشح إلى اخدود بدون مرشح كانت 34 % بكثافة المطر الأدنى التي تصل الى 30 (مم / ساعة) و 12.5 % في كثافة المطر الأعلى التي تصل الى 58 (مم / ساعة) ، في حين أن نسبة العابر كانت 37 % و 13 % للحد الأدنى والحد الأقصى لقطر الرواسب ، على التوالي.

اثبتت النتائج أن استخدام النموذج الرقمي لمحاكاة هذه الظواهر يعطي نتائج مقبولة ، وكان الحد الأقصى للخطأ فيها أقل من 16 % . يوفر نموذج التنبؤ بتحليل الأبعاد طرقاً فعالة للتنبؤ بسلوك النسبة العابر من كلي مع مرشح إلى كلي بدون مرشح . يتم الاستفادة من النموذج العددي الحصول على معادلة إحصائية لحساب  $(Mf/Mg)$  , حيث يعطي استخدام نموذج SPSS لتقدير نسبة  $(Mf/Mg)$  نتيجة تصل الى  $R^2 = 0.88$  وفق ظروف العمل .



وزارة التعليم العالي والبحث العلمي

جامعة كربلاء كلية الهندسة

قسم الهندسة المدنية

## تحسين كفاءة شبكة تصريف مياه الامطار باستخدام تصميم مرشح

الرسالة مقدمة الى قسم الهندسة المدنية/كلية الهندسة في جامعة كربلاء كجزء من متطلبات نيل  
درجة الماجستير في علوم الهندسة المدنية(البنى التحتية)

من قبل

**كرار عبدالله محسن**

باشرف

الاستاذ الدكتور

واقد حميد حسن

الاستاذ الدكتور

باسم خليل نايل